ROCK MAGNETISM AND PALEOGEOPHYSICS

Volume 1

Published by the

Rock Magnetism and Paleogeophysics

Research Group in Japan

December 1973

Tokyo

PREFACE

This is a continuation to the annual progress reports of our group published formerly under the titles ANNUAL PROGRESS REPORT OF THE ROCK MAGNETISM RESEARCH GROUP IN JAPAN (for the years 1963, 1964, and 1965) and ANNUAL PROGRESS REPORT OF THE PALAEOGEOPHYSICS RESEARCH IN JAPAN (for 1967 and 1968). Since the last volume of 1968, publication of annual reports has been discontinued for several years mostly because of financial difficulties. However, the publication is again made possible through the activities of our group in the Geodynamics Project. We hope to continue the publication in the coming years.

As the previous progress reports were so, this volume also is a collection of summaries of provisional results of various works carried out in our research group; no refereeing being made for individual papers. This volume can be referenced, but if a paper in this volume is published in another journal, readers are requested to refer the paper from that journal. We hope that this volume will be used as a summary of advance information of recent works on rock magnetism and paleogeophysics in Japan.

We would like to acknowledge the partial financial support for this publication and for the investigations included in this volume from the Ministry of Education as part of the Geodynamics Project. This volume constitutes a scientific report of the Rock Magnetism and Paleogeophysics Research Group in the Geodynamics Project in Japan.

28 December 1973

Masaru Kono

Editor

CONTENTS

ROCK MAGNETISM AND PALEOGEOPHYSICS SYMPOSIA

Two symposia were held in 1973; 19 and 20 March at Geophysical Institute, University of Tokyo, and 24 and 25 July at Saru-ga-kyo, Gumma Prefecture. Titles of the papers presented at these symposia are as follows:

19 March

M. Kono	Tokyo Univ.	Paleointensities of the Geomagnetic Field
K. Yaskawa	Osaka Univ.	Details of Measurements of Magnetization in the Lake Biwa Sediments
S. Sasajima	Kyoto Univ.	On the Blake Event
N. Kawai	Osaka Univ.	Problems Concerning to the Geomagnetic Field
H. Yoshimura	Tokyo Univ.	Dynamo Action in the Chromosphere of the Sun
T. Rikitake	Tokyo Univ.	Review of Non-Stationary Dynamos
K. Maenaka	Hanazono Univ.	Magnetic Properties of Volcanic Ashes
I. Muroi	Osaka Sci. Education Center	Measurements of Anisotropy of Susceptibility
N. Niitsuma	Tohoku Univ.	On the Japanese Paleomagnetic Stratigraphy

20 March

K. Ono	Geol. Survey	A Few Remarks from a Geologist
N. Fujii	Tokyo Univ.	Problems of Ultramafic Rocks
M. Shimada	Osaka Univ.	Magnetic Properties of Kimberlites
H. Ito	Shimane Univ.	Paleomagnetism of Granites
H. Kinoshita	Tokyo Univ.	On Superconducting Magnetometer
Y. Tomoda and K. Kobayashi	Tokyo Univ.	Magnetic Smooth Zone
N. Isezaki	Meteor. College	Magnetic Lineation Patterns and N-R Event
S. Uyeda	Tokyo Univ.	On Plate Motions

24 July

T. Yoshimura	Niigata Univ.	Alteration of Rocks
N. Yamashita	Shinshu Univ.	Shin'etsu-Bozu Zone
T. Nomura	Gumma Univ.	Geological Structures of the Western Part of the Gumma Prefecture
A. Tazaki	Osaka Univ.	Application of Superconductivity to Rock Magnetism
T. Nagata	Tokyo Univ.	Magnetic Properties of the Lunar Rocks
N. Sugiura	Tokyo Univ.	Thermomagnetic Curves of Meteorites and the Lunar Rocks
N. Kawai[1], T. Nakajima[1], K. Hirooka[2], K. Kobayashi[3] and K. Yaskawa[1]	1 Osaka Univ., 2 Fukui Univ., 3 Tokyo Univ.	Images of the Earth Imprinted under the Water --- Continuous, High-Resolution Measurements of the Geomagnetism
H. Domen	Yamaguchi Univ.	On Chemical Demagnetization

25 July

O. Oshima	Tokyo Univ.	Chemical Composition of Fe-Ti Oxides in Volcanic Rocks
T. Katsura	Tokyo Inst. Tech.	Synthesis and Thermodynamics of Spinel Solid Solutions Including Fe_3O_4
M. Joshima[1], M. Ozima[1], and H. Kinoshita[2]	1 Univ. Tokyo, 2 Meteor. Coll.	
K. Kitazawa	Tokyo Univ.	Magnetic Properties of JOIDES Basalts
K. Momose	Shinshu Univ.	On Chemical Remanent Magnetization

ROCK MAGNETIC STRUCTURES OF OCEANIC CRUST

BY

MINORU OZIMA AND MASATO JOSHIMA

GEOPHYSICAL INSTITUTE, UNIVERSITY OF TOKYO
BUNKYO-KU, TOKYO, JAPAN

Abstract

Primary titanomagnetite formed in an oceanic ridge undergoes progressive maghemitization with a time constant of about a few ten million years when oceanic crust moves laterally from a ridge.

One of the fundamental assumptions in interpreting oceanic magnetic lineation anomaly is that remanent magnetization acquired in an oceanic ridge has been preserved while oceanic crust moves laterally from the ridge. However, recent studies on magnetization of many submarine basalts have revealed that ferromagnetic minerals in submarine basalts undergoes progressive oxidation with time (1, 2). Since such oxidation may affect the primary remanent magnetization resulting in a violation of the assumption (3, 4), it is important to know the extent of oxidation in oceanic crust.

Thermomagnetic curves of submarine basalts show generally a characteristic irreversible change both in air and vacuum heating (2, 5, 6). This is explained as unmixing of titanomaghemite to Fe rich titanomagnetite and other less magnetic phases (2, 6). Although the occurrence of titanomaghemite in submarine basalts appears to be very general, titanomagnetite were also found in fresh submarine basalts dredged from the mid-Atlantic ridge at 45°N (7). It is now generally agreed that primary ferromagnetic minerals in submarine basalts are titanomagnetite and the titanomagnetite oxidizes to titanomaghemite. Suboceanic environment in which H_2O is easy of access appears to favour the particular oxidation process (2), that is, maghemitization or low temperature oxidation. Although the importance of such maghemitization process in suboceanic crust has been more and more recognized, little is known either of time involved, or the depth affected by maghemitization in oceanic crust. Hence, we attempted to estimate the time constant for maghemitization process and the depth of the maghemitized layer in oceanic crust.

Time constant for maghemitization: We chose six submarine basalts which are large enough to yield measurable amount of ferromagnetic mineral separates (Table 1). Because of their very fine grain size, it was difficult to separate ferromagnetic minerals free from silicate inclusions. Chemical analyses showed that the sum of FeO, Fe_2O_3 and TiO_2 constitues generally more than 80 % of the total weight, but for two samples (Piq. 1 and AM 49) it is less than 60 percent (Table 1). Except Piq. 1 which shows slight pyroxene peaks besides major cubic peaks in an X-ray diffractogram, other samples show only peaks corresponding to a cubic structure, indicating that the separated ferromagnetic minerals are essentially of a single phase with a cubic structure. For samples with high impurities (Piq. 1 and AM 49), a chemical

composition (Fe^{2+} : Fe^{3+} : Ti ratio) of the separated minerals may not represent those of the ferromagnetic components. However, AM 49 shows a reversible thermomagnetic curve in vacuum which is characteristic of titanomagnetite, indicating that the chemical analysis on the separates does represent a chemical composition of the ferromagnetic components. A chemical composition (Fe^{2+} : Fe^{3+} : Ti ratio) of the ferromagnetic component in Piq. 1 may be subject to some error.

Chemical compositions are plotted in a TiO_2 - FeO - Fe_2O_3 diagram (Figure 1). As is evident from Figure 1, except AM 49 all others are

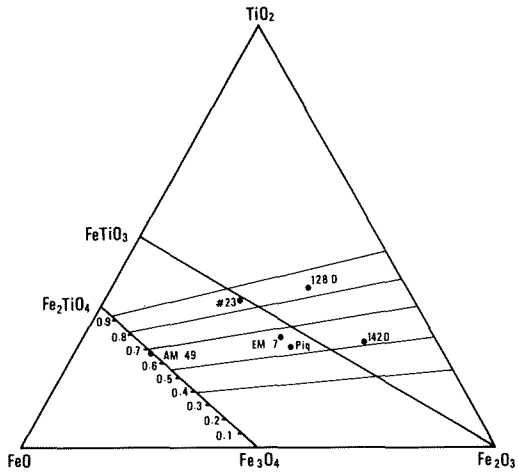

Figure 1. Ternary diagram showing a chemical composition of ferromagnetic minerals separated from submarine basalts. x-values (Ulvospinel content) are shown by figures along Fe_2TiO_4 - Fe_3O_4 join.

cation-deficient titanomagnetite (titanomaghemite). Assuming that the cation-deficient titanomagnetite are secondary oxidation products of primary titanomagnetites, we can estimate the chemical composition of the primary titanomagnetite by extrapolating each titanomaghemite point to an ulvospinel-magnetite join along a redox line (Ti/Fe = const. line) the redox lines being shown in the figure by thin lines. The extrapolation then indicates that ulvospinel contents in the submarine basalts range from 50 to 85 %, the average being a little higher than that for subareal basalts. Also noteworthy is that two samples are oxidized even beyond the ilmenite-hematite join, whereas AM 49 dredged from the mid-Atlantic ridge axis is almost stoichiometric titanomaghetite.

From a chemical composition we can calculate an oxidation parameter z for each sample in which z is defined as (8)

$$Fe^{2+} + \frac{z}{2} O \rightarrow zFe^{3+} + (1 - z)Fe^{2+} + \frac{z}{2} O^{2-} \qquad (1)$$

In Figure 2, z is plotted against K-Ar age of the samples. It is clearly seen from the figure that the degree of oxidation or the value of z increases with an increase of the age of submarine basalts, indicating a progressive maghemitization with age. Assuming that maghemitization obeys a first order rate process, the oxidation parameter z can be expressed as

$$z = 1 - e^{-t/\tau} \qquad (2)$$

which is similar to an expression used by Creer et al.(9) for high temperature oxidation process of titanomagnetite. In Equation 2, τ denotes the time constant of the process. In Figure 2, curves

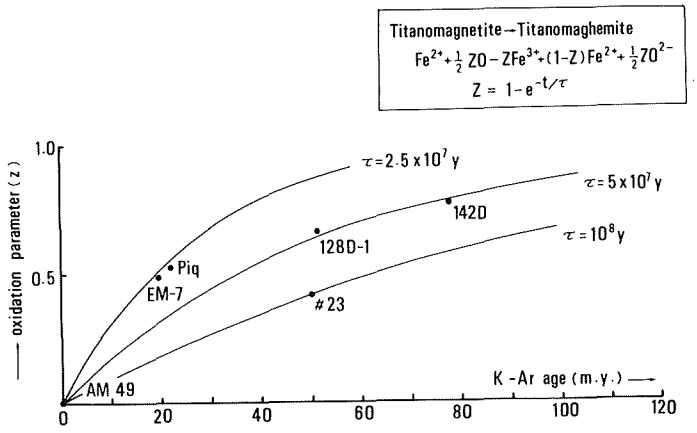

Figure 2. Oxidation parameter z against K-Ar age of submarine basalts. See the text for the explanation of curves.

representing Eq.(2) are shown for various values for the time constant τ. Experimental data seem to be roughly represented by a theoretical curve with $\tau = 5 \times 10^7$ y. Actual maghemitization process in submarine basalts must be a very complex depending on various factors such as grain size, initial chemical composition, P_{O_2} etc. Hence, a first order rate process must be a very crude approximation. Nonetheless, the experimental data (Figure 2) seem to indicate that maghemitization has taken place with a time constant of a few ten million years in these submarine basalts.

From a laboratory experiment on oxidation of artificial titanomagnetite grains to titanomaghemite, Readman and O'Reilly (10) suggested a time constant of about one million years, assuming a first order rate process for the oxidation. The difference between the Readman-O'Reillys' value and the present estimate must be due to the difference in the grain size, since the mean crystal size of the artificial titano-

magnetite studied by Readman and O'Reilly is about 400 A, whereas the grain size of ferromagnetic minerals in submarine basalts are generally larger than a few microns.

Vertical extension of maghemitization: Except EM-7 all samples in Figures 1 and 2 were dredged from the top of seamounts. Hence, the conclusion reached here may refer only to a very surficial part of oceanic crust. To understand a vertical extension of maghemitization in oceanic crust, we need to study drilled samples penetrating to a considerable depth. At present only one core is available to us; which is basalts from Experimental Mohole (5). In this case small fragments were available at almost every 1 meter interval in the whole drilled core of about 14 meters. In Figure 3, Curie temperature is

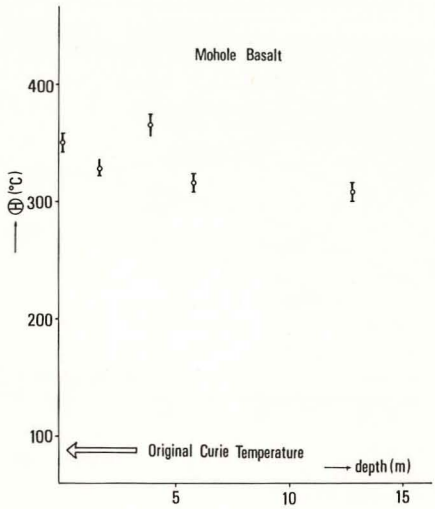

Figure 3. Curie temperature against depth from the top of basalt flow (Mohole basalt). Original Curie temperature (indicated by an arrow) is estimated by assuming that the primary ferromagnetic minerals were unoxidized titanomagnetite.

plotted against a depth from the top of the flow: Curie temperature is higher in the surface part than in the interior. This is easily understood if we assume that diffusing oxygen atoms from the surface is responsible to oxidation. Oxidation parameter z may be expressed approximately by

$$\frac{dz}{dt} = D \frac{d^2 z}{dx^2} \qquad (3)$$

where D is a diffusion coefficient of oxygen atom and x is a depth from the surface. The diffusion equation for z can then be solved to determine D with the use of data for dz/dt (see Figure 2) and dz/dx (= dⒽ/dx/dⒽ/dz), in the latter dⒽ/dx is estimated from Figure 3 and dⒽ/dz from experimental data on synthesized titanomaghemite.(11) The value of D estimated is about 5×10^{-7} cm /sec. The skin depth d for

maghemitization process can then be defined as $d = \sqrt{2Dt}$. For example the skin depth would be about 10^3 meters for Cretaceous oceanic crust (~ 10^8 years). Since oxidizing condition must vary considerably from a place to a place in suboceanic crust, the above conclusion derived from a single experimental result should not be generalized. Here, it is sufficient to suggest that maghemitization may extend to significant depth in older oceanic crust.

Implications: In Figure 4 we show a view of rock magnetic structures of oceanic crust. Primary titanomagnetite formed in an oceanic ridge

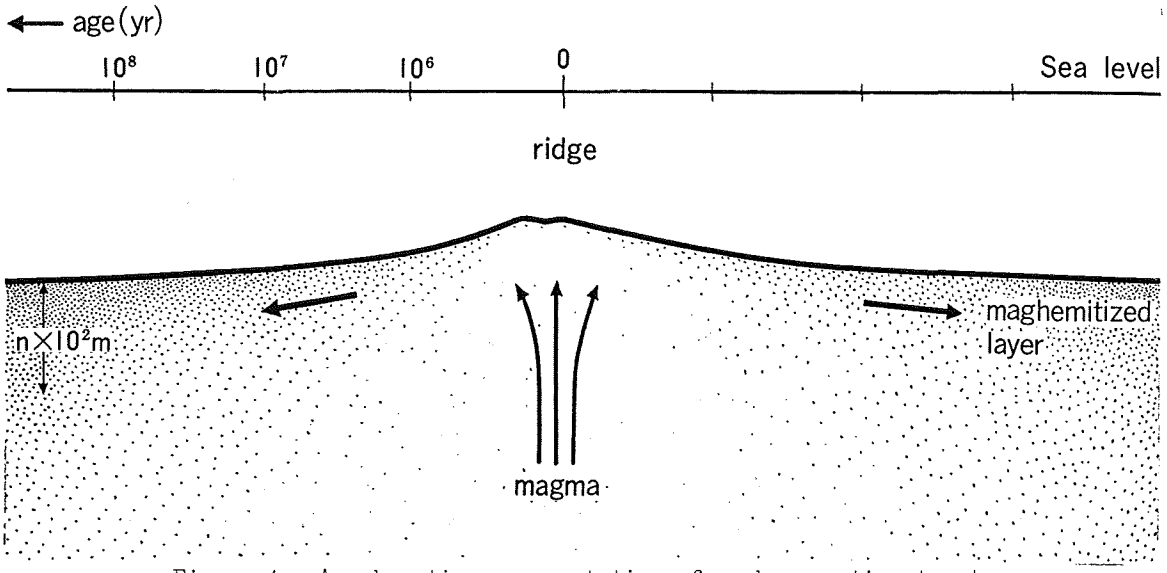

Figure 4. A schematic representation of rock magnetic structures of oceanic crust, indicating progressive maghemitization with age of the crust.

subsequently undergoes maghemitization resulting in an increase of Curie temperature and a reduction of a saturation magnetization (11). Time constant for maghemitization would be about a few ten million years. A decrease in a saturation magnetization with progressive degree of maghemitization should result in a reduction of NRM of submarine basalts. Johnson and Merrill (4) did find a decrease in the intensity of an initial ARM (anhysteretic remanent magnetization) and a development of CRM (chemical remanent magnetization) when ARM-carrying titanomagnetite grains were oxidized to titanomaghemite. Hence, considering that the time constant for such maghemitization is about a few ten million years, it is interesting to speculate that the reduction of NRM (natural remanent magnetization) intensity may be responsible to Cretaceous magnetic smooth zone. Moreover, a development of a secondary ferromagnetic phase (titanomaghemite) in the presence of the geomagnetic field may result in an acquisition of CRM whose direction could be entirely different from the primary NRM. Although it is still not conclusive whether a newly acquired CRM during maghemitization is really strong enough to affect a primary NRM (12), one should

at least be very careful in interpreting an observed magnetic anomaly lineation pattern in terms of a remanent magnetization acquired in an oceanic ridge.

We thank Professors V. Vacquier, A. Miyashiro and Dr. R. Doell for submarine basalts and Dr. E. Schwarz for reading a manuscript.

References

1) Schaeffer, R. M. and Schwarz, E. I., Can. J. Earth Sci., 7, 268 (1970).
2) Ozima, M. and Ozima, M., J. Geophys. Res., 75, 2051 (1971).
3) Nagata, T. and Kobayashi, K., Nature, 197, 476 (1963).
4) Johnson, P. and Merrill, R. T., J. Geophys. Res., 78, 4938 (1973).
5) Cox, A. and Doell, R. R., J. Geophys. Res., 67, 3997 (1962).
6) Ozima, M. and Ozima, M., J. Geophys. Res., 76, 8080 (1971).
7) Irving, E., Park, J. K., Haggarty, S. E., Aumento, F., and Loncarevic, B., Nature, 228, 1 (1970).
8) O'Reilly, W. and Banerjee, S. K., Phys. Letters, 17, 237 (1965).
9) Creer, K. M., Ibbetson and Drew, W., Geophys. J., 19, 93 (1970).
10) Readman, P. W. and O'Reilly, W., Phys. Earth Planet. Interion, 4, 1021 (1970).
11) Ozima, M. and Sakamoto, N., J. Geophys. Res., 76, 7035 (1971).
12) Marshall, M., Am. Geophys. Un. Trans., 54, 126 (1973).
13) Ozima, M. and Saito, K., Earth Planet. Sci. Letters (in press).

ON DISCRIMINATION OF RESPECTIVE REMANENT MAGNETISMS OF TITANOMAGNETITE AND TITANOMAGHEMITE

Kan'ichi Momose and Susumu Inagaki
Department of Geology, Faculty of Science, Shinshu University,
Matsumoto, Japan

Titanomagnetite(β-phase) grains in nature have sustained a secondary alteration to produce partly titanomaghemite(γ-phase). If such a stable remanent magnetism as the CRM might be generated in the altered fraction —— titanomaghemite, observed natural remanent magnetism(NRM) should represent a composition of two magnetic vectors respectively due to the fractions in the β and γ- phases, so that discrimination of each NRM is naturally a matter of serious importance for palaeomagnetic study.

The writer is to declare a possible method of discrimination of each of the NRMs by a thermal treatment in which until recently he has employed.

First, the Curie temperature(Tc) is to be obtained from original titanomagnetite fraction that has not sustained a secondary alteration.

Next, the presence or absence of any remains of remanent magnetism due to titanomaghemite(γ-phase) may be checked by thermal demagnetization at a temperature corresponding to Tc of titanomagnetite(β-phase).

However, the magnetic behaviour of the fraction in γ-phase varies with change in chemical composition of primary titanomagnetite, in other words the content(x) of $TiFe_2O_4$ in the titanomagnetite series ; hence it is difficult to find out Tcs respectively pertinent to titanomagnetite and titanomaghemite.

To overcome this difficulty, the experimental sample the writer now treats for this purpose is required to have such properties as in the following:

1) Under the reflection microscope, existence of the γ-phase fraction should be recognized within ferromagnetic grains.

2) Thermomagnetic curves of the sample should be irreversibly traced, as shown in the figure, through heating and cooling processes, and this fact suggests the breakdown of the γ-phase fraction took place at high temperature, resulting disappearance of the adherent remanent magnetism. Eventually, it becomes possible to obtain the Curie temperature Tc_2 of this sort of samples (Mituko Ozima and E.E.Larson,1967 ; Kunio Kobayashi and K. Momose,1969).

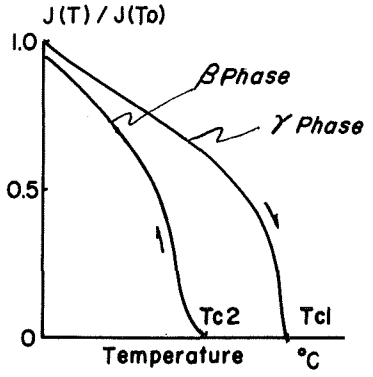

The Tc_1 thus obtained may demonstrate a high stability of the γ-phase fraction against heating up to a temperature corresponding to Tc_1.

If the γ-phase fraction holds a stable NRM, it is possible to estimate, accordingly to examine whether or not the role of this NRM might bear a significant influence on the original NRM of the sample.

In the writer's experiment carried out on a certain lava, three samples from the same lava indicated their Tc_1s being respectively at 560°,550°C and 500°C, whereas their Tc_2s all measured 410°C after heating up to 900°C in vacuo. The NRM of this rock could mostly be removed by thermal demagnetization at temperature corresponding to Tc_2.

On the other hand, an agreement was ascertained between direction of the NRM having remained slightly even after the thermal demagnetization cited above, and that of original sample which was demagnetized in an alternating field of 150 Oe. These results have made the writer conclude that the remains of magnetism due to the γ-phase fraction are assigned to the VRM.

Considering that this sample acquires, however, a considerable VRM during about twenty hours storage after thermal demagnetization, a stable remanent magnetization may not possibly have taken place in the γ-phase fraction owing to big particle sizes of ferromagnetic minerals.

By taking advantage of this check method, the writer will continue to test rocks containing fine particles of ferromagnetics.

References

Kobayashi, Kunio and K. Momose(1969) Etudes sur le Quaternaire dans le Monde, VIII INQUA congress,959.

Ozima, Mituko and E.E. Larson(1967) Journ. Geomag. Geoelectr.,Vol.19,117.

MAGNETIZATION OF OCEANIC BASALTS

Masato JOSHIMA

Geophysical Institute, University of Tokyo, Bunkyo-ku,
Tokyo, Japan

1. Introduction

It is now generally recognized that submarine basalts contain highly oxidized titanomaghemites. In spite of the importance of titanomaghemites in magnetization process of suboceanic crust, magnetic properties of titanomaghemites are not fully understood (Irving,1970, Ozima and Ozima,1971). Because of difficulties in synthesizing such minerals,submarine basalts which contain highly oxidized titanomaghemites, should offer an excellent chance to study the magnetic properties. This paper is a report of the results of X-ray and chemical analyses of titanomaghemites separated from submarine basalts.

Ozima and Sakamoto(1971) and Readman and O'Reilly(1972) reported the properties of titanomaghemites synthesized by wet grinding method. Ozima and Sakamoto could only produce titanomaghemites up to z = 0.3, where z is the oxidation parameter, beyond which titanomaghemites were further unmixed to magnetite and ilmenite. Using the same technique of Ozima and Sakamoto, Readman and O'Reilly reported a synthesis of titanomaghemite up to z = 1.0. However, lattice parameters and Curie temperatures they obtained were significantly different from those reported by Ozima and Sakamoto.

At present, it is difficult to judge which of the two results should be taken as more reliable. I have measured lattice parameters and Curie temperatures of titanomaghemites separated from several submarine basalts, in the hope that the study would resolve the above question.

2. Curie Temperatures and Lattice parameters of the Separated Minerals

Dredge locations and depths, and Curie temperatures of the samples are given in Table 1.

Rocks were crushed and ground in water to prevent oxidation and then magnetic minerals were separated by a hand magnet. In this separation, the most serious difficulty was to avoid oxidation because of extremely fine grain sizes of the minerals. To make sure that oxidation did not take place, we compared the Curie temperatures of the separated samples with those of original rocks. The results indicate that appreciable amount of oxidation did not take place by this grinding in water (Table 2).

For the six samples which were shown to be one phase by means of X-ray diffraction analysis, we measured Curie temperatures, lattice parameters, and saturation magnetizations, and did chemical analyses (Table 2).

In order to compare the results with data of synthesized titanomaghemites, lattice parameters and Curie temperatures of the samples are plotted on the equi-Curie temperature and equi-lattice parameter diagrams of Ozima and Sakamoto (1971) (Fig.1), and on those of Readman and O'Reilly(1972) (Fig.2). As seen in the figures, the present data do not agree with either of the contours of equal Curie temperature and lattice parameter. Curie temperatures (lattice parameters) of the submarine basalts seem too high (low) compared with the synthetic minerals of the same composition.

Table 1. Samples

Sample	Dredge Location Long.	Lat.	Depth	Curie Temp.	Remarks
AM49	30°01'N	42°04'W	4280 m	180-200°C	
W10-3	22°10'N	45°12'W	3000	230-250	Lamella
Cobb	46°46'N	130°49'W	34	520-528	
Piq.1	14°12'S	77°36'W	4910	376-396	
AM50	30°01'N	42°04'W	4280	660-690	
Vac.23	21°29'N	159°32'E	1250	267-281	
Erimo	40°54'N	144°50'E	4000	524-545	Lamella
128D-1	9°15'N	158°20'W		283	
142D-10	18°00'N	169°05'W		431-448	
133D	12°04'N	165°50'W		559	
144D-2	21°32'N	167°56'W		573	
Phillippine Sea				282-290	

Table 2. Magnetic Properties of the Separated Minerals

Sample	Curie Temperature	(Rock)	Lattice Parameter	Saturation Magnetization	x	z
AM49	153°C	(180-200°C)	8.470 Å	17.27 emu/g	0.567	0.008
Piq.1	390	(376-396)	8.358		0.494	0.512
Vac.23	292	(267-281)	8.399	8.75	0.805	0.407
128D-1	286	(283)	8.360	5.91	0.794	0.656
142D-10	434	(431-448)	8.364	24.27	0.485	0.762
Phillippine Sea	283	(282-290)	8.402	16.94	0.714	0.439

x ; Ulvospinel content in unoxidized state
i.e., x $Fe_2TiO_4 \cdot (1-x)\ Fe_3O_4$
z ; Oxidation parameter

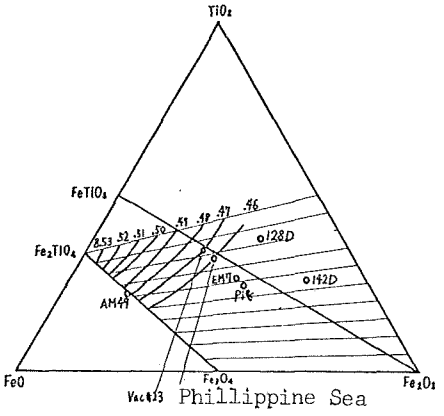

Fig.1a Circles(Our data) and contour lines(Ozima and Sakamoto) of equi-lattice parameter in a ternary diagram.

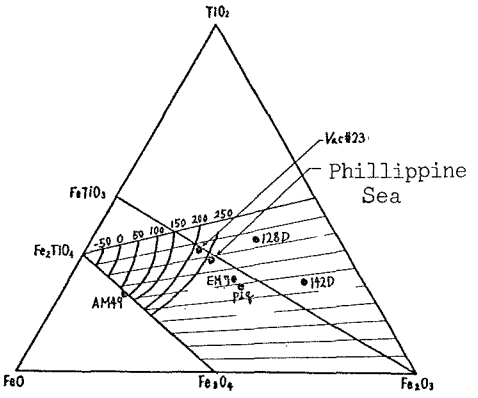

Fig.1b Circles(Our data) and contour lines(Ozima and Sakamoto) of equi-Curie temperature in a ternary diagram.

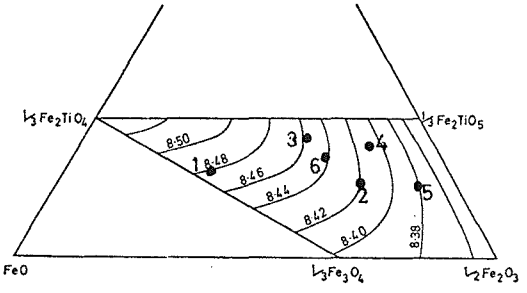

Fig.2a Circles(Our data) and contour lines(Readman and O'Reilly) of equi-lattice parameter in a ternary diagram.

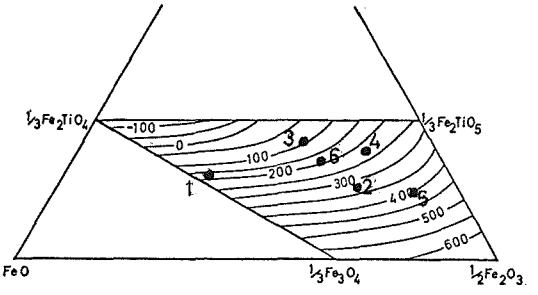

Fig.2b Circles(Our data) and contour lines(Readman and O'Reilly) of equi-Curie temperature in a ternary diagram.

1; AM49, 2;Piq.1, 3; Vac.23, 4; 128D-1, 5; 142D-10, 6; Phillippine Sea

Löffler(1963) showed that mixing of Al^{3+},Mg^{2+},and $Cr^{3+}$with magnetite and γ-hematite lowers both Curie temperatures and lattice parameters of them. According to Creer and Stephanson(1972), the effect of impurity ions in the lattice parameter of titanomagnetites is expressed as

$$a = 8.394 + 0.136*(Ti) - 0.147*(Al) - 0.034*(Mg) \quad \text{------} \quad (1)$$

where (Ti),(Al),and(Mg) are molecular numbers of individual ions. Concentration of Fe,Ti,Al,and Mg in magnetic minerals of Vac.23 were measured by means of X-ray microanalyser ; (Al_2O_3)=1.8 mole % and (MgO)=4.56 mole %. By means of chemical analysis the values of (Al_2O_3)=1.56 mole % and (MgO)=1.46 mole % were obtained for the Phillippine Sea sample. Then, a simple-minded application of eq.(1) may indicate that lattice parameter would be lowered by the effect of Al^{3+} and Mg^{2+} by 0.02 Å for Vac.23, and 0.015 Å for the Phillippine Sea sample. The difference between the values of lattice parameters of synthesized titanomaghemite (Ozima and Sakamoto,1971) and that of minerals in submarine basalts is 0.02-0.07 Å. The difference between our data and those of Readman and O'Reilly is 0.01-0.06 Å. As eq.(1) was obtained for titanomagnetite, it may or may not be applied to titanomaghemite. Even if impurity ions lower the lattice parameters of titanomaghemites in a same way as in eq.(1), the effect on the Curie temperatures should then be to lower and not to raise them.

Other factors may exist which lower lattice parameters and increase Curie temperatures. Also, another possibility is that the separated ferromagnetic minerals are not perfectly in a single phase, but contain two or more phases which cannot be detected by X-ray diffraction or chemical analysis.

Acknowledgements

I wish to thank especially Prof. M.Ozima for continual guidance. For supplying samples, I am very grateful to ; Prof.A.Miyashiro, State University of New York at Albany ; Prof.V.Vacquier, M.R.Jarrard, and Mr.T.Hilde, Scripps Institution of Oceanography ; Prof.R.T.Merrill, University of Washington ; Prof.K.Kobayashi, Ocean Research Institute of University of Tokyo.

Refference

Creer,K.M. and A.Stephanson (1972) J.Geophys.Res. 77 3698.
Irving,E. (1970) Can.J.Earth Sci. 7 1528.
Löffler,H.,F.Frölich and H.Stiller (1965) Geophys.J.Roy.Astro.Soc. 9 411.
Ozima,M. and M.Ozima (1971a) J.Geophys.Res. 76 2051.
Ozima,M. and N.Sakamoto (1971) J.Geophys.Res. 76 7035.
Readman,P.W. and W.O'Reilly (1972) J.Geomag.Geoelectr. 24 69.

NOTES ON INTEGRATED EFFECT OF REPEATED SHOCKS ON REMANENT MAGNETIZATION OF IGNEOUS ROCKS

Takesi NAGATA

National Institute of Polar Research, Itabashi, Tokyo.

1. Introduction

In a previous paper (Nagata 1971), general characteristics of the shock remanent magnetization $J_R(H+SHo)$, the advanced shock effect on IRM, $J_R(SH+Ho)$, and the shock demagnetization $J_R(H+HoS)$ of igneous rocks were described. Here, $J_R(H+SHo)$ represents the remanent magnetization acquired by giving a compressive shock momentum S on a rock sample in the presence of a magnetic field H ; $J_R(SH+Ho)$ the isothermal remanent magnetization acquired in H of a rock sample which was shocked by S in non-magnetic space before H is applied ; $J_R(H+HoS)$, the remanent magnetization after the ordinary IRM, $J_R(H+Ho)$ is shocked by S in non-magnetic space. In this notation, H+ means an application of H and Ho a release of a sample from H, while S is given by

$$S = \int_t P(t)\,dt \quad , \tag{1}$$

where P(t) represents a mechanical compressive shock of a short duration as a function of time (t).

As for $J_R(H+SHo)$, experimental results have been summarized for small values of H and large values of S as

$$J_R^{//}(H+SHo) = K^{//}H \cdot S, \qquad J_R^{\perp}(H+SHo) = K^{\perp} H \cdot S, \tag{2}$$

where // and $\perp$ represent respectively a case that the direction of H is parallel to the axis of S and another case that the direction of H is perpendicular to the axis of S, and $K^{//}$ and $K^{\perp}$ denote materials constants, where

$$K^{\perp} \simeq \frac{3}{4} K^{//} \ . \tag{3}$$

As for $J_R(SH+Ho)$, experimental result are summarized as

$$J_R(SH+Ho)/J_R(H+Ho) = F(S/H), \tag{4}$$

$$F(0) = 1, \quad F(S/H) > 1 \quad \text{and} \quad F(S/H) \simeq NS/H$$

for large value of S/H,

where N denotes a positive numerical constant.
As for $J_R(H+HoS)$,

$$J_R(H+HoS)/J_R(H+Ho) = G(S/H) \ ,$$

$$dG(S/H)/d(S/H) = -M < 0 \quad \text{for small values of } S/H \tag{5}$$

$$\lim_{(S/H)\to\infty} G(S/H) = 0$$

On the other hand, Shapiro and Ivanov (1967) have pointed out that the

and

$$J_R(H+HoS_1 \cdots Sn) - K_\infty \; J_R(H+Ho)$$
$$= (K_1 - K_\infty) J_R(H+Ho) \exp\{-\beta (n-1)\} \qquad (15)$$
$$(\text{ for } \quad n \geqq 1 \;).$$

Hence

$$J_R(H+HoS_1 \cdots Sn) = J_R(H+Ho)\left[K_\infty + (K_1 - K_\infty)\exp\{-\beta (n-1)\}\right]. \qquad (16)$$

Similarly

$$J_R(H+S^*HoS_1 \cdots S_n) =$$
$$= J_R(H+S^*Ho)\left[K_\infty + (K_1 - K_\infty)\exp\{-\beta (n-1)\}\right]. \qquad (17)$$

The experimental results of shock demagnetization of SRM are as follows:

Sample	H	S*	S	K_1	K_∞	β
	(Oe)	(Bar.Sec)	(Bar. Sec)			
NV-B	1.69	0.117	0.117	0.356	0.098	0.326
	1.69	0.117	0.0292	0.540	0.360	0.142
	1.69	0.0292	0.117	0.128	0.121	0.428
	1.69	0.0584	0.117	0.119	0.088	0.935
NV-K	1.37	0.0424	0.0424	0.408	0.085	0.595
	3.37	0.0424	0.0272	0.664	0.420	0.272
	3.37	0.0283	0.0283	0.535	0.210	0.522
	3.37	0.0283	0.0424	0.122	0.027	0.364

3. $J_R(S_1 \cdots Sn\, H+Ho)$

It seems that the most significant key phenomenon in a direct connexion with the physical mechanism of various effects of mechanical compressions or shocks on the remanent magnetization of rocks is the advanced compression effect (Nagata and Carleton 1968, 1969a, b) and the advanced shock effect (Nagata 1971) on IRM, which are symbolically noted by $J_R(P+PoH+Ho)$ and $J_R(SH+Ho)$ respectively. Since $J_R(P+Po)=0$ and $J_R(S)=0$ but generally $J_R(P+PoH+Ho) > J_R(H+Ho)$ and $J_R(SH+Ho) > J_R(H+Ho)$, the state of $J_R(P+Po)=0$ or $J_R(S)=0$ must be distinguished from $J_R(0)=0$. It has been experimentally proved that the inner condition of $J_R(P+Po)$ or $J_R(S)$ state can be reduced to $J_R(0)$ by the ordinary AF-demagnetization procedure of the maximum alternating field $\tilde{H}$, because

$$J_R(P+Po\tilde{H}H+Ho) = J_R(H+Ho) = J_R(0\,H+Ho),$$
$$J_R(S\tilde{H}H+Ho) = J_R(H+Ho),$$

as far as $\tilde{H}$ is sufficiently large.

It has been proposed (Nagata 1971) on the other hand that the remarkable integrated effect of repeated shocks in the SRM and shock demagnetization phenomena could be interpreted as due to the physical principle

that the entropy of a magnetized sample concerned always increases whenever possible by applied repeated mechanical shocks of fluctuating magnitudes. In this connexion, experimental examinations of a possibility of the integrated effect of repeated shocks in non-magnetic space in advance of an acquisition of IRM, (i.e. a possible dependence of $J_R(S_1 \cdots\cdots SnH+Ho)$ on n, should be most interesting. Fig. 1 shows a summary of results of experimental studies on the dependence of $J_R(S_1 \cdots SnH+Ho)/J_R(H+Ho)$ on n for sample NV-K for different values of S and H, where $S_1 = \cdots = Sn = S$. It seems in the figure that $J_R(SH+Ho)$ is slightly smaller than $J_R(SSH+Ho)$ for small values of S/H, but $J_R(S_1 \cdots SnH+Ho)$ is practically constant for $n \geqq 2$. Approximately speaking, therefore, there is no appreciable integrated effect of repeated advanced mechanical shocks on IRM, that is

$$J_R(S_1 \cdots SnH+Ho) = J_R(SH+Ho). \quad (18)$$

Results of similar experiments on sample NV-B have led to the same conclusion, though the accuracy of measurements for this sample is less than that for NV-K.

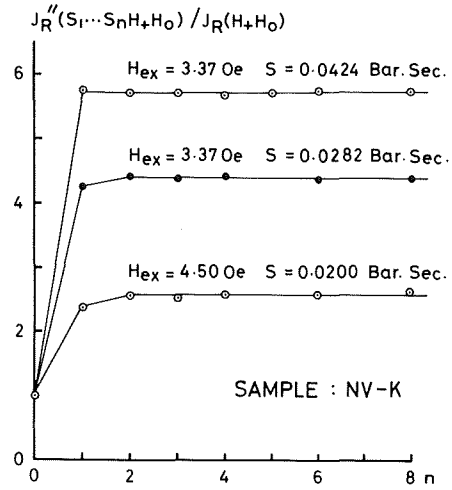

Fig. 1 Constancy of repeated advanced shock effect, which is practically independent of n. Sample NV-K.

4. Theoretical Discussions of Experimental Results

As already discussed (Nagata 1971), it seems that the most self-consistent and unified theoretical interpretation of the phenomena of SRM, shock demagnetization and advanced shock effect on IRM is based on the idea that both the magnetostatic force introduced by a magnetic field and the magnetoelastic force introduced by a mechanical shock irreversibly drive the 90° domain walls so that the total potential energy takes the minimum possible value at individual stages during the whole course of respective experimental processes. As for the internal resistive force which resists against the externally applied forces, Rayleigh's relationship between H and IRM (i.e. $J_R(H+Ho) = bH^2$) macroscopically represents the relationship between the external and internal forces in this theory. The above-mentioned physical principle is exactly identical to the basic physical idea of Nagata-Carleton's theory of piezo-remanent magnetization (Nagata and Carleton 1969 a b).

In Nagata-Carleton's theory, an acquisition of PRM for large values of P and small values of H has been given by

$$J_R(H+P+PoHo) = \frac{16}{5\pi} bHHc \qquad \text{for } Hc \geqq 2H, \qquad (19)$$

and the pressure demagnetization effect for small values of P is represented by

$$J_R(H+P+PoHo) = J_R(H+Ho)\left(1 - \frac{16}{15\pi}\frac{H_c}{H}\right) \quad \text{for} \quad H_c \leqq H, \qquad (20)$$

Here, $$H_c = \frac{3\lambda_s}{2J_s} P = h_c P \quad , \qquad h_c \equiv \frac{3\lambda_s}{2J_s} \quad , \tag{21}$$

where λ_s represents the isotropic magnetostriction coefficient.

(A) Then, let us now assume in the case of mechanical shock effect that the effective value of Hc working on individual 90° domain walls has statistical fluctuations in each shocks, an individual Hc value being expressed as

$$H_c = H_c^o + \xi \quad , \tag{22}$$

where the distribution function $p(\xi)$ of ξ is represented by a finite symmetric function around $\xi = 0$ such as

$$\begin{aligned} p(\xi) &= \frac{1+\gamma}{2h_o^{1+\gamma}} (h_o - \xi)^\gamma \quad \text{for} \quad 0 \leqq \xi \leqq h_o \ , \\ &= \frac{1+\gamma}{2h_o^{1+\gamma}} (h_o + \xi)^\gamma \quad \text{for} \quad -h_o \leqq \xi \leqq 0 \ . \\ &\qquad (\gamma \geqq 0) \end{aligned} \tag{23}$$

For the whole set of 90° domain walls, therefore, the average value of Hc is always H_c^o , and

$$\int_{-h_o}^{o} p(\xi)d\xi = \int_{o}^{h_o} p(\xi)d\xi = \frac{1}{2} \quad .$$

(B) As the second assumption, we may consider that repeated shocks following the first shock can give rise to additional effects on individual walls only when the effects result in a decrease of the magnetostatic energy. These two basic assumptions, (A) and (B), would be reasonably well acceptable as an approximation.

(a) $J_R(H+HoS_1 \cdots Sn)$
In Nagata -Carleton's theory,

$$J_R(H+HoP+Po) = \frac{1}{2} J_R(H+Ho) + \frac{1}{2} J_R(H+Ho)\left(1 - \frac{32}{15\pi} \frac{H_c^{(-)}}{H_c}\right), \tag{24}$$

$$\text{for} \quad H_c \leqq H \ ,$$

where $H_c^{(+)}$ and $H_c^{(-)}$ denote respectively Hc working on (+) walls on which Hc affects into the same direction as the effect of H and that on (-) walls on which H affects into the direction opposite to that of H. Let us now consider the integrated effect of repeated shocks. The probability that n th shock is larger than (n-1) th shock is 1/2 i.e. $p(S_n > S_{n-1}) = 1/2$. Then, expressing the average value of Hc of all $(S_2 > S_1)$ walls by $H_c = H_c^o + h_2$, we get

$$h_2 = h_o \left\{ 1 - \left(\frac{1}{2}\right)^{\frac{1}{1+\gamma}} \right\}. \tag{25}$$

In general, $$h_n = h_o \left\{ 1 - \left(\frac{1}{2}\right)^{\frac{n-1}{1+\gamma}} \right\} \ . \tag{26}$$

Then, replacing $J_R(H+HoP+Po)$ in (24) by $J_R(H+HoS_1 \cdots Sn)$, $H_c^{(-)}$ in (24) can be replaced by

$$\begin{aligned} H_c^{(-)}(n) &= H_c^o + h_n = H_c^o + h_o \left\{ 1 - \left(\frac{1}{2}\right)^{\frac{n-1}{1+\gamma}} \right\} \\ &= H_c^o + h_o \left[1 - \exp\left\{ -\frac{\ln 2}{1+\gamma} (n-1) \right\} \right] \ . \end{aligned} \tag{27}$$

Thus,

$$J_R''(H+HoS_1 \cdots Sn) = J_R(H+Ho)\left[\left(1-\frac{16}{15\pi}\frac{H_c^o+h_o}{H}\right.\right.$$

$$\left.\left.+\frac{16}{15\pi}\frac{h_o}{H}\exp\left\{-\frac{\ln 2}{1+\gamma}(n-1)\right\}\right]. \qquad (28)$$

If we put

$$1-\frac{16}{15\pi}\frac{H_c^o+h_o}{H} = K_\infty, \quad 1-\frac{16}{15\pi}\frac{H_c^o}{H} = K_1, \quad \frac{\ln 2}{1+\gamma} = \beta,$$

then (28) becomes

$$J_R(H+HoS_1 \cdots Sn) = J_R(H+Ho)\left[K_\infty + (K_1 - K_\infty)\exp\left\{-\beta\,(n-1)\right\}\right],$$

which is exactly the same as (16)

J_R $(H+S^*HoS_1 \cdots Sn)$ also can be theoretically derived in the same way to become identical to (17).

(b) $J_R(H+S_1 \cdots SnHo)$

In accordance with Nagata-Carleton theory,

$$J_R(H+P+PoHo) = \frac{16}{15\pi}\,b\,H_c\,H_c^{(+)} + \frac{32}{15\pi}\,b\,H\,H_c^{(-)}$$

$$\text{for} \qquad H_c \geqq 2H \qquad (29)$$

If $H_c \gg H$, (in a more mathematically exact expression, if $H_c > 4H$ for individual pairs of (+) and (−) 90° domain walls),

$$J_R(H+S_1 \cdots Sn\,Ho) = \frac{32}{15\pi}\,b\,H\,H_c^o + \frac{16}{15\pi}\,bH\,(H_c^o + h_n)$$

$$= \frac{16}{5\pi}\,b\,H\,H_c^o + \frac{16}{15\pi}\,b\,H\,h_o\left[1-\exp\left\{-\frac{\ln 2}{1+\gamma}(n-1)\right\}\right]. \qquad (30)$$

Putting then

$$\frac{16}{5\pi}\,b\,H\,H_c^o = J_R(H+SHo) = K\,J_R(\infty), \quad \frac{16}{15\pi}\,b\,H\,H_o = J_R^*(\infty),$$

$$\frac{\ln 2}{1+\gamma} = \alpha,$$

(30) becomes identical to (12)

(c) $J_R(S_1 \cdots Sn\,H+Ho)$

In Nagata-Carleton theory,

$$J_R(P+Po) = \frac{16}{15\pi}\,b\left\{H_c^{(+)}\right\}^2 - \frac{16}{15\pi}\,b\left\{H_c^{(-)}\right\}^2 = 0 \qquad (31)$$

If $H_c^{(+)} \neq H_c^{(-)}$, $J_R(P+Po)$ must have either positive or negative remanent magnetization, and consequently a certain finite amount of the magnetostatic energy must appear, whence $H_c^{(+)} = H_c^{(-)}$ as far as any acquisition of a finite magnetostatic energy in H=0 space is forbidden. In the case of $J_R(S)$ or $J_R(S_1 \cdots Sn)$, the situation must be the same as in the case of $J_R(P+Po)$. Namely, the allowable values of Hc for individual shocks must be

$$H_c^{(+)} = H_c^{(-)} = H_c^o + \xi \qquad (-h_o \leqq \xi \leqq h_o) \qquad (32)$$

for each pairs of domain walls. The probability that both $H_c^{(+)}$ and $H_c^{(-)}$

simultaneously take a same value of $H_c^o + \xi$ should be negligibly small. Since the average value of $H_c^o + \xi$ is H_c^o, we may write

$$J_R(S_1 \cdots Sn) = J_R(S) = \frac{16}{15\pi} b \left[(H_c^o) - (H_c^o)^2 \right] = 0 \quad . \tag{33}$$

Then (33) theoretically leads to

$$J_R\ (S_1 \cdots SnH{+}Ho) = J_R\ (SH{+}Ho) = \frac{16}{15\pi}\ b\,H\,H_c^o \quad , \tag{34}$$

for sufficiently large values of H_c^o/H. That is, there is no integrated effect of advanced repeated shocks on IRM.

***** **** *****

References

Nagata, T., (1971), Introductory notes on shock remanent magnetization and shock demagnetization of igneous rocks, Pure. Appl. Geophys. 89, 159-177.

Nagata, T. and Carleton, B. J., (1968), Notes on piezo-remanent magnetization, J. Geomag. Geoele., 20, 115-127.

Nagata, T. and Carleton, B. J., (1969a), Notes on piezo-remanent magnetization of igneous rocks, II, J. Geomag. Geoele., 21, 427-445.

Nagata, T. and Carleton, B. J. (1969b), Notes on piezo-remanent magnetization of igneous rocks III, theoretical interpretation of experimental results, J. Geomag. Geoele., 21, 623-645.

Shapiro, V. A. and Ivanov, N. A. (1967), Dynamic remanence and the effect of shocks on the remanence of strongly magnetic rocks. Doklady Akad. Nauk, USSR, 173, 1065-1068.

THE VOLMETRIC HISTOGRAM OF NICKEL CONCENTRATION IN METAL PARTICLES OF LUNAR AND METEORITE SAMPLES

Naoji SUGIURA and Takesi NAGATA

Geophysical Institute, University of Tokyo, Tokyo, Japan

1. Introduction

There is a wide range of nickel concentration in the metallic particles of lunar samples (Reid et al. (1971) ; El Goresy et al. (1971) ; Goldstein et al. (1972)). The wide range of Ni has been interpreted as due to the paragenesis sequence from the melt. A metal phase solidified earlier in the sequence contains more nickel, which is siderophile than the metal solidified later. However, there are many exceptions which show a poor relation between the nickel content and the paragenesis sequence (El Goresy et al. (1971)). To understand the origin of lunar metal, it will be important to produce precise histograms of nickel concentration. From the thermomagnetic curves, we have made the histograms, which are volumetric, different from the ordinary histograms derived by microprobe analysis. These histograms show a great similarity to those of meteorites.

2. Method of analysis

Denoting $Js(T)$, $k(T, \theta)$ and $C(\theta)$ as

$Js(T)$; Saturation Magnetization of lunar sample, which contains some kinds of metals, as a function of temperature T ;

$k(T, \theta)$; Saturation magnetization of a metal whose Curie point is θ ;

$C(\theta)$; Weight fraction of a metal whose Curie point is θ ,

there holds an equation

$$Js(T) = \int_0^a k(T, \theta) \cdot C(\theta) d\theta \quad , \tag{1}$$

where a is the highest Curie point of the sample. As $k(T, \theta)$ is known and $Js(T)$ is a measured value, (1) is an integral equation with respect to $C(\theta)$. Dividing the temperature range into p equal intervals, the following matrix and vectors can be defined ; i . e.

$$\begin{array}{lll} J = (j_i) & j_i = Js(ih) & (i = 0, 1, 2, \cdots p-1), \\ K = (k_{ij}) & k_{ji} = K(ih, jh) & (i = 0, 1, \cdots p-1, \ j = 1, 2, \cdots p), \\ C \equiv (C_j) & C_j = C(jh) & (j = 1, 2, \cdots p), \end{array} \tag{2}$$

where $h = a/p$.

Then, the above integral equation can be converted to a linear equation

$$J = KC \quad . \tag{3}$$

Beyond Curie temperature (i.e. when $i \geq j$) $k_{ij} = 0$, so K becomes a triangular matrix. In actual computations, the estimate of $C(\theta)$ for p equal intervals can start from the highest temperature interval.

This method is an approximate analysis of a thermomagnetic curve. Because of observational errors, however, the approximate method may be practically sufficient for the purpose of the present analysis.

3. Assumptions

(i) For the standard values of $K(T, \theta)$, $Js(T)$ of pure iron which is nomalized by T/θ is adopted and the $\gamma \rightarrow \alpha$ transition at transition point θ' is approximated by a function

$$\frac{1}{1+b^{(T-\theta')}} \quad , \qquad (4)$$

where b is a constant depending on a cooling rate of experiment. In our experiment ($dT/dt = 200^{o}C/hour$), $b \cong 1.25$.
(ii) The $\gamma \rightarrow \alpha$ transition temperature is shown in Fig. 1 which is derived from the data of Bozorth (1951) and modified by our microprobe analysis data. As the alloy contains cobalt up to a few per cent, we must use a ternary diagram for a precise analysis. Since no ternary diagram is available at present, a binary system of Fe and Ni is assumed in the present work.
(iii) The saturation magnetization at room temperature is approximated, in accordance with Bozorth(1951) , by

$$K(273^{o}C, \theta) = 220.0 - 0.125 \times \rho(\theta)^2 ,$$

where ρ represents the nickel weight per cent corresponding to θ .
(iv) In our experiments, two cycles of thermomagnetic analyses have been made for all samples. In the present analysis, the second cooling curve is analyzed for individual samples, because the contribution of super-paramagnetism is negligibly small. The taenite phase which can be separated from the kamacite with the aid of the analysis of heating curve is very small in all samples, whence the presence of taenite is neglected except for one sample (#60255).
(v) The temperature range (h) for individual intervals is $8^{o}C$ above $T = 590^{o}C$ and $12.5^{o}C$ below $T = 590^{o}C$. To construct the histograms, $C(\theta)$ values are added for each four intervals for the temperature range above $590^{o}C$ and for each two intervals below $590^{o}C$.

4. Result

In the course of analyzing these observed data, $Js(T)$ is so approximated by a computer that the relative error is smaller than one per cent. The histograms are shown in Fig. 2 , where Co represents a component whose observed Curie point is higher than $770^{o}C$ and therefore attributable to cobalt. Some histograms of $C(\theta)$ for meteorites are shown in Fig.3 for comparison. In Fig. 2, the peak of $C(\theta)$ about pure iron phase may be due to a pure metalic iron produced as the break down product (El Goresy et al. 1972) which is out of interest of the present work. Then, the following features can be observed in the histograms.
(i) No significant difference is observed among the lunar rock types; i.e. fines, breccias, and igneous rocks.
(ii) A similarity between the lunar and meteorite samples can be observed; namely the peak at $5 \sim 7$ wt per cent Nickel is dominant in all lunar samples which contain magnetically irreversible alloy. This peak is not so evident in the histograms obtained by the microprobe analysis. This difference between the two kinds of histogram may be due partly to statistical

errors, and/or due to a relation between the grain size and Nickel content which has been known in the case of lunar soil sample (Goldstein et al. (1972) ; Wlotzka et al. (1972)). The peak at 5 ~7 wt % Ni could be interpreted from the view point of paragenesis sequence, if the sample is reheated or cooled so slowly that the samples can be in equilibrium. From the phase diagram of Fe-Ni, however, there must be two peaks in the histogram corresponding to the α and γ phase boundary. So there may be some process to put the meteoritic metal into the lunar samples. Actually, it has become obvious from metallographic analyses that there are many meteoritic metals in the fines and breccias (Goldstein et al. (1972)), and in an igneous rock (Axon and Goldstein (1972)). To interpret the histogram from the view point of the idea of a migration of meteorite metals, there is a problem that the histograms for the ordinary chondrite are sharply cut at 6 ~ 7 % while the lunar ones are broadly distributed up to 11 wt per cent nickel. Although there may be some ways to produce the alloy containing about 15 % Ni during the impact metamorphism of meteorite (Goldstein et al. 1970), it has not yet been clear how the alloys of 8 ~ 11 wt per cent Nickel can be produced. A possible interpretation of this problem is an assumption that the Carbonaceous chondrite are the ancestors of lunar materials. This interpretation can be supported also by the fact that the metal phase of carbonaceous chondrite contains high and variable amount of cobalt, which is the case of the lunar metals (Goldstein and Yakowitz 1971).

References

Axon H. J., and J. I. Goldstein (1972) Earth Planet. Sci. Letters 16, 439.

Bozorth R. M. (1951) Ferromagnetism p 31.

El Goresy, A., P. Ramdohr, and L. A. Taylor (1971) Earth Planet Sci. Letters 13, 121 .

El Goresy, A., L. A. Taylor, and P. Ramdohr (1972) Proc. Third Lunar Sci. Conference No. 1 333.

Goldstein J. I., E. P. Henderson and H. Yakowitz (1970) Proc. Apollo 11 Lunar Sci. Conference. 1, 499

Goldstein J. I. and H. Yakowitz (1971) Proc. Second Lunar Sci. Conf., 1, 117.

Goldstein J. I., H. J. Axon, and C. F. Yen (1972) Proc. Third Lunar Conference 1, 1037.

Reid A. M., C. Meyer, R. S. Harmon, and R. Brett (1970) Earth Planet Sci. Letter 9. 1.

Wlotzka, F., E. Jagoutz, B. Spettel, H. Baddenhausen, A. Balacescu, and H. Wanke (1972) Proc. Third Lunar Sci. Conference 1, 1077.

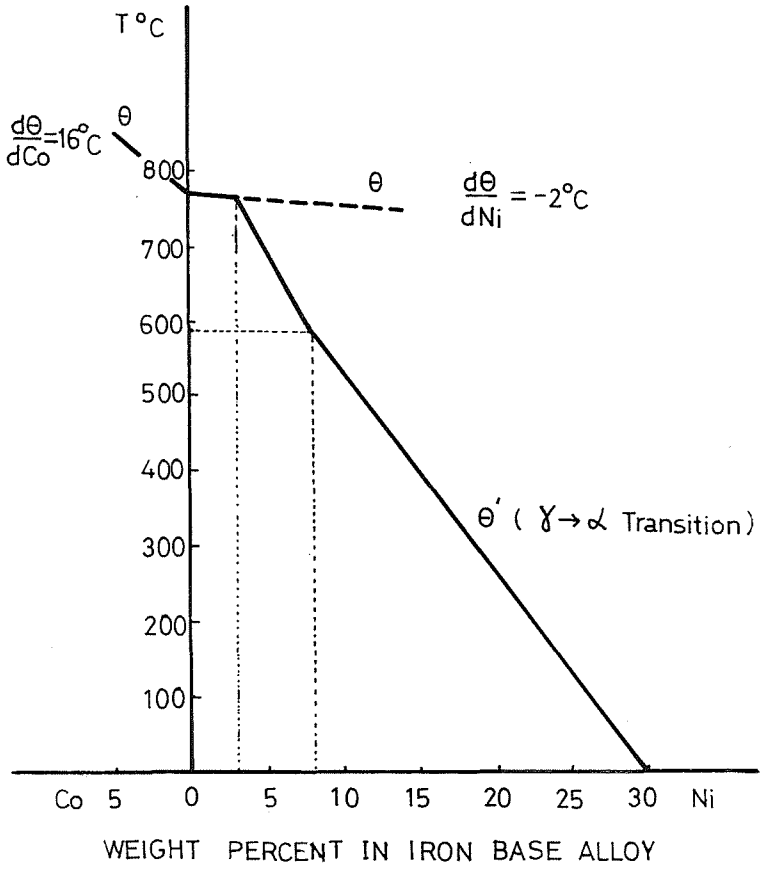

Fig. 1. Simplified phase diagram of Fe-Ni-Co system

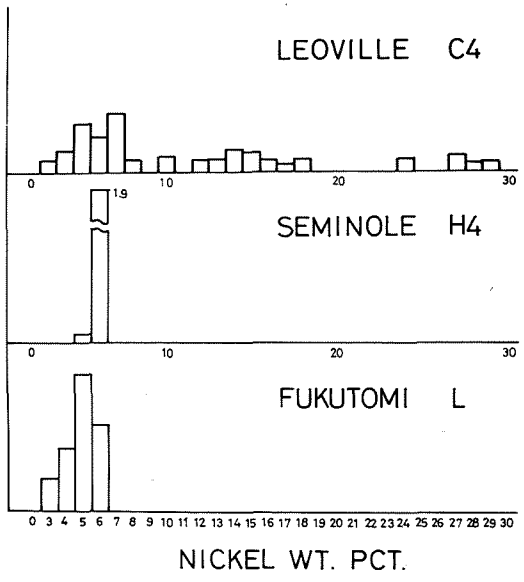

Fig. 3. Histograms of Nickel concentration for meteorite samples.

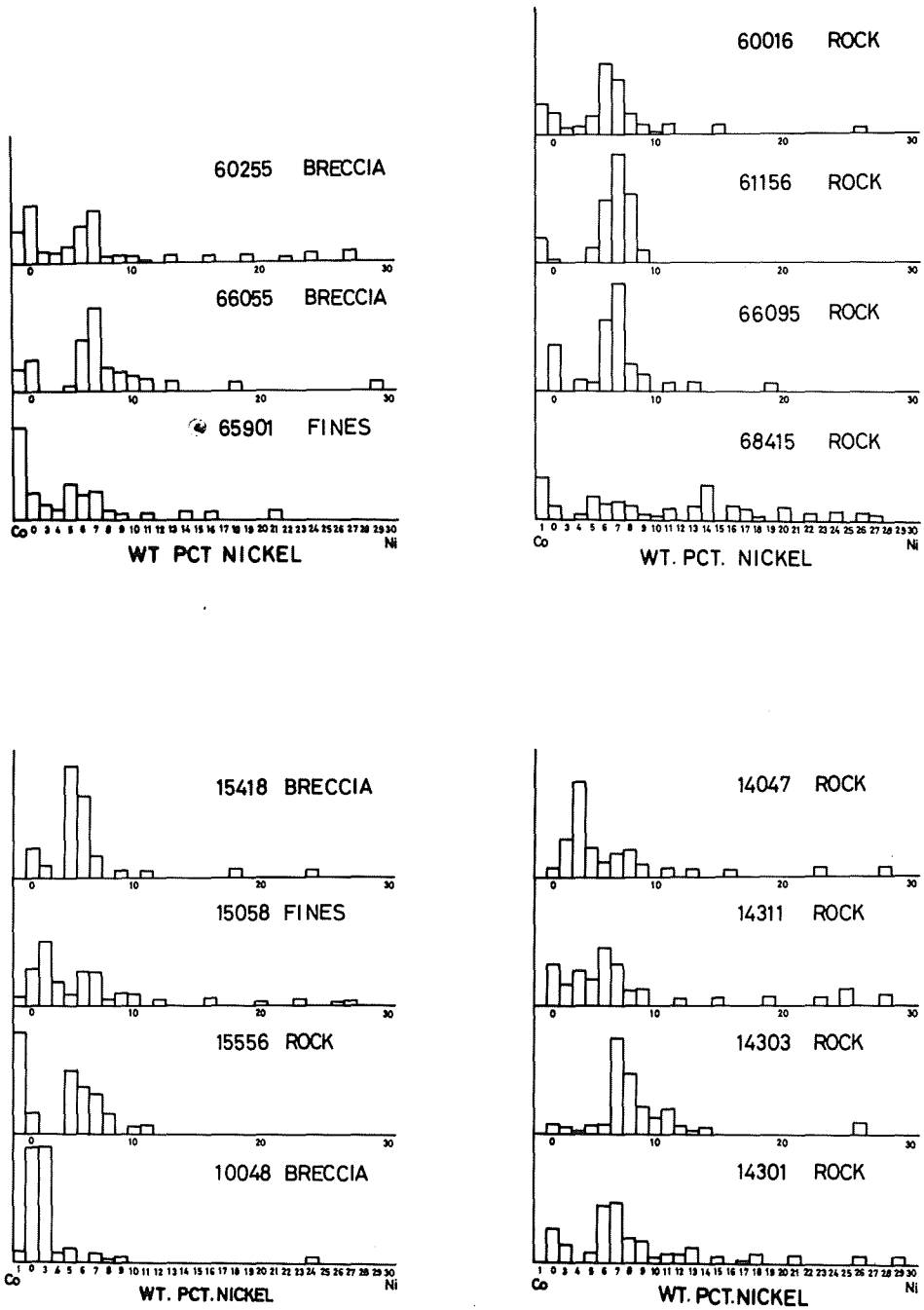

Fig. 2. Histograms of Nickel concentration for lunar samples

MEASUREMENTS OF ULTRASONIC WAVE VELOCITIES OF SOLID UNDER HIGH PRESSURES AND HIGH TEMPERATURES
-SUPPLEMENT TO STUDIES ON SEISMO-MAGNETIC PHENOMENA-

Hajimu KINOSHITA
Meteorological College, Chiba Pref.
and
Hideyuki FUJISAWA
Earthquake Research Institute, University of Tokyo, Tokyo

1. Introduction

Seismo-magnetic effect is one of the most important problems in the practical field of the earth sciemces(Stacey, 1969). This effect is understood as a change of local geomagnetic field (inner part and induced by the crust) due to accumulation of elastic (and/or non-elastic strain energy in the crustal materials prior (or due) to occurrence of shallow earthquakes. From stand point of ferromagnetism this is attributable to some inverse effects of magnetoelasticity (Lee, 1955). It is,therefore, necessary to study mechanical properties of ferromagnetic minerals characteristic to the crustal materials so that we are better able to understand thei magnetoelastic behaviors under high pressures and temperatures realized in the earths crust. Change of mechanical constants due to change in pressure and temperature is partly observed by measurements of ultrasonic wave velocities. Owing to recent revolutional progress in electronic techniques we are easily able to construct a measuring system of this sort.

2. Measuring Systems

We have made up two types of circuits for measurements of ultrasonic wave velocities of solid materials. Basic idea of the system is well known (McSkimin, 1961; Mattaboni and Schreiber, 1966), and detailed contents of our electronic circuits are described elsewhere (Fujisawa, Kinoshita and Hachimine, 1974). Therefore we will show only simple diagrams of our equipments in Figs. 1 and 2. Both of them are essentially based on the same idea;i.e. measurement of ultrasonic wave velocities by means of reflection and interference. First circuit (FKH-1, Fig.1) is commonly used in many laboratories but is more costly compared to the second one (FKH-2, Fig.2) because it does have to contain an oscilloscope of high quality. In FKH-2 we have merely to use a simple oscilloscope with a stable triggering circuit.

Right now we are trying to get used to measuring techniques for very small samples (3 mm or less in dimensions) so that we are able to measure ultrasonic wave velocities of solid under high pressure produced by a static pressure

machines. In the case of measurement of small sample, we have to check, first of all, effects of thickness of the transducers (PZT or Qz), since thickness of samples is in the same order compared to that of transducers. Roughly speaking, we are sure to get readings of velocity values with ±0.5% both in accuracy and reproducibility for aluminum poly crystals at room temperature and atmospheric pressure. Further results will be discussed in other papers.

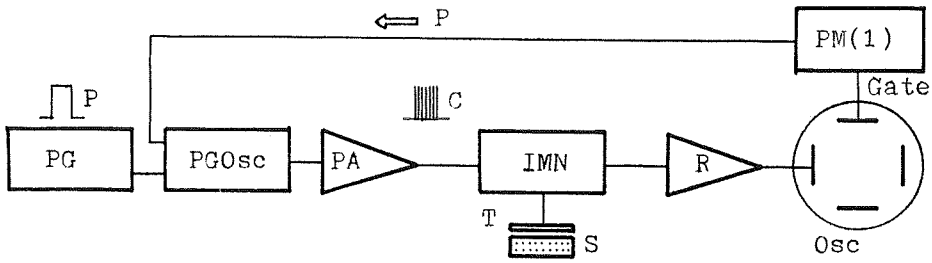

Fig.1 Block diagram of FKH-1.

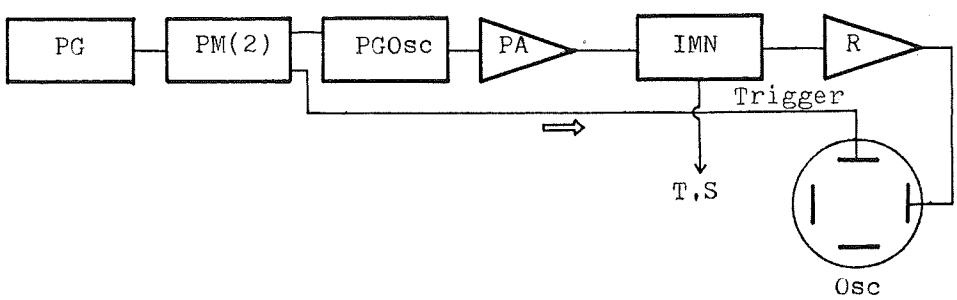

Fig.2 Block diagram of FKH-2.

Explanations to Figs. 1 and 2.

PG:Pulse generator (non-stable multivibrator type, 0-1MHz).
PGOsc:Pulse-gated oscillator(carrier frequency 10-50MHz).
PA:Power amplifier.
IMN:Impedance matching network.
T:Transducer (electric wave vs. mechanical oscillation).
S:Sample (with optical flat surface).
For high temperature measurements, some buffer rod with high-Q value being inserted between T and S.
R: Wide-band receiver (differential video amplifier).
PM:Pulse modulation circuit; (1)attached to Osc and (2) to PG.
P:Pulse (with various types of time sequences).
C:Carrier (enveloped by P).
⟸:Directions of pulse transfer.
Osc:High speed oscilloscope.

References

Fujisawa, H., H. Kinoshita and T. Hachimine (1974) J. Seism. Soc. Japan (in print).
Lee, E.W. (1955) Rep. Progress in Phys. 18, 184.
Mattaboni, P. and E. Schreiber (1966) Rev. Sci. Instr. 37, 1625.
McSkimin, H. J. (1961) J. Acoust. Soc. Am. 33, 12.
Stacey, F. D. (1969) Phys. of the Earth, John Wiley and Sons, 120.

ARCHAEOMAGNETIC STUDY IN HOKURIKU DISTRICT

Kimio HIROOKA

Geological Laboratory, Faculty of Education, Fukui University

Up to 1971, archaeomagnetic studies in Japan had been carried out intensively by several authors (Watanabe, 1958, 1959: Yukutake, 1961: Kawai et al.,1965, 1968: Hirooka, 1971). But all of these results except one datum were obtained by measuring samples collected from the localities in the region of the Pacific Ocean side of the Japanese Islands. The only exceptional datum was obtained from an old kiln of medieval time in Fukui Prefecture (Hirooka, 1971).

Recently, several results of archaeomagnetic study in Hokuriku District, the northern part of central Japan appeared separately in the archaeological reports of excavation of individual site (Kawai et al., 1971: Hirooka, 1972, 1973: Hirooka et al., 1972). Present author recently obtained new data from three sites which were excavated since1971 in this District. These sites are Suzu Old-kiln site (Suzu City, Ishikawa Prefecture), Shimokōbata Ruins (Sabae City, Fukui Prefecture), and Hosorogi Old-ironworks (Kanazu Town, Fukui Prefecture).

At Suzu Old-kiln site, samples were collected from a kiln called Hōjūji-3, whoes age is estimated to be in Early or Middle Muromachi Era (Muromachi Era : 1334-1573 A.D.) or a little older than that from the shape of potteries excavated. This kiln was repared several times in a manner of making the new floor on top of the older one, so that we have several floors in the vertical section of the kiln basement. The samples submitted to archaeomagnetic measurements were taken from the youngest two floors.

More than 20 baked earths were found in Shimokōbata Ruins. These were baked by the fire of cremation of ancient times. Collected samples were from four well baked places which were named K-1,K-7, K-8 and K-9. There very few archaeological evidences indcating the age of these cremations. Several potsherd of Heian Era (794-1185 A.D.) were excavated from the same stratigraphic horizon of these baked earths. This fact can only bound the age of the site to be in a time during from Heian Era to the 18th Century.

In the area called Hosorogi in Kanazu Town, Fukui Prefecture are found many kilns which were used for reducing iron oxide to pig iron in the ancient. Two kilns which were numbered 1 and 2 were excavated in 1971 and archaeomagnetic samples were obtained from both of them. Fission-track age determination was carried out as to Kiln-1 and the obtained age shows 1300 $\pm$ 290 B.P.(Nishimura, personal communication).

The orientation of samples was measured referring to the geomagnetic north by using a specially designed magnetic compass (Hirooka, 1971) and corrected to the value referring to the geographic north with the value of the present declination which was determined from the direction of the sun at every site.

All the archaeomagnetic data so far obtained in Hokuriku District are summerized here. In Table 1 are listed up the name, kind of site, geographic coordinate, and age estimated from the archaeological evidencies of the sites, and the localities of these are as shown in Fig. 1.

Table 1.

No.	Site	Kind of Site	Geographic Coordinate	Age
1.	Tsukasaki Ruins	Dwelling pits (fireplaces)	36.60°N, 136.70°E	Middle of Late Yayoi Period (ca. 200 A.D.)
2.	Hosorogi Old-ironworks	Kilns	36.23°N, 136.26°E	Nara or Heian Era (?) 1300±290 B.P.(F.T. age)
3.	Echizen Old-kiln Site	Kiln	35.94°N, 136.04°E	1260±20 A.D.
4.	Suzu Old-kiln Site	Kiln	37.41°N, 137.22°E	Early or Middle Muromach Era
5.	Old Kutani Kiln Site	Kilns	36.20°N, 136.42°E	Kiln-1 1656 A.D.* Kiln-2 1688-1704 A.D.** Kiln-Yoshidaya 1824-1826 A.D.
6.	Wakasugi Old-kiln Site	Kiln	36.40°N, 136.49°E	1810-1837 A.D.
7.	Shimokōbata Ruins	Crematory (baked earths)	35.96°N, 136.21°E	Younger than Middle of Heian Era (?)***

F.T. age : Fission-track age

* One potsherd on which this age was written is found in the kiln.

** It is considered from old records that they stopped to use this kiln during these ages.

*** Samples were obtained from four places named K-1, K-7, K-8, and K-9. K-8 and K-9 are older than the other two.

The results of the studies are tabulated in Table 2, and the declination and the inclination changes are shown in Fig. 2. The secular change curves drawn from the study of the southwestern Japan (Hirooka, 1971) are also shown in the figure. There seems to be no significant difference between the archaeomagnetic field direction of the southwestern Japan and that of Hokuriku District. But it is very dificult to prove the above-mentioned fact because of the two problems. One is the small amount of

Table 2.

No.	Name of Sampling Place	D	I	$_{95}$	K	N	Reference
1.	Mean of 8 fireplaces	4.2	64.0	3.8	23.56	61	Hirooka(1972)
2.	Kiln-1	-11.4	59.6	4.0	98.11	14	This paper
	Kiln-2	-14.4	53.5	2.8	199.24	14	This paper
3.	Kamioshidani	20.0	51.6	9.5	30.53	9	Hirooka(1971)
4.	Hōjūji-3						
	Top layer	12.7	56.0	2.1	471.46	11	This paper
	2nd layer	12.0	53.1	3.9	241.58	7	This paper
5.	Kiln-1	8.0	49.3	3.0	122.71	19	Kawai et al.(1971)
	Kiln-2	5.6	42.9	4.0	149.25	10	Hirooka et al.(1972)
	Kiln-Yoshidaya	-1.6	47.3	2.3	384.94	11	Hirooka et al.(1972)
6.	Wakasugi-1	4.3	48.1	2.7	143.20	20	Hirooka(1973)
7.	K-8	0.5	50.6	5.9	61.01	11	This paper
	K-9	5.3	54.1	3.9	65.29	22	This paper
	K-1	8.4	51.5	10.0	84.69	4	This paper
	K-7	4.9	47.8	4.2	154.61	9	This paper

No. : same in table 1.
D : declination
I : inclination
$_{95}$: Fishers cone of confidence at P=0.05
N : namber of samples

available data. We must accumulate more data for each district. The other problem is the ambiguity in age of the sites. Accurate archaeological estimation of of age can be done only in the case that the excavated things are correlated very well to the historical records. But usually it is not in the case. Scientific methods of age determination such as C^{14}, fission-track and other methods seems to be very difficult to achieve the accuracy with which we can distinguish the difference of archaeo-secular change between districts. So we need much more data of well known age for this study.

References

Hirooka, K. (1971) Mem. Fac. Sci., Kyoto Univ., Ser. Geol. & Mineral., 38, 167.
Hirooka, K. (1972) Report of the Excavation Research of Tsukasaki Ruins, 49 (in Japanese).
Hirooka, K. (1973) Preliminary Report of the Excavation Research of Wakasugi Old Kiln Site, 33 (in Japanese).

Hirooka, K., T. Nakajima and N. Kawai (1972) Old Kutani Kiln : Preliminary Report of the 2nd Excavation Research, 49 (in Japanese).
Kawai, N., K. Hirooka, S. Sasajima, K. Yaskawa, H. Ito and S. Kume (1965) Ann. Geophys., 21, 574.
Kawai, N., K. Hirooka, K. Tokieda and T. Kishi (1968) 1967 Ann. Progress Rep. Palaeogeophys. Res. Japan, 81.
Kawai, N., K. Hirooka, K. Yaskawa and T. Nakajima (1971) Old Kutani Kiln : Preliminary Report of the 1st Excavation Research, 33 (in Japanese).
Watanabe, N. (1958) Nature, 182, 383.
Watanabe, N. (1959) J. Fac. Sci. Univ. Tokyo, Sect. 5, 2, 1.
Yukutaka, T. (1961) Bull. Earthqu. Res. Inst., 39, 467.

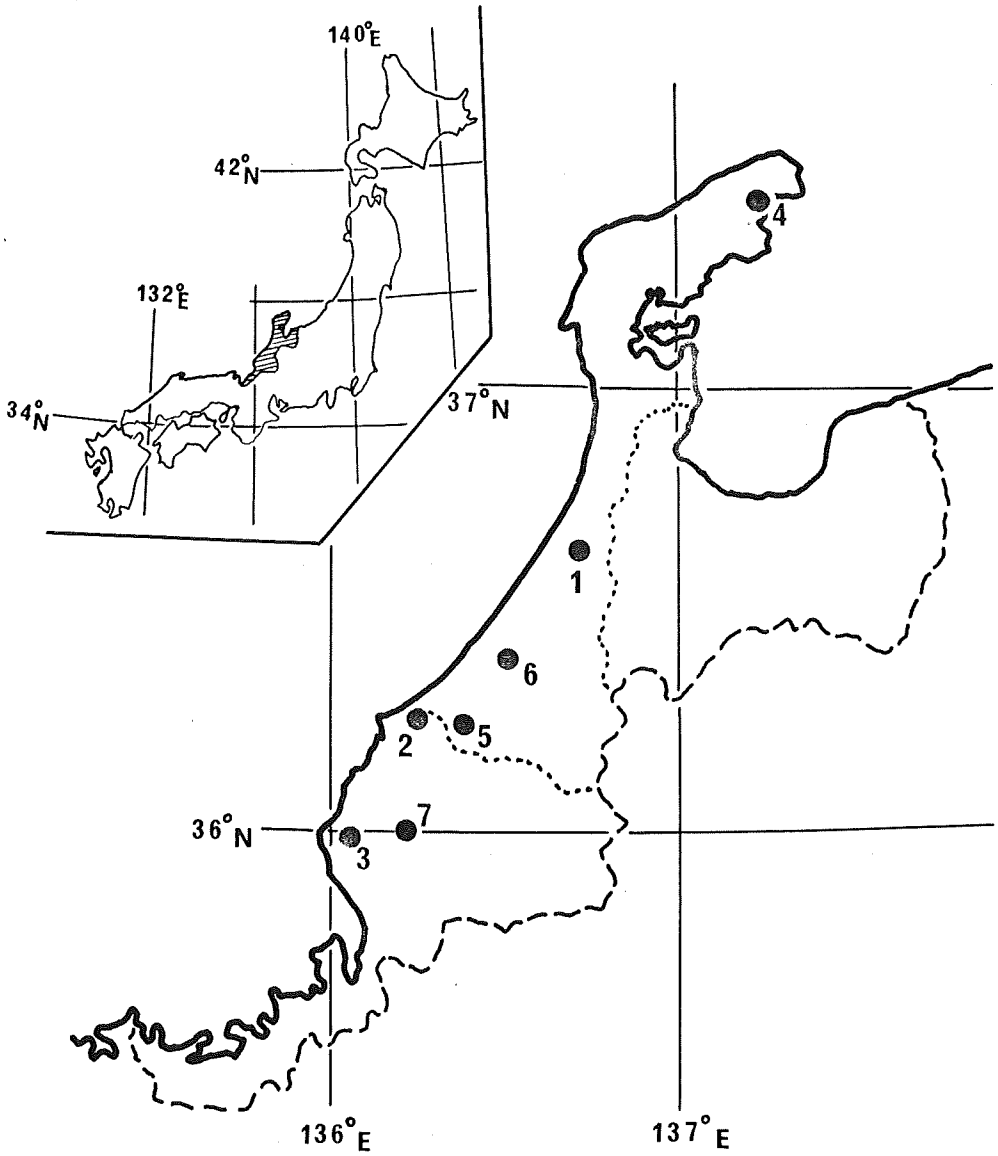

Fig. 1. Localities of Sampling Sites

Site no. is same in Table 1.

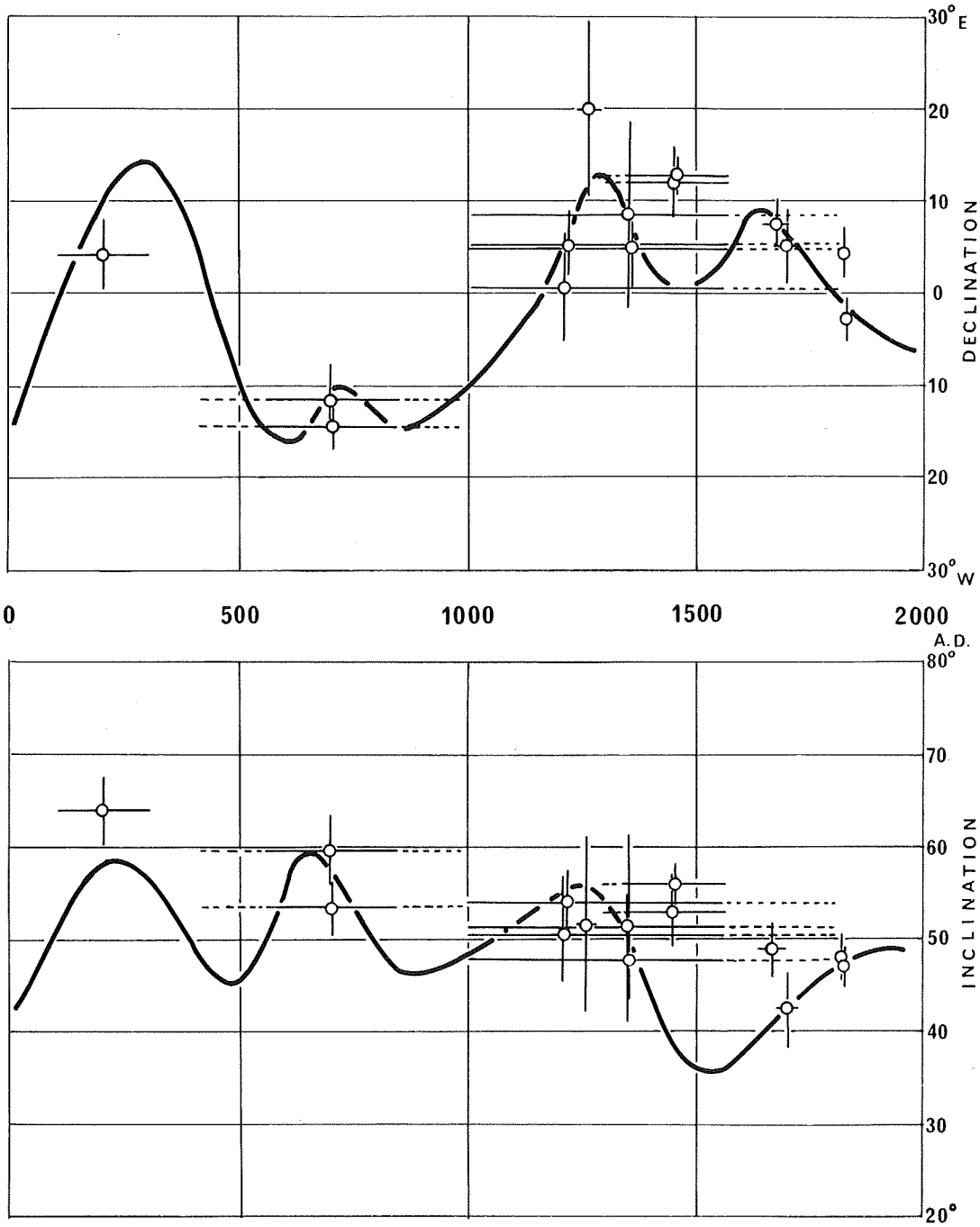

Fig. 2. Secular variations of the declination and the inclination of Hokuriku District

Thick curves are the variations obtained from the archaeomagnetic study of the southwestern Japan (after Hirooka, 1971).

SECULAR GEOMAGNETIC VARIATION IN THE RECENT 60,000 YEARS FOUND FROM THE LAKE BIWA SEDIMENTS

Tadashi NAKAJIMA and Naoto KAWAI

Department of Physics, Faculty of Engineering Science, Osaka University, Toyonaka, Japan

Introduction

The past geomagnetic field is fossilized within general sediments that formed in water. Among others, the Lake Biwa sediments obtained by Horie (1972) provided a good piece of information regarding geomagnetic polarity events in the Brunhes geomagnetic epoch (Kawai et al., 1972; Nakajima et al., 1973; The research Group for Palaeomagnetism of Lake Deposits, 1973).

Being not only continuous but also more precise in details than those from the ocean sediments, the data may disclose the secular variation in a time span extending back to the remote past of the geological age. The lake basin is made up of green grayish strata that piled up incessantly at a changing rate whose mean is estimated using C^{14} method to be 42.6 cm/1,000 yr (Horie et al., 1971; Yaskawa, 1973).

As the sediments were forming it took approximately 47 years till the thickness increased by 2 cm. Cubic specimen with this thickness is quite favourable for the observation by using astatic as well as spinner magnetometer. Besides, each layer contains ferromagnetic minerals which give the sediments the intensity of about 7×10^{-6}cgs emu/cc. A sequence of cubic specimens, each being 8 cc in volume, was prepared along the core axis from the head downwards successively. A record of the geomagnetism with high resolution (obtained at every 47 years interval) was thus obtained as shown in the next paragraph.

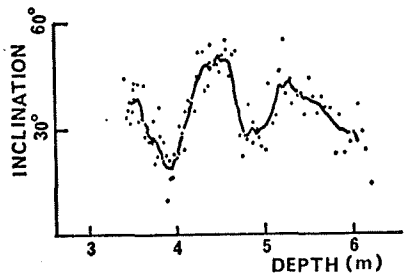

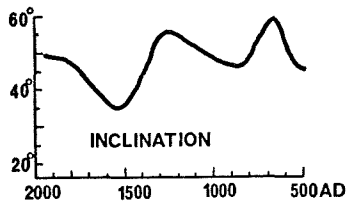

Fig. 1 Change of inclination (Lake Biwa).

Fig. 2 Change of inclination (Southwest Japan; after Hirooka, 1972).

Secular variation in the historic time

In the uppermost part of the boring core is preserved the record of geomagnetic variation from recent back to the historic or even more antique past. Change in the inclination, declination, and intensity of the field have all been obtained.

In Fig. 1 are shown the obtained data on the inclination of NRM arranged on a scale showing

increasing depth of the core. The sediments of the uppermost 3 m were lacking in the core pipe. This may have arisen either from the compaction of oozy upper mud or from the extrusion of it out of the pipe. Actual geomagnetic record starts, therefore, from 3 m as assigned by Horie (1972). Fig. 2 is placed below Fig.1. In the former is shown the change of inclination with age obtained from the archaeomagnetic studies in Southwest Japan (Kawai et al., 1965; Hirooka, 1971). It is evident that the two curves up and down resemble with each other so conspicuously that the dating of the boring core is directly available when maxima and minima are assumed to coincide in the two curves.

Similar adjustment of the age is possible in the case of declination as shown in both Figs.3 and 4. Adjustment of age was thus carried out in two ways, one using declination change, and the other inclination change. Despite of the independence, two shows striking coincidence. Accordingly it was possible to determine the rate of recent deposition which changed from time to time in the historic time. Results of the estimation are shown in Table 1. The variation in the declination and that in the inclination are traceable back to the prehistoric time as shown later.

Next, in Fig. 5 intensity of NRM is plotted against the depth. As we are going down along the core axis we fined that the intensity inceases and reach the first peak at the depth of 4.5 m. This is then followed by the first valley and second peak at 5.3 and 5.9 m respectively. The decreasing intensity through the second peak unfortunately encounters a gap of measurement which continues from a depth of 6.2 m to that of 7.0 m. During sampling in the lake a part of the core at the pipe end was lost. The sediments in the vicinity of the end extruded from the pipe whilst the later was being tugged up to the lake surface and fell down in water. So far we have four main archaeomagnetic intensity data including the new one from Lake Biwa. They are shown in Fig. 5 for the sake of

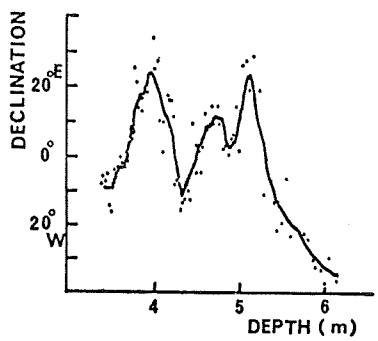

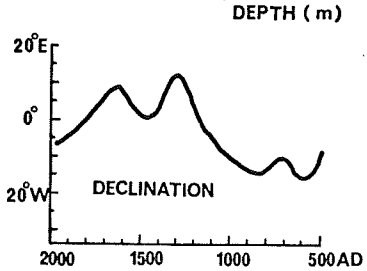

Fig. 3 Change of declination (Lake Biwa).

Fig. 4 Change of declination (Southwest Japan; after Hirooka, 1972).

Table 1

Depth (m)	Age (yrBP)		Rate of Deposition (mm/year)
3.4	0		
			1.25
3.9	400	(I_{min}, D_{max})	
			2.00
4.2	550	(D_{min})	
			2.00
4.5	700	(I_{max})	
			2.00
4.6	750	(D_{max})	
			1.14
5.0	1100	(I_{min})	
			1.50
5.3	1300	(I_{max})	
		mean	1.65

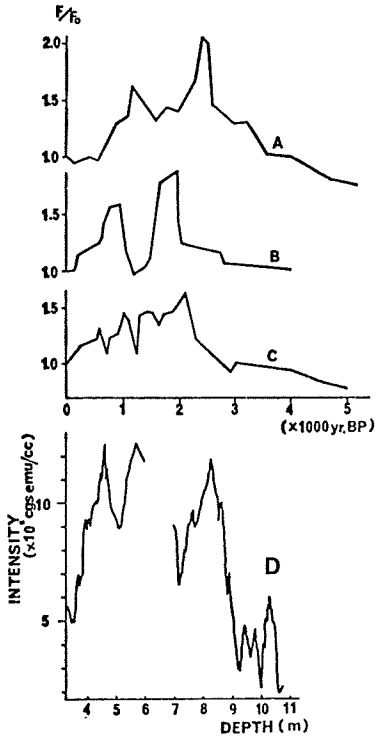

Fig. 5 Change of intensity. A,B,C; Data summerized by Bucha (1971) from Czechoslovakia, America, and Japan, respectively. D; Present study.

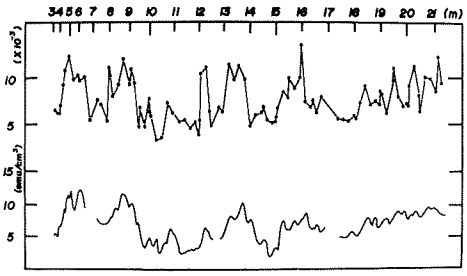

Fig. 6 Ratio of intensity of NRM to that of I_sRM. Lower curve shows the change of intensity of NRM.

comparison. Similar fluctuation can be seen in the four curves, each showing local geomagnetic field changes.

Recently a report appear on the acquisition of DRM by one ocean sediments (Kent, 1973). A proportionality of the intensity of NRM to the applied field was very well established by his experiments. Intensity value devided by that of the saturation remanence, that is, I(NRM)/I(I_sRM) was determined in each specimen of our lake sediments. They are shown in Fig. 6, together with the change of NRM itself. No remarkable discrepancy came out from the comparison, suggesting that the concentration of ferromagnetic particles seems to be uniform and reasonably same everywhere in the strata examined so far. The lake sediments may, therefore, be regarded as magnetometer with which to measure approximately the past field effectively.

The intensity was about 2.0 and 2.3 times greater at the first peak and the second peak respectively in comparison to the present one. Even the field intensity at the first valley was greater than the present one by 25 %. The geomagnetic dipole field continued to drop since the time of Gauss's first harmonic analysis. Recent data show that the rate became increased approaching to 6%/130 years. When mean rate of the decrease was estimated from the lake sediments, it turned out to be more than 5%/100 years or so. The nearly straight line will come across with zero line not in the remote future but within only 1,000 years posterior to the present. McDonald and Gunst (1968) emphasized the same importance on a basis of their harmonic analysis.

Prehistoric secular variation

No accurate scaling of age but depth is available since we have no standard based on the results of the archaeomagnetism in the prehistoric secular variation . Furthermore the geomagnetic record met unfortunately

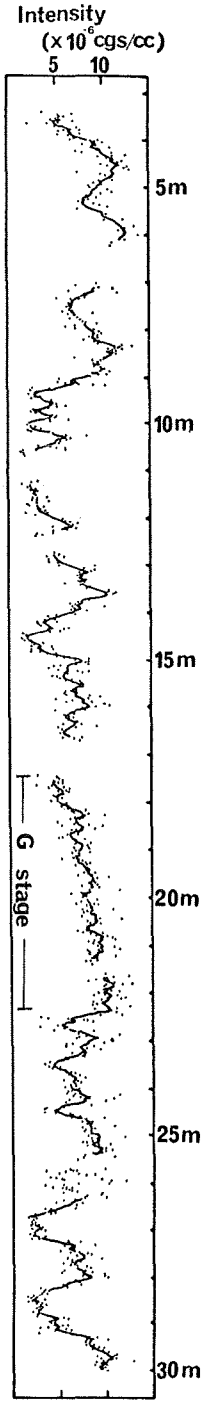

Fig. 7 Change of intensity.

six gaps of measurements. Each occurred as the results of unavoidable extrusions of sediments from the pipe end at the time of the renewing sampling pipe in the lake. Although the inclination change can be inferred relative to the vertical axis of the core, the declination change can not be joined up well in case the gap length was relatively long. So, the informations regarding the variation is restricted to both intensity and inclination change.

First the intensity change is dealt with as follows. The change in a long prehistoric span of time is shown up in Fig. 7. It covers the stage from approximate age of 60,000 years to 6,000 years ago according to the depth vs age estimation carried out by Yaskawa (1973). In the data the existing fluctuation is large enough to surprise us. The largest intensity is about six times greater than the smallest. Nearly same value of intensity continued for a short duration and then rapidly followed by the different value of the intensity from time to time. When mean was, therefore, taken for a desired length of time separately and successively, the span can be devided into at least more than three sub-groups. In one of them the mean is highest and remains in the range from 11 to 13×10^{-6} cgs emu/cc. In the second one it is weakest and remains in the range from 2 to 3×10^{-6} cgs emu/cc, whereas in the last one in a range from 6 to 8×10^{-6} cgs emu/cc respectively.

In the stage we call G in Fig. 7, however, a gradual shift of intensity appears from depth of 17.4 m to that of 22.4 m. It becomes greater from 5 to 12×10^{-6} cgs emu/cc with increasing depth accompaning very small fluctuation. In other part of time span the change take place rapidly stepwise. From one level in one short stage to the other level in the other stage it jumps up and down swiftly.

Next, the change of inclination we obtained is shown up in Fig. 8. The value varies with amplitude which is nearly same as that of archaeomagnetic variation, exept six moments as shown by A,B,C,D,E, and F on the figure. Values of inclination at A, B, D, E, and F are extremely low or negative. In contrast, that at C is quite high. The direction of the field was evidently abnormal at each time. Nakajima et al. (1973) reported a short period abnormal direction at A (18,000 yrBP) and assigned it as an excursion. Barbetti and McElhinny (1972) reported also that an excursion existed at about 30,000 yrBP. Despite that the

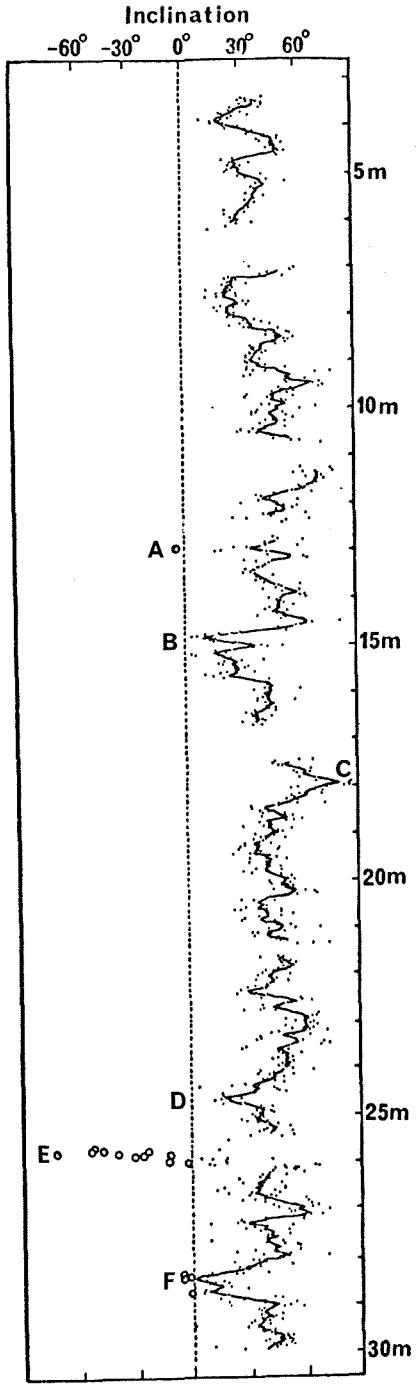

Fig. 8 Change of inclination.

path of virtual pole movement in one excursion resembles to that of the other, these two are different in age of the appearance. Present data of almost continuous geomagnetic record indicate that Barbetti's excursion may correspond to that of B moment.

Negative values of inclination appear also at E and F moments as well as A. Such relation between the intensity and inclination during these moments as follows seems important to be further studied. Intensity is extremely low at F, while it was changing (or) oscillating from low to high in the E moment.

References

Barbetti, M. and M. McElhinny (1972) Nature 239, 327.

Bucha, V. (1971) in Dating Techniques for the Archaeologist edited by H. N. Michael and E. K. Ralph (MIT Press).

Hirooka, K. (1971) Mem. Fac. Sci. Kyoto Univ. Ser. Geol. Mineral., 38, 167.

Horie, S. (1972) Palaeolimnology of Lake Biwa and the Japanese Pleistocene.

Horie, S., O. Mitamura, S. Kanari, H. Miyake, A. Yamamoto,and N. Fuji (1971) Disaster Prev. Res. Inst. Univ. Kyoto Annuals 14, 745.

Kawai, N., K. Yaskawa, T. Nakajima, M. Torii, and S. Horie (1972) Proc. Japan Acad. 48, 186.

Kawai, N., K. Hirooka, S. Sasajima, K. Yaskawa, H. Ito and S. Kume (1965) Ann. Geophys. 21, 574.

Kent, D. V. (1973) Nature 246, 32.

Nakajima, T., K. Yaskawa, N. Natsuhara, N. Kawai, and S. Horie (1973) Nature Physical Science 244, 8.

McDonald, K. L. and R. H. Gunst (1968) J. Geophys. Res. 73, 2057.

The Research Group for Palaeomagnetism of Lake Deposits (1973) J. Geomag. Geoelectr. 25 (in press).

Yaskawa, K. (1973) Sed. Geol. (in press).

RATE OF SEDIMENTATION FOR YOUNG LOOSE SEDIMENT

For the palaeomagnetic investigation of the core from the deep sea or the lake bottom

Katsumi YASKAWA

Department of Physics, Faculty of Engineering Science, Osaka University, Osaka, Japan

1. Introduction

The rate of sedimentation is usually expressed in terms of the thickness of sediment accumulated per unit time. In order to give the rate of sedimentation as a velocity, it is sufficient to estimate the age at two known depth levels in a sediment, because the thickness of the sediment can be regarded as a linear function of time, when the depth levels under consideration lie deep enough to compact the sediment to a final density. At the upper part of the sediment, however, the compaction is still going on, and the thickness cannot be regarded as a linear function of time. The above-mentioned definition of the rate of sedimentation is no longer appropriate to such a young soft sediment. In order to make it of effect irrespective of the age of sediment, old or young, it is necessary to express the rate of sedimentation with the mass of dry sediment accumulated on a unit area for a unit time. This definition seems to be correct when the sediment is composed of inorganic matter, but it does not seem to be also right in the case when the sediment is mainly composed of organic substances such as pollen, remains of plankton etc.. The reason why the dry sediment is employed is because its mass can be regarded to be free from the padding effect due to the volume of the pore-spaces in the sediment. Therefore, it is not allowed for each component of the sediment to lose water of itself when the sediment is heated and dried up. This is rather difficult to be done.

The rate of sedimentation should be defined as a differential coefficient of depth with respect to time. It is clear from this definition that, if proper relation is obtained between a depth level of a certain sediment and its time of deposition, the rate of sedimentation can easily be determined at any depth level in the sediment. Thus, the thickness (the depth from the bottom) of a sediment is first discussed and formulated in this paper as a function of time under the assumption that the material of the sediment has been supplied homogeneously over a great extent of area and continuously for a long period.

As an example to apply this consideration to an actual case, the sediments of Lake Biwa are taken. Although there are thin layers of volcanic ashes in the sediments of the lake, as a whole, the material of the sediment in the deep region of this lake is so uniform and appears to have been deposited so continuously, that the formula seems to be available to

provide the depth-age relation for the sediments of the lake and give the correct rate of sedimentation at any depth level.

2. Compaction of sediment in the gravity field

Let us consider a cylinder with fully hydrous mud of a volume V_0 in it, and a piston made of a kind of filter, through which only water can pass, on it. If we place a weight on the top of the piston to push it down with a constant pressure P for a long period, the piston will gradually decend until the ratio of water to solid material in the mud reaches a certain value. The equilibrium volume V decreases as the weight on the piston increases towards a final volume V_m. The relation between the volume and the weight can be expressed by the equation

$$(V-V_m)/(V_0-V_m)=\exp(-AP), \qquad (1)$$

where A is an arbitrary constant to be experimentally determined.

Now let us consider the volume of mud deposited in the water. Let ΔH be the thickness of the mud supplied on the bottom per annum, and for n years the thickness becomes

$$H=n\cdot\Delta H$$

without compaction. However, as the water is gradually squeezed out, the actual thickness h will be less than H with compaction:

$$h=\sum_{i=0}^{n}\Delta h_i < n\cdot\Delta H=H$$

$$\Delta h_0=\Delta H.$$

Supposing a vertical column with unit area in the mud of thickness h, we can obtain the volume supplied in the i-th year from the equation (1):

$$(\Delta h_i-\Delta h_m)/(\Delta H-\Delta h_m)=\exp(-AP_i), \qquad (2)$$

where Δh_m and P_i are the minimum volume of ΔH and load pressure on Δh_i respectively. Therefore, the actual total volume of this column for n years can be expressed as

$$h=\sum_{i=0}^{n}\Delta h_i=\sum_{i=0}^{n}(\Delta h_m+(\Delta H-\Delta h_m)\exp(-AP_i)). \qquad (3)$$

Putting D_0 the apparent density of the supplied hydrous mud before compaction, g the gravity, S and G the ratios of the minimum volume Δh_m and of the volume of the solid material in the hydrous mud to the original volume ΔH, m the mass of the solid material supplied for a year, the density of which is D, m_w the mass of the water in the hydrous mud supplied for a year and D_w the density of the water, we have

$$D_0=(m+m_w)/\Delta H=(G\cdot\Delta H\cdot D+(\Delta H-G\cdot\Delta H)D_w)/\Delta H=GD+(1-G)D_w. \qquad (4)$$

Therefore, if we accept $D_w=1$ as the density of water,

$$G=(D_0-D_w)/(D-D_w)=(D_0-1)/(D-1). \qquad (5)$$

On the other hand, as the load pressure P_i on Δh_i is expressed as follows:

$$P_i=(m-D_w m/D)i\cdot g=G\cdot\Delta H(D-D_w)i\cdot g$$

and using G of (5),

$$P_i=(D_O-D_W)ig\Delta H=(D_O-1)ig\Delta H, \qquad (6)$$

equation (3) becomes

$$h=nS\cdot\Delta H+(1-S)\Delta H\sum_{i=0}^{n}\exp(-A(D_O-1)\Delta Hig). \qquad (7)$$

Letting n tend to infinity and putting

$$x=\lim_{n\to\infty}\Delta H\cdot i=\lim_{n\to\infty}(H/n)i \quad \text{and}$$

$$dx=\lim_{n\to\infty}\Delta H=\lim_{n\to\infty}(H/n)$$

lead the equation to

$$h=SH+(1-S)\int_0^H\exp(-A(D_O-1)gx)dx$$

$$=H+(1-S)\left[-\exp(-A(D_O-1)gx)/(A(D_O-1)g)\right]_0^H$$

$$=H+(1-S)(1-\exp(-A(D_O-1)gH))/(A(D_O-1)g). \qquad (8)$$

In general, it can hardly be expected that the total mass of the hydrous mud supplied for a year and/or the original density have been constant for many years. They ought to be functions of time. In the case, however, that homogeneous material of sediment is continuously supplied with a constant rate, we can regard them to be constant, and from (4), that is,

$$D_O=(m+(\Delta H-m/D)D_W)/H$$

we get

$$\Delta H=m(1-D_W/D)/(D_O-D_W)=m(1-1/D)/(D_O-1), \qquad (9)$$

and

$$H=m(1-1/D)t/(D_O-1).$$

Substituting this H into the equation (8), we finally obtain the following equation:

$$h=Sm(1-1/D)t/(D_O-1)+(1-D)(1-\exp(-Am(1-1/D)gt))/(A(D_O-1)g). \qquad (10)$$

3. An application of the equation

Recently S. Horie of Kyoto University succeeded in obtaining successive core samples with length of about 200 m in the deep region of Lake Biwa. This core has four definite levels dated either radiometrically or palaeomagnetically as shown in Table 1, giving four number pairs of h and t to the equation (10).

Table 1

Depth (m)	Age (yr)	Method
0.8 ± 0.05	1,430 ± 95	Radio carbon
4.5 ± 0.15	3,650 ± 105	Radio carbon
11.5 ± 0.20	14,980 ± 460	Radio carbon
52	111,000	Magnetic

If we connect these data points with a smooth line, we will get a curve which does not run through the origin of the depth and age cordinates. From the equation (10), however, the function h(t) is zero at t=0 and its second derivative is always negative as long as t is positive, that is,

$$d^2h/dt^2=-Am^2g(1-S)(1-1/D)^2\exp(-Am(1-1/D)gt)/(D_o-1),$$

because $A>0$, $S<1$, $D>1$ and $D_o>1$. In other wards, the curve of the function is concave towards the time axis through the origin. Therefore, it is obvious that these depth-age data cannot satisfy the relation (10) without transforming h-axis to the right by t_o parallel to the t-axis. The reason why we must introduce t_o as initial time is probably as follows: The uppermost layer of the sediments corresponding to t_o was too soft and unstable to collect it by a core sampler or, in the extreme case, it was still in the state of hydrous mud, so that it might have flown out from the core sampler. Using these four number pairs, we can in principle determine t_o and the three coefficients of the equation (10) as follows:

$$h=0.0426(t-1090)+561.8(1-\exp(-0.000365(t-1090))), \quad (11)$$

where h is measured in centimeter and t in year. By comparing the coefficients of the equation (10) to those of the equation (11), we obtain the following values:

$$\left.\begin{aligned} &S=0.172 \\ &Ag(D_o-1)=0.00147 \\ &m(1-1/D)/(D_o-1)=0.248. \end{aligned}\right\} \quad (12)$$

On the other hand, at the depth level deep enough for h to be regarded as a linear function of t, the bulk density D_b of the sediments can be expressed as follows,

$$D_b=(m+m_w)/\Delta h_m=(vD+(\Delta h_m-v)D_w)/\Delta h_m,$$

where m and m_w are the mass of solid material and water in the volume Δh_m, D and D_w are the density of them and v is the volume of the solid material included in Δh_m. Considering that $\Delta h_m=S\Delta H$ and $v=G\Delta H$,

$$D_b=(G\Delta HD+(S\Delta H-G\Delta H)D_w)/S\Delta H=(G(D-D_w)+SD_w)/S.$$

Taking $D_w=1$ as the density of water and using relation (5) i.e.

$$G=(D_o-1)/(D-1),$$

we obtain

$$D_b=(D_o-1)/S + 1$$

or $$D_o=S(D_b-1) + 1 \quad (13)$$

Let the bulk density of the sufficiently compressed sediments be about 1.9 and the mean density of the solid material of the sediments be about 2.6, then using (12) and (13), we can determine D_o, A and m (the rate of sedimentation expressed in terms of the mass):

$$\left.\begin{aligned} &D_o=1.155 \\ &A=0.00951/g\fallingdotseq 9.70\ 10^{-6} \\ &m=0.0623\ (gr/cm^2/yr). \end{aligned}\right\} \quad (14)$$

Toyoda et al. (1968) measured the mass of deposits in the deep region of the lake, every month in 1963 and 1964, using so-called sediment traps. The result of these measurements shows that the rate of sedimentation reaches its maximum value,

i.e. 3 to 6 ($gr/m^2/day$) or 0.1 to 0.2 ($gr/cm^2/yr$), in April and May, and its minimum, i.e. 0.1 ($gr/m^2/day$) or 0.004 (gr/cm2/yr), in winter. The value m=0.0623 ($gr/cm^2/yr$) of (14) is just between their maximum and minimum, and indicates in good agreement with the approximate mean value of their result.

4. Discussions

As mentioned already, the rate of sedimentation should be grasped as the differential coefficient of the depth h from the bottom surface with respect to the time t of deposition. In case of the old compact part of sediment, this differential coefficient is regarded as a constant irrelevant to depth or time, but in case of the young loose part of the sediment the coefficient cannot be constant and varies its value with the change of depth or time. This is quite inconvenient in practice when we want to compare the rate of sedimentation at different places. To compare the rate of sedimentation satisfactorily at different places, the author would like to propose to introduce a concept of the converted rate of sedimentation d_∞ defined as follows:

$$d_\infty=(dh/dt)_{t=\infty}=Sm(1-1/D)/(D_0-1).$$

The value of this converted rate of sedimentation at the deep region of Lake Biwa is calculated as $d_\infty=0.0426$ (cm/yr). Using d_∞, we can easily compare the velocity of accumulation of deposits at any place in any condition, regardless of age and depth, young and loose or old and compact.

Recently the core samples from 10 to 15 m long have become to be collected from the deep sea bottom and discussed about their rate of sedimentation, which has usually been treated as a constant to the depth from the bottom. The rate of sedimentation, however, cannot be treated as a constant down to at least 12m from the bottom, inferred from the case of Lake Biwa as will be seen from the equation (11).

Reference

Toyoda, Y., S. Horie and Y. Saijo (1968) Mitt. Internat. Verein. Limnol. 14, 243.

REVERSALS IN BRUNHES NORMAL POLARITY EPOCH

Katsumi YASKAWA

Department of Physics, Faculty of Engineering Science,
Osaka University, Toyonaka

A continuous series of specimens was taken from the core 200 m long of the deep-sediments of Lake Biwa for palaeomagnetic investigation. The core is composed chiefly of gyttja and fine clay which are quite homogeneous, showing continuous and gradual deposition in the deepest region of the lake. The rate of sedimentation is considered to be 42.6 cm/1,000 yrs from the age estimation. This value is several hundred times greater than that of the sediments in the deep-sea bottom. Therefore, the palaeomagnetic investigation of the core will give us much more precise and detailed feature of the time-variation of the past geomagnetic field than that of deep-sea core does.

The sediments of the lake have been dated by radio carbon method at three depth levels (Horie et al., 1971) at the same place where this core was taken, i.e. 1,430, 3,650 and 14,980 yr B.P. at 0.8, 4.5 and 11.5 m from the bottom surface respectively. Based mainly on these three pairs of data, the following depth-age relation was proposed for this core (Yaskawa, in preparation):

$$h=0.0426(t-1090)+561.8(1-\exp(-0.000365(t-1090))),$$

where h is the depth from the lake bottom (cm) and t is the age (yr). Recently Nishimura and Yokoyama (1973) got new depth-age data by fission track method using zircon in the volcanic ash layers of the core, i.e. the ages at the depth levels of 38, 63 and 100 m are 80,000, 110,000 and 180,000 yr B.P. respectively. These depth-age data are a little younger than the age calculated by the relation but not so different.

Just before the specimens were sampled, the core was cut through its central axis and divided into two semicircular columns. Then plastic cases of about 2 cm cube with one side open were pushed into the core along its axis seriatim in such a way that a plane opposed to the open side of each cubic case was kept parallel to the plane of the semicircular column and other two opposed planes of the case were perpendicular to the core axis. The specimens in these cases were oriented and numbered before being taken out from the core.

The measurement of natural remanent magnetization (NRM) was made by an astatic magnetometer. Before the measurement of all the specimens the stability of NRM was checked by means of the progressive alternating field demagnetization method for several tens of the specimens picked up by random

sampling from the whole. As the result of this demagnetization, it has been made clear that, although some of them have such unstable component of remanence as can be erased by demagnetization up to 100 Oe, the stability of the remanence is considerably high, that is, half of the original intensity remained even after the demagnetization of 400 Oe of peak alternating field and no remarkable change of the direction was observed up to 600 Oe. Thus, the remanence after demagnetized at 100 Oe alternating field can be regarded as the fossil magnetism acquired at the time of deposition or a little later.

Before the measurement of the whole series of specimens, a preliminary survey was made at intervals of 5m down the core with an astatic magnetometer (Kawai et al., 1972). The result showed that there may have been at least three short reversed events during the Brunhes normal polarity epoch. If the depth-age relation mentioned above is accepted, the ages for these reversals can be determined as tabulated in Table 1. On the other hand, the curve of inclination as a function of depth is well correlated to that of some deep sea core (Ninkovich et al., 1966 and Wollin et al., 1971) which has the time scale given on the basis of the age at Brunhes-Matuyama boundary, showing good agreement with the values in the Table.

Table 1

Depth (m)			Age (yr B.P.)		
From 50.0	to	55.0	from	104,000	to 117,000
80.5		85.0		176,000	186,000
130.0		132.5		292,000	298,000

The palaeomagnetic measurement of the whole series of specimens, covering 30 m of the upper part of the core was finished and all the details of the results have been reported by the research group for plaeomagnetism of lake deposits (1973). One of the most important results is that there may have been excursions of geomagnetic pole twice for the time range covering these 30 m of the core, i.e. at about 13 m (Nakajima et al., 1973) and at about 26 m deep. The ages for these excursions are estimated at about 18,000 and 49,000 yr B.P., using the above-mentioned depth-age relation.

To reconstruct the ancient pole position, it is necessary to get the declination as well as the inclination of geomagnetic field at the time, but, since the core was divided into more than 160 pieces, it is difficult to trace back the variation of declination beyond the boundary between each core piece. Fortunately the specimens taken from the lower half of the core pieces Nos B21 and B55, in which the excursions were found, have almost the same direction of magnetization. Assuming their mean azimuth of magnetization zero

(north direction), the declinations of the rest specimens of these core pieces were determined relative to it. Using these pairs of declination and inclination, the pole-paths during these excursions were obtained.

Recently Barbetti and McElhinny (1972) reported the palaeomagnetic results of Australian ancient fire-places, and showed the change of geomagnetic field direction at about 30,000 yr B.P.. It is remarkable that the pole-path calculated from their results is quite similar to those of the excursions observed in the core from the lake. Unfortunately both ages of Japanese excursion, however, are different from that of Australian excursion. The age of Australian excursion is reported to be about 30,000 yr B.P. by radio carbon dating, and is just between Japanese two excursions whose ages were estimated at 18,000 and 49,000 yr B.P. as mentioned already.

As can be clearly seen in the Table, there existed three short reversal polarity events in the Brunhes normal epoch at intervals of about 90,000 to 100,000 yrs.

The pattern of inclination change or intensity change around the first excursion is similar to that around the second excursion. This may show the existence of a periodic variation of geomagnetic field at intervals of about 30,000 yrs.

The age of the bottom depth of the results reported (30 m) by the research group for palaeomagnetism of lake deposits (1973) can be estimated at about 60,000 yr B.P.. Therefore, it is clear that there is no reversals worthy to call polarity event like so-called "Laschamp" or "Gothengurg" at least for these 60,000 yrs.

References

Barbetti, M. and M. McElhinny (1972) Nature 239, 327.
Horie, S., O. Mitamura, S. Kanari, H. Miyake, A. Yamamoto and N. Fuji (1971) Disaster Prev. Res. Inst. Univ. Kyoto Annuals 14, 745.
Kawai, N., K. Yaskawa, T. Nakajima, M. Torii and S. Horie (1972) Proc. Japan Acad. 48, 186.
Nakajima, T., K. Yaskawa, N. Natsuhara, N. Kawai and S. Horie (1973) Nature Phys. Sci. 244, 8.
Ninkovich, D., N. Opdyke, B. C. Heezen and J. H. Foster (1966) Earth Planet. Sci. Letters 1, 476.
Nishimura, S. and T. Yokoyama (1973) Proc. Japan Acad. 49, 615.
The Research Group for Palaeomagnetism of Lake Deposits (1973) J. Geomag. Geoelectr. 25, in press.
Wollin, G., D. B. Ericson, W. B. F. Ryan and J. H. Foster (1971) Earth Planet. Sci. Letters 12, 175.

POSSIBLE BLAKE EVENT AS REVEALED IN A PYROCLASTIC FLOW OCURRING IN SOUTHERN KYUSHU, JAPAN

Sadao SASAJIMA

Department of Geology and Mineralogy, University of Kyoto

1. Introduction

There are several number of famous calderas in Kyushu, of which the largest one is thought to be the Aira caldera having a central cone, the Sakurajima active volcano. A palaeomagnetic investigation of some pyroclastic and lava flows around the caldera has been carried out with special stress on its volcanotectonics. The volcanostratigraphy in this area is fairly well established by several Japanese geologists. A map showing sampling area is illustrated in Figure 1.

During the couse of studies, it has been found that the reversed NRM of the Inuzako pyroclastic flow (abbr. PF. hereafter) intercalated in the upper part of sequence could be correlated with the Blake event of the Brunhes Normal Epoch. Unfortunately the Blake event has not yet been confirmed with any continental rocks because of its very short duration, though little doubt is cast about the real existence of the Blake event; several scientists have succeeded in confirming the event in their magnetostratigraphic results of cores (Wollin et al, 1971; Eardley et al, 1972; Kawai et al, 1972), since the pioneer work by Smith and Foster (1969).

2. Palaeomagnetic Result

Samples were partially demagnetized in a peak field of 160 -200 Oe to remove unstable components, and an example of a.f. demagnetization is shown in Figure 2. As seen in this diagram the original divergent direction of NRMs of the Inuzako PF. is significantly improved in grouping after a partial demagnetization. Palaeomagnetic data obtained are summarized in Table 1 and Figs. 3,4.

In this table volcanic strata of sampling sites are arranged by the author referring to the studies reported by Aramaki (1969), Ôki et al. (1970) and Tsuyuki et al. (1970) with descending order from the younger to the older. The uppermost two pyroclastic flows, the Ito and Tsumaya, have been dated with ^{14}C- method as 23,000± yrs. B.P. in good precision (Kigoshi et al.,

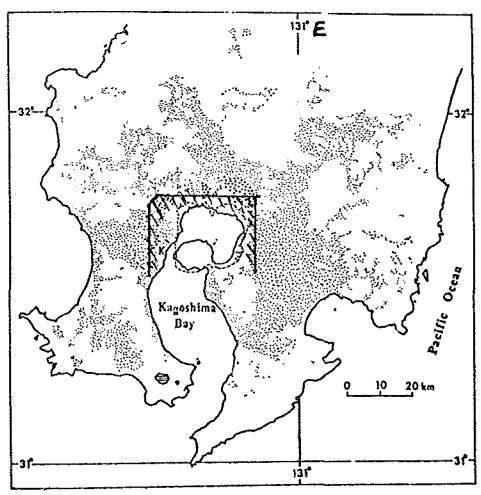

Fig. 1. Map showing the sampling area. broken line shows outline of Aira caldera, and dotted area, of distribution of Ito PF. K: Kagoshima City.

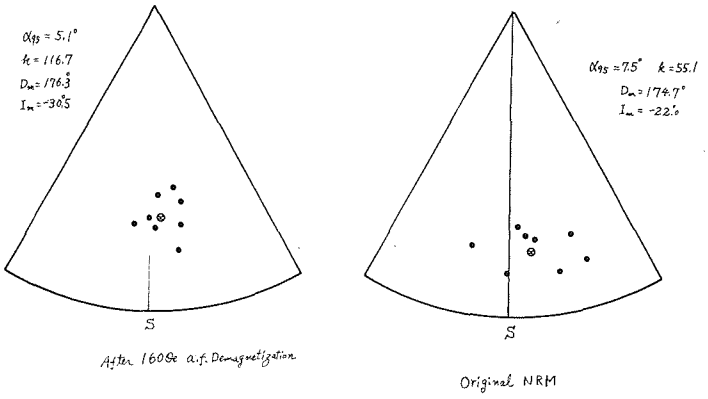

Fig. 2. Change of grouping of NRMs after a.f. demagnetization of 160 Oe. (Inuzako PF.).

Table 1.

Site	Strata	No.	D_m	I_m	$\alpha 95$	k	V.G.P. φ	V.G.P. λ	dp	dm	Jn emu/g
9	Itô PF.	6	8.7°	52.8°	3.3°	538	82.4°	214.7°	3.2°	4.6°	1.1×10^{-3}
8	Tsumaya PF.	6	7.6	45.4	11.2	37	82.3	247.4	8.9	14.0	7.7×10^{-5}
3	Chikuri PF.	7	346.0	40.3	9.7	40	75.3	12.1	7.0	9.9	1.9×10^{-3}
2	Hyôkiyama PF.	5	344.9	35.1	5.5	192	72.3	4.6	3.6	6.3	9.4×10^{-4}
7	Iwato PF.	7	4.8	45.5	6.4	89	84.3	262.0	51.	8.1	6.0×10^{-4}
11	Shikine And.	8	40.3	53.2	6.2	81	56.0	204.4	5.9	8.6	3.0×10^{-4}
4	Shinkawa PF.	6	347.7	42.1	7.5	81	77.4	13.2	5.6	9.2	3.7×10^{-3}
12	Inuzako PF.	8	176.3	-30.5	5.1	117	75.3	324.1	3.2	5.7	2.1×10^{-4}
5	Shimokado PF.	7	352.8	46.5	4.3	194	82.3	20.8	3.5	5.5	1.2×10^{-3}
10	Yoshino WT.	8	9.7	49.2	4.9	127	81.5	226.1	4.3	6.5	1.3×10^{-3}
6	Goino PF.	5	359.7	33.8	6.2	154	77.9	310.2	4.0	7.1	9.1×10^{-4}
1	Umegaya And.	5	335.7	43.5	3.2	615	66.0	19.6	2.5	4.0	2.2×10^{-4}
13	Obama WT.	9	204.0	-18.9	4.0	161	58.9	257.4	2.2	4.2	5.6×10^{-4}
	* Mean values		357.2	42.3	6.0	65	83.4	333.0	4.5	7.0	

PF.: Pyroclastic flow, And.: Andesite, WT,: Welded tuff
Site numbers are the same as for Figures 3 and 4.
* : being excluded Shikine And. with anomalous direction and the lowest two strata which are far older than the above members.

1972). According to the age determination made by Nishimura and Miyachi (1973) by the use of fission-track technique, the Shinkawa PF. and the lower member of Kakuto PF. have been dated 72,000 and 110,000 yrs. B.P. respectively. And the Shimokado PF. is correlated stratigraphically with the horizon lying beneath the lower member of the Kakuto PF. mentioned above, therefore, it is most likely that the Inuzako PF. was formed at any time between 72,000 yrs. and a little older time than 110,000 yrs. B.P. Accordingly it may be reasonable to suppose that the reversed NRM of Inuzako PF. represents the Blake event.

The age of the Blake event has been estimated first by Smith and Foster (1969) to span 108,000-114,000 yrs. B.P., while slightly different intervals, 104,000-117,000 yrs. B.P., have been given more recently by Kawai et al. (1972) from bottom sediments cores of the lake of Biwa, in central Japan. However, the Blake event has not yet been evidenced by any continental rocks perhaps because of its very short duration.

The distribution of Inuzako PF. deposits is rather limited in its area on the northwestern part of Kagoshima city (Ôki et al.,1970). They belong to a single cooling unit composed of non-welded and welded cycle, though they have maximum thickness of 40m. Their origin is subaerial but they occur unconformably between two different marine sedimentary layers, therefore, we can not unfortunately trace the time continuously before and after their formation.

The virtual pole positions (VGP) for all directions of NRMs and for the mean direction of the younger ten layers are shown altogether in Fig. 4. It should be noted in the figure that the distribution range of VGPs for the younger layers is quite similar to that of the archaeosecular variation for the past 2,000 years obtained from Southwest Japan (Hirooka, 1971), and that the mean VGP for the younger layers is situated in the position somewhat distant from the geomagnetic north pole than the north pole.

We can not say so much about the geomagnetism which was maintained during the Blake event only from the time spot datum of Inuzako PF., but it may be safe to say that the dipole axis was not so much inclined during the times, if any, as compared with its obliqueness at present.

On the other hand, magneto-mineralogical investigations have been performed in association with the problem of self-reversal. Thermomagnetic and X-ray crystallographic analyses, and reflection microscopic observation of constituent ferromagnetic minerals which are responsible for NRM of the rocks have been made in detail. As the result it appears that an appreciable amount

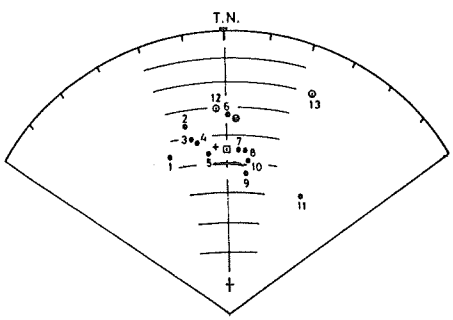

Fig.3. Remanent directions in Schmidt's projection.

⊡ : mean direction of 10 sites.
⊗ : direction; geomagnetic dipole.
+ : present geomagnetic field at Kagoshima city.

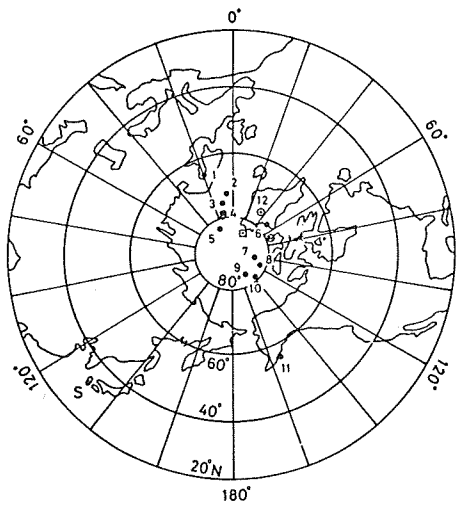

Fig. 4. Distribution map of VGPs. symbols, same as for Fig. 3.

of hemoilmenites with rhombohedral crystallographic structure coexist with the main component, Ti-poor titanomaghemites having spinel structure. Results of measurements are as follows:

Hemoilmenite; Curie point, Tc=70°C, a_{Hex}=5,079 Å, c_{Hex}=13,955 Å
V_{Hex}=311.6 Å^3,
Ti-poor maghemite; Tc=560°C, a=8.355±0.002 Å^3.

The hemoilmenite composition with such a molar volume corresponds to $Ilm._{0.76} \cdot Hem._{0.24}$ after Lindsley (1964), while according to the magnetization versus composition diagram by Ishikawa (1962), hemoilmenite with the curie point, 70°C, corresponds to $Ilm._{0.68} \cdot Hem._{0.32}$. This discrepancy could be explained chiefly by an effective replacement of Mn^{II} into Fe^{II} of the natural hemoilmenite (Buddington and Lindsley, 1964). It seems likely that Ti-poor maghemite characterized by the above-mentioned constants can be specified as a highly oxidized titanomaghemite (O'Reilly and Readman, 1971). It is convinced petrogenetically that such a coexistence of prominently oxidized products is substantiated by the extraordinary hydrous nature of 'nuée ardente'.

Thermal demagnetization experiment to examine change of remanent polarity of the rocks has disproved the possibility due to self-reversal origin: No appreciable change of the remanent direction has been observed with increasing temperature up to 550°C during thermal demagnetization run. Furthermore, af. demagnetization tests of a pilot specimen prior to routine demagnetization treatments also proved to keep constantly the same reverse polarity up to 800 Oe.

From discussions on the result described above, the following conclusions can be drawn. (1) The reversed NRM of Inuzako PF. could not have been caused by the self-reversal properties, but formed under the ambient field of the Blake event. (2) Two coexisting titaniferous ferromagnetic minerals, hemo-ilmenite and titanomaghemite, contained in the Inuzako PF. are recognized without our resistances as oxidation products suggestive of a greatly increased intensity of oxidation, which governed the volcanic magma chamber. (3) It seems likely that the dipole axis of the Blake event was not so much inclined, if any, as compared with the inclination of the present dipole axis.

References

Buddington, A.F. and D.H. Lindsley (1964) J. Petrol. 5, 310.
Hirooka, K. (1971) Mem. Facul. Sci., Kyoto Univ., Ser. Geol. Mineral. 38, 167.
Ishikawa, Y. (1962) J. Phys. Soc. Japan, 17, 1835.
Kawai, N., K. Yaskawa, T. Nakajima, M. Torii and S. Horie (1972) Proc. Japan Acad., 48, 186.
Kigoshi, K., T. Fukuoka and S. Yokoyama (1972) J. Japan. Assoc. Volcanol., 17, 1.
Lindsley, D.H. (1964) Carnegie Inst. Wash. Yearb. 64, 144.
Nishimura, S. and M. Miyachi (1973) J. Mineral. Petrol.& Econ. Geol., 68, 225.
Ôki, K. and S. Hayasaka (1970) Mem. Facul. Sci., Kagoshima Univ., No.3, 67.
O'Reilly, W. and P.W. Readman (1971) Zeitsch. Geophys. 37, 321.
Smith, J.D. and J.H. Foster (1969) Science, 163, 565.
Tsuyuki, T., S. Hayasaka, M. Maeno, K. Oki and Y. Momikura (1970) Mem. Facul. Sci., Kagoshima Univ., No.3, 93.
Wollin, G., D.B. Ericson, W.B.F. Ryan and J.H. Foster (1971) Earth Planet. Sci. Lett., 12, 175.

GEOMAGNETIC REVERSAL RECORDED IN THE LATE PLEISTOCENE SEDIMENTS

Ken-ichi MANABE

Department of Earth Science, Faculty of Education,
Fukushima University, Hamada-cho, Fukushima-shi.

Paleomagnetic studies have been carried out on late Pleistocene sediments, developed along the Pacific coast of Fukushima Prefecture. Five terraces are well developed in the area and they are named by number in ascending order (Nakagawa, 1961).

In this study, approximately 100 oriented samples were collected from the Tsukabara Formation which correlated with the Third Terrace formation by Nakagawa (1961, 1967). The Tsukabara Formation consists of lower gravels, middle silts, and upper sands and gravels at the type locality (37°35'N, 141°02'E). Marine shells and fossil plants have been found in them. From the results of the paleontological and stratigraphical investigations, the Tsukabara Formation has been considered to be deposited in the age of last interglacial (Suzuki and Nakagawa, 1971).

Specimens on which the remanent magnetization was measured were sampled from the middle part of the Tsukabara Formation, with a nearly equal separation of 20 cm (Fig. 1). These specimens were partially demagnetized in an alternating field of 100 Oersted to remove unstable components. Remanent magnetic directions were measured by means of a parastatic magnetometer with three magnets described by Thellier (1967).

The intensity of remanent magnetization after cleaning in alternating field ranges from 10^{-5} to 10^{-7} emu / cc. Magnetic directions and intensities averaged over the 2 to 3 specimens from each horizon are shown in fig. 2.

Three zones of reversed magnetization (A,B and C) were recognized in the middle part of the Tsukabara Formation. The inclination change is associated with a declination change over the same interval

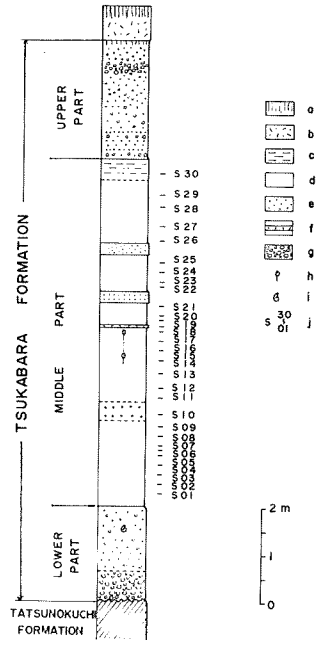

Fig. 1. Stratigraphic column of the Tsukabara Formation at the type locality.
(a. soil, b. loam, c. clay, d. silt, e. sand, f. volcanic ash, g. gravel, h. plant fossil, i. molluscan fossil, j. sampling horizon)

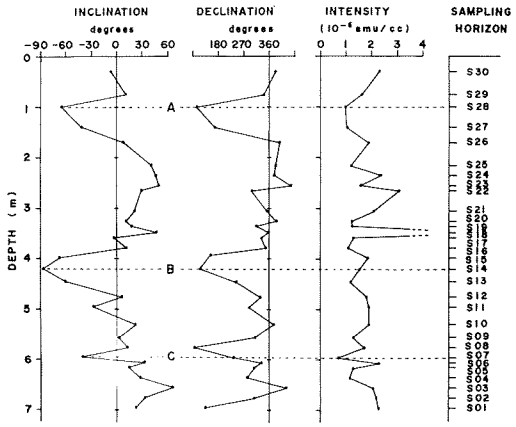

Fig. 2. Summary of paleomagnetic results after cleaning in alternating field of 100 Oersted. Each data point represents an average of measurement on 2 to 3 specimens from one horizon.

except zone C. Therefore the upper two reversals (A and B) are considered to be attributed to geomagnetic reversals. These reversals may be comprised in one reverse event within the Brunhes normal epoch, because of short interval between zone A and zone B.

Although the exact date is uncertain, the geomagnetic reversal recorded in the middle part of the Tsukabara Formation may be correlated with the Blake event as originally found by Smith and Foster (1969) in the North Atlantic deep-sea cores, on the basis of geological and paleontological evidences.

Kukla and Koči (1972) also examined some Pleistocene sediments from Czechoslovakia. They noted evidence for a geomagnetic reversal at the end of the last interglacial stage, and the reversal was correlated with the Blake event.

References

Kukla, G.J. and Koči, A. (1972) Quaternary Research 2, 374.
Nakagawa, H. (1961) Tohoku Univ. Contr. Inst. Geol. Paleont. 54, 61.
Nakagawa, H. (1967) Osaka City Univ. Jour. Geosci. 10, 37.
Smith, J.D. and Foster, J.H. (1969) Science 163, 565.
Suzuki, K. and Nakagawa, H. (1971) Tohoku Univ. Sci. Rep. 42, 187.
Thellier, E. (1967) in: Methods in Palaeomagnetism, ed. Collinson, D.W., Creer, K.M. and Runcorn, S.K. (Elsevier, Amsterdam).

THE OSCILLATION OF FIELD IN THE MATUYAMA GEOMAGNETIC EPOCH AND THE FINE STRUCTURE OF THE GEOMAGNETIC TRANSITION

Naoto KAWAI*, Tadashi NAKAJIMA*, Kimio HIROOKA**, and Kazuo KOBAYASHI***

*) Department of Physics, Faculty of Engineering Science, Osaka University
**) Department of Geology, Faculty of Education, Fukui University
***) Ocean Research Institute, University of Tokyo

I) Introduction

Recently we have tried to evolve a technique to acquire a continuous geomagnetic record with high fidelity and resolution from general sediments ceaselessly formed in water. The feasibility was examined using one boring core of sediments taken from the northern Pacific basin. The trial, despite the first attempt, provide a good piece of informations regarding the Brunhes normal, Matuyama reverse polarity epoch involving the Jaramillo geomagnetic event and excursions.

II) Sample and Micro-astatic magnetometer

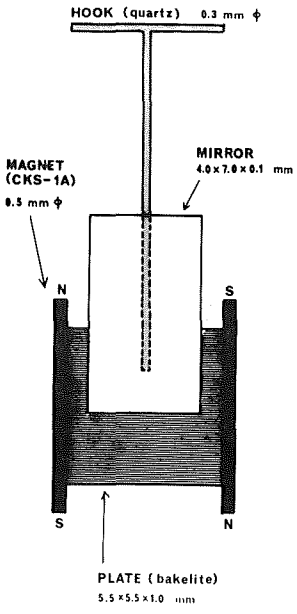

Fig.1 Micro-astatic magnetometer.

From a spot in the north Pacific basin with the longitude 170°05'W and latitude 38°26'N we have obtained a boring core of sediments of the Quaternary and Tertiary periods incessantly piled up presumably at the ocean bottom. The core was acquired by the research vessel Hakuho-maru, cruise KH70-2.

In our laboratory a sensitive micro-astatic magnetometer as shown in Fig.1 was set up to detect the weak magnetic vector preserved in the sediments. Permanent magnets we used is so small as 0.5 and 5 mm in diameter and length respectively that leaking flux out of the free poles can hardly disturb remanence of the specimen which has to be placed close to the magnetometer during measurement. No effect of remagnetization was observed even when the core surface was approached to a distance 3 mm aparted from the poles.

III) Experimental Results

1) Underneath the above-mentioned magnetometer the core column was rotated around the central axis, while the later was kept

vertically. Horizontal component of fossil magnetism recorded in the upper part of the column was, thus, determined from the deflection of the magnetometer.

Next the uppermost piece of the column with thickness of 1 mm was sliced off using a non-magnetic knife of beryllium cupper. The remaining column, after being shifted exactly 1 mm towards the magnetometer, was rotated again around the axis to be farther measured. This simple procedure was repeated more than 2,000 times till the column reduced the height to approximately 2 m from the top. The uppermost section gives the strongest magnetic torque with which the magnetometer can be deflected. The torque arising from the neighbouring section and those lying farther below becomes progressively small as the distance r from the magnetometer increases. The rate of the decrease in the present measurement was confirmed experimentally to be almost proportional to $1/r^3$. Each value in the above-mentioned measurements is still a moving average of the vectors remained in the upper several sections, it bears, however, an extremely heavy weight impressed upon the uppermost one.

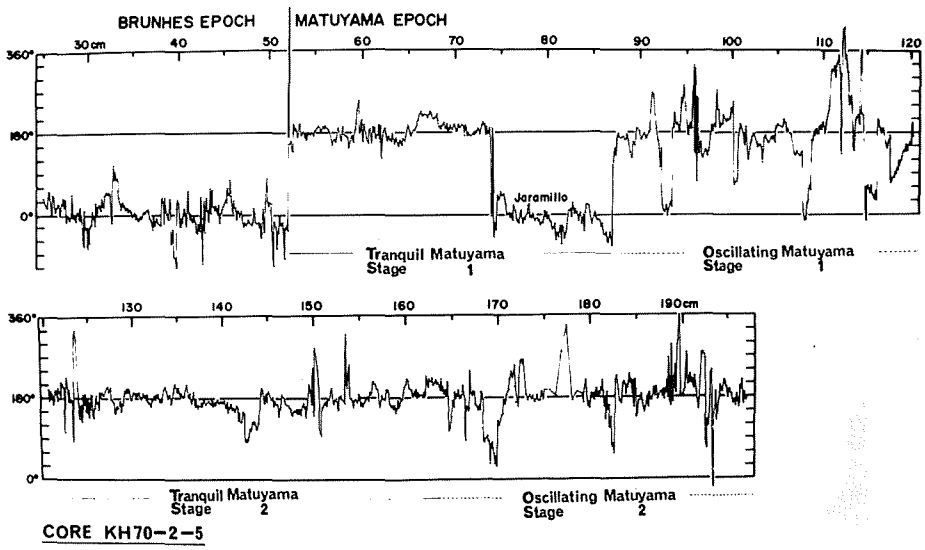

Fig.2 Change of declination with depth of sediments.

According to the estimated rate of sedimentation (Kobayashi et al., 1971; Kobayashi, 1972), each section requires 500 years to be formed in the particular part of the basin. The change of magnetic field with increasing depth from 25 to 197 cm as shown up in Fig.2 can, therefore, be assumed as a continuous geomagnetic variation deciphered from the buried sediments at every 500 year intervals. In the upper column above a depth of 52 cm measured declinations were mostly normal, in the same direction as that of the present field. Almost antiparallel declination,

however, was found to have appeared at least more than 5 times and seems to have persisted for only a short while. Since inclination during the polarity change was not examined as yet, the changes can not be regarded as due to such a frequently recurring excursion of the Brunhes'pole as we confirmed recently from Lake Biwa (Kawai et al., 1972; Nakajima et al., 1973). At the depth of 52 cm a reverse declination appeared suddenly and continued till 74 cm. The curve showing the change at this depth is so steeply rising that the boundary separating normal and reverse declination is found only within 1 mm section of the core, suggesting that the declination change in the transition is more swift and rapid than that have been considered so far. Cox et al.(1967) and Niitsuma (1971) assumed it to take more than 4,000 years in the change.

The first depth was assigned by Kobayashi et al,(1971 and 1972) as the boundary separating the Matuyama from the Brunhes epoch. The second and third ones were assumed as those with which the Jaramillo event could be clearly marked out of the prolonged Matuyama epoch. Radiometric dating of rocks with corresponding polarity shows that these three occurred at 0.69, 0.89 and 0.95 m.y., respectively.

From depths 52 to 87 cm and also from depths 124 to 142 cm the value of declination dose not fluctuate greatly except two swift shifts occurring at the upper and lower Jaramillo transition zone.

The name "Tranquil Matuyama" was used to call these steady geomagnetic fields. On the other hand in the rest stage of the Matuyama epoch the geomagnetic field were so oscillating significantly that the normal field was followed by a reverse field and vice versa alternatively, although the total duration of reversed polarity is much longer than that of normal. "Oscillating Matuyama" is proposed by the present authors for this behaviour of field to be distinguished from the tranquil Matuyama field.

2) Although all boundaries separating one from the other were surveyed in detail, much remains to be further investigated. Among all others the fine structure of each polarity transition is in need of an urgent clarification. A part of the core column that involves the Brunhes-Matuyama boundary was, therefore, pick up first from our storage.

From its upper surface a pipe having square aross section 3.5x3.5 mm was pushed in vertically. The small core thus obtained was then sliced up so that a sequence of plate sections with thickness of 2 mm can be made. The intensity, inclination and declination of the fossil geomagnetism were determined under a micro-astatic magnetometer, rotating each section around the three mutually perpendicular axes fixed to the column. In the vicinity of the boundary one more column was prepared, taking it from the sediments adjacent to the former as shown in Fig.3. The upper plane of each section in the main column and that in the auxiliary column differ from each other exactly 1 mm in height. One can survey the fine structure of the transition, therefore, when these sections were measured in the order of increasing

section number and arranged as shown in Fig.4.

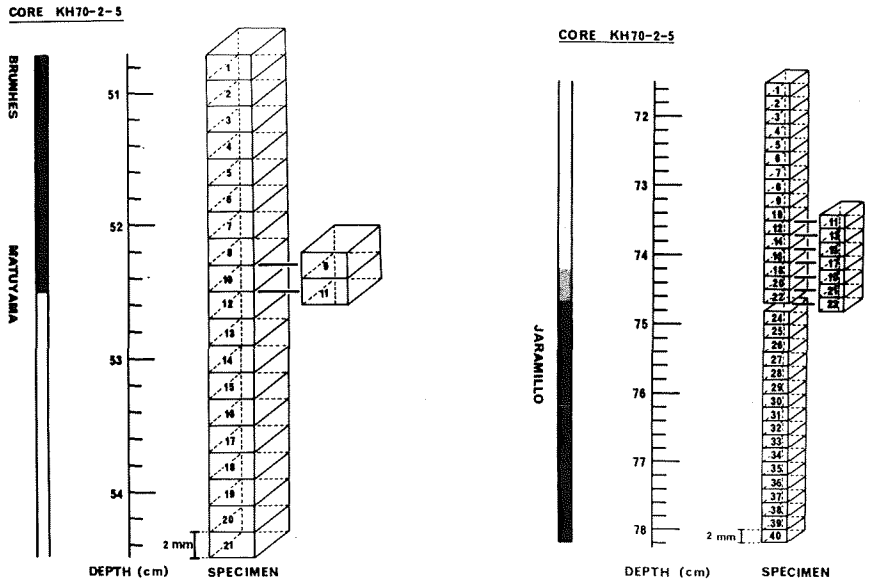

a) Brunhes-Matuyama boundary b) Upper Jaramillo boundary
Fig.3 Sequence of plate sections.

A dotted vertical line was drawn through a depth at which the intensity of fossil magnetism was smallest. This line came across with the curves showing both the inclination and declination change with depth. We can see that a intensity minimum appeared prior to the directional change. The value decreased to one quarter of the normal one. Subsequently after this minimum, the inclination began to decrease towards the horizontal plane but no change could be seen in the declination as yet. At the depth about 3 mm above the minimum the declination finally started to turn over towards the Brunhes normal direction. The overturn was rapid and completed only within 2 mm. If the rate of sedimentation were assumed to have remained almost same in the entire Matuyama epoch, the minimum persisted only for 500 years or so, while the sudden overturn took place approximately 2,000 years later than the minimum. Complete change of inclination was sandwiched between the above-mentioned intensity drop and the declination swing.

The upper Jaramillo boundary was surveyed also by using the sliced section as shown in Fig.5. Although general tendency prevailing the transition is almost same, the minimum has a more broadened bottom than that of the Brunhes-Matuyama boundary. Furthermore, one more overturn can be seen at a horizon exactly 2 mm above the main transition zone. Whilst the inclination was fluctuating, the declination swung simultaneously.

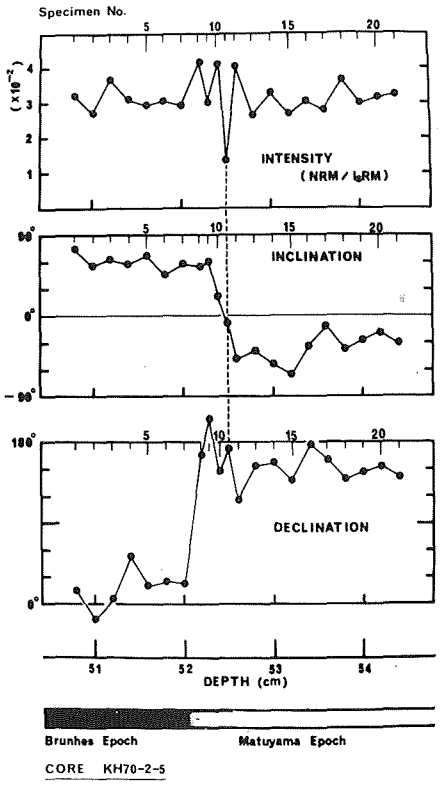

Fig.4 Change of geomagnetic field with depth (Brunhes-Matuyama boundary).
Intensity (NRM)/saturation remanence (I_SRM) was plotted in the uppermost figure.

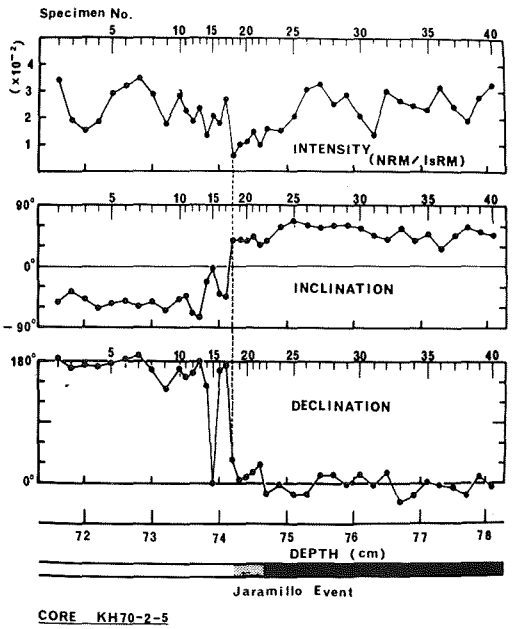

Fig.5 Change of geomagnetic field with depth (Upper Jaramillo boundary).

IV) Discussions

1) Doell and Cox (1965) have propounded the view that the Pacific ocean is a place where no remarkable secular anomaly exists. They considered that any actual anomaly is due to the non-dipole geomagnetic fields which continuously westward (relative to the mantle) causing the secular variation. In order to explain the absence of anomaly in the Pacific they took into account the physical property of the mantle deep beneath the ocean that is especially conductive, absorbs easily the moving magnetic flux and dissipates it into heat. However, the secular field of the Matuyama epoch is, as has been shown in Fig.2, rather noisy suggesting that their arguments might not be tenable here. Even in the tranquil Matuyama stage declination frequently fluctuates in one thousand years with the amplitude over 30°, the value too large to be looked for experimental errors.

The so-called Pacific quietness or "dipole window" is indeed missing in the entire Matuyama epoch.

2) The rapid overturn of declination we confirmed in both the two transitions (Figs. 4 and 5) is hardly understandable on a basis of any classical magneto-hydro-dynamic model made up of dynamo having free decay time longer than the time length of each transition. A probability of finding one decaying dynamo in a particular period of the transition is in general so small. It would become far smaller indeed, if the field should have been mated with and overcomed by an accidentally growing other independent dynamo producing opposite poloidal field. Unfortunately no model is still satisfactory to account for the oscillating Matuyama stage.

Independently from these models the present experiments can clearly indicate that a new field with opposite polarity had already been generated along the rotational axis of the earth and coexisted with the pre-existing field since the intensity drop, and also that the new one grew rapidly later to have exceeded the former feild in intensity.

Worth mentioning finally is that we have no reason to restrict this coexistence to have arisen only at the time of the polarity transition. Instead, we can safely extend the occurrence over to the entire Matuyama or even to the Brunhes epoch. If so, the tranquil Matuyama field is the consequence of a reversely compensated resultant vectors of the two antiparallel poloidal fields, whereas the oscillating one is the consequence of the unbalance that arose whilst one of the almost same two vectors was fluctuating in intensity relative to another. The alignment of the two magnetic fields resembles greatly that of the antiferromagnetic spins in several solids.

References

Cox, A. and G.B.Dalrymple (1967) J.Geophys.Res., 72, 2603.
Cox, A. (1969) Science, 163, 237.
Doell, R.R. and A.Cox (1965) J.Geophys.Res., 70, 3377.
Kawai, N., K.Yaskawa, T.Nakajima, M.Torii, and S.Horie (1972) Proc. Japan Acad., 48, 186.
Kobayashi, K., K.Kitazawa, T.Kanaya, and T.Sakai (1971) Deep-Sea Research, 18, 1045.
Kobayashi, K. (1972) in Physics of Ocean Floor edited by Y.Tomoda p.p. 235, Tokyo University Press(in Japanese).
Nakajima, T., K.Yaskawa, N.Natsuhara, N.Kawai, and S.Horie (1973) Nature Physical Science, 244, 8.
Niituma, N. (1971) Tohoku Univ., Sci.Rep., 2nd Ser.(Geol.), 43, 1.

Expression of fluctuations of the geomagnetic field intensity in deep-sea sediment cores

Kazuo KOBAYASHI and Shigeki MIZUTANI
Ocean Research Institute, University of Tokyo

More than thirty deep-sea sediment cores have been collected from widely-distributed areas of the Pacific Ocean and adjacent seas by the R.V. Hakuho-maru using a piston corer. Their natural remanent magnetization (NRM) has been measured in detail and levels with reversed magnetic polarity have been found in nearly half of the cores. Age of each level of the cores has been determined by correlating the levels of polarity transitions with a standard time scale of the sequences of reversals in the earth's magnetic polarities for these 4 million years. Micropaleontological study of two equatorial cores (KH 68-4-18, KH 68-4-20) has confirmed the magnetic correlation (Kobayashi et al, 1971).

Direction of NRM in each polarity period is usually quite uniform. In several cores having high stability against alternating field demagnetization the standard deviation of declination and inclination in one polarity period is within 10 degrees except a few specimens in transitional levels. In these the effect of laboratory demagnetization by a field of 50 to 100 oersteds is so small that the original direction and intensity of NRM before any demagnetization can provide information on the ancient magnetic field.

In contrast to direction, intensity of NRM has appreciable fluctuations in any cores. It decreases to nearly one-tenth of the average intensity at each polarity transition. Even in an interval of constant polarity it changes with an amplitude amounting to one-third of the averaged value. Although the intensity of NRM depends upon the amount and quality of ferromagnetic minerals contained in the sediment, our preliminary result of saturation remanence (artificial remanent magnetization acquired under the influence of a field of about 5,000 oe) has indicated that distribution of ferromagnetic minerals in any core is very uniform throughout the whole core (from top to bottom) with only one exception of a thin black highly magnetized layer (near the top of KH 68-4-25 core) in which magnetite is concentrated. Therefore the observed fluctuation in intensity of NRM of sediment cores is a record of secular variation in intensity of the earth's magnetic field.

Decrease in intensity of NRM at any levels of core at which the direction of NRM is reversed may partly be due to mechanism of magnetization blocking in deep-sea sediment. The shipboard observation of piston cores and triggering gravity cores has witnessed that the top sediment of about 30 cm is very fluid with high porosity. It has been widely accepted that sediment acquires remanent magnetization when the detrital magnetic grains fall down in water and statistically align their magnetic orientation under the influence of the earth's magnetic field. Then the deposited material holds the original remanent magnetization even if the earth's field is reversed after the deposition. However, if the

sediment is still so fluid that magnetic particles can slowly rotate toward the direction of the ambient field probably aided by the Brownian motion of suspensoid, resultant intensity of remanent magnetization would decrease when the field is reversed. As the porosity becomes smaller and particles can not at all rotate any further in deeper levels beneath the bottom surface under compaction by the overlying sediment, such a decrease in intensity must occur within a short interval, say 30 cm or so. In this aspect decrease in intensity of NRM at the polarity reversals can be a faithful record of the change in the field intensity only when the length of decrease is longer than 30 cm.

Recently Opdyke et al (1973) have found a long piston core of sediment formed in the Matuyama epoch with a very high rate of sedimentation, i.e. 9 cm/10^3yr and shown that the length of decrease in the NRM intensity is approximately 35 cm (thus about 4,000 years). Since this length is much longer than that mentioned above, this mode of change in NRM intensity is not due to any internal mechanism of viscous rotation of magnetic particles, but certainly represents the actual variation of the geomagnetic field intensity.

In our cores the rate of sedimentation is much smaller, usually in a range of several millimeters per thousand years. Then the width of intensity troughs at levels of reversals can be larger than that of the real variation. In these cores directional records of reversals of very short events are likely to be lost by the same mechanism and only the decrease in the NRM intensity is preserved as a fossil of these events.

When the field is kept in one direction, on the other hand, such a decrease in NRM intensity due to viscous reversing of magnetic particles as seen at the levels of the field reversals does not occur but only a slight broadening of peaks and troughs in the NRM fluctuation may be observed. Periods of fluctuation in intensity of the earth's field can be revealed from the NRM intensity. Regarding the relative amplitude of fluctuation of the field intensity little can be said in the present stage because the field dependence of depositional remanent magnetization has not been experimentally established with the deep-sea sediment. However the patterns of NRM intensity variation in several sediment cores are so coincidental with one another, when they are plotted as a function of time as shown in Fig. 1 as an example, that these variations seem likely to be an expression of the actual secular variation of the ancient field intensity.

In some cores the topmost parts of sediment have been lost by either a type of sea-bottom currents or failure of coring. Some cores have discontinuities of sedimentation rate during one polarity period (between two adjacent reversals). Magnetic stratigraphy method has no power to determine at which levels and how such hiatuses occurred. We would like to propose to compare the patterns of variation in the NRM intensity and to correlate each level of cores with one another. A core KH 68-4-18 (Fig. 2) has been selected as a standard because none of the shipboard observation, paleomagnetic polarity correlation and micropaleontological study indicate any discontinuity in the core sediment. It has thus been proved that a core taken in the Antarctic sea

(KH 68-4-49) has a distinct hiatus at about 350 thousand years ago (Fig. 3). Before that time rate of sedimentation is approximately 3 cm/10^3yr and afterward it decreases to less than one-tenth, which appears to imply the drift of boundaries of the polar ice areas.

Table: Cores cited in text

No.	Latitude	Longitude	Water Depth	Core Length
KH 68-4-18	01°59'N	170°01'W	5,390 m	983 cm
KH 68-4-49	69°28'S	169°53'W	4,200	973
KH 70-2- 5	38°26'N	170°06'W	5,140	1,055

(see Cruise Report of the R.V. Hakuho-maru, KH 68 and KH 70-2 for details)

Reference

Kobayashi, K., K. Kitazawa, T. Kanaya and T. Sakai, Magnetic and micropaleontological study of deep-sea sediments from the west-central equatorial Pacific, Deep-Sea Research, 18, 1045-1062, 1971.

Opdyke, N.D., W. Lowrie and D.V. Kent, Details of magnetic reversals recorded in a high deposition rate deep-sea core, IAGA General Scientific Assembly, Kyoto, 309 (Abstract) 1973.

Ocean Research Institute, Preliminary Rep. of the Hakuho Maru Cruise KH 68-4, ed. Y. Horibe, 1970.

Ocean Research Institute, Preliminary Rep. of the Hakuho Maru Cruise KH 70-2, ed. Y. Horibe, 1971.

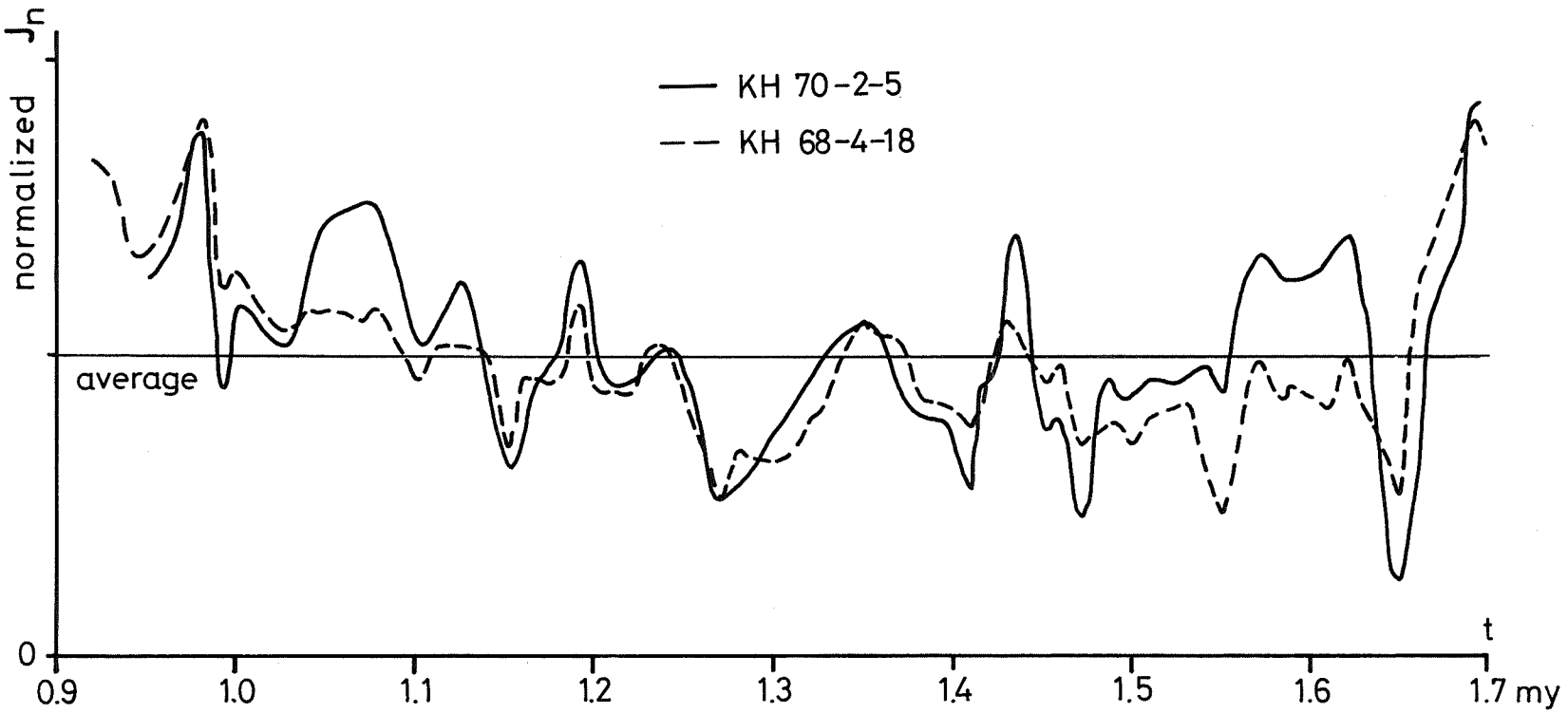

Fig.1 Comparison of patterns of the NRM intensity of two deep-sea cores (between the Jaramillo and Olduvai events)

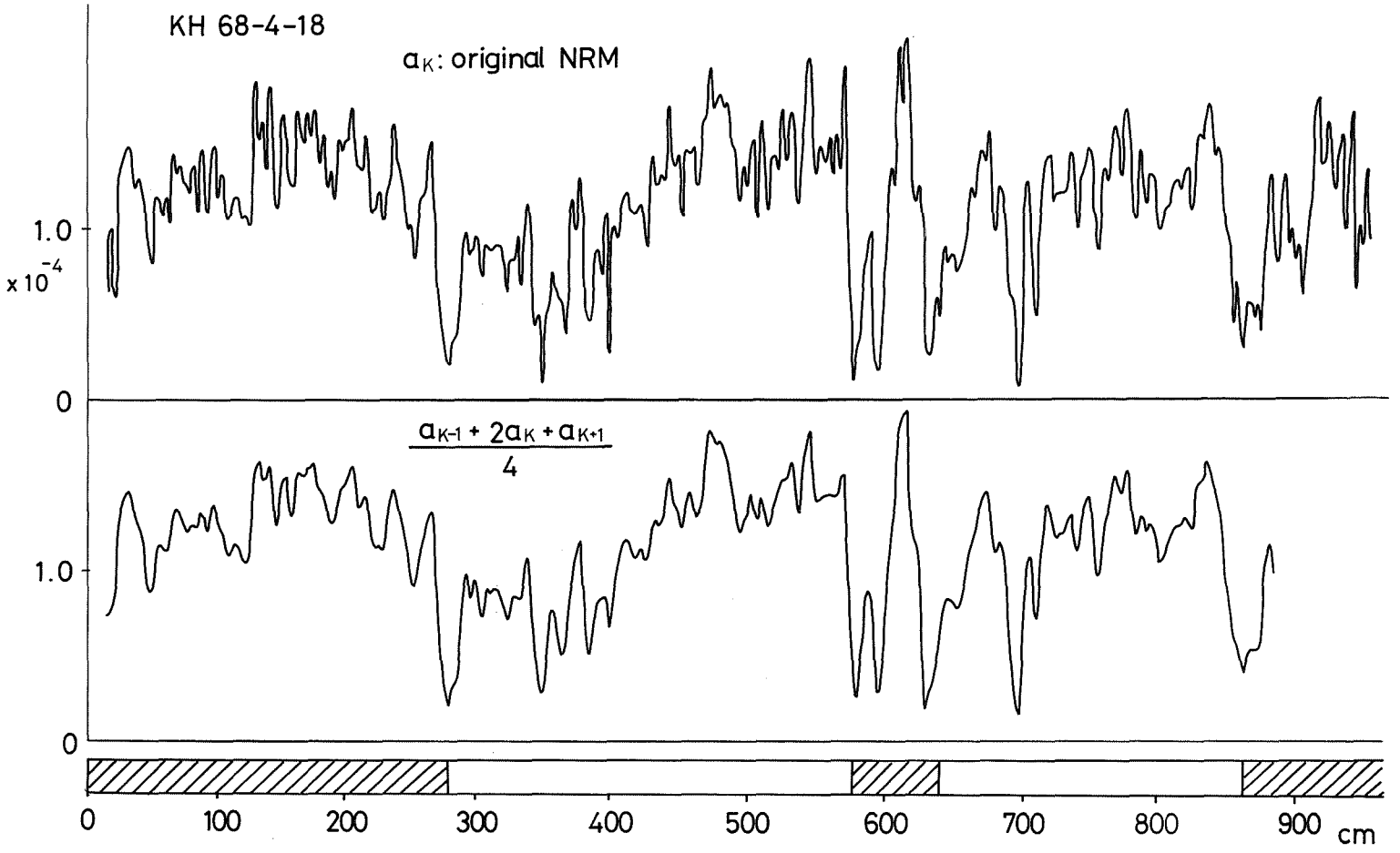

Fig.2 Intensity of the NRM in the core KH68-4-18
above: original
below: smoothed curve given by the running means of the original values.

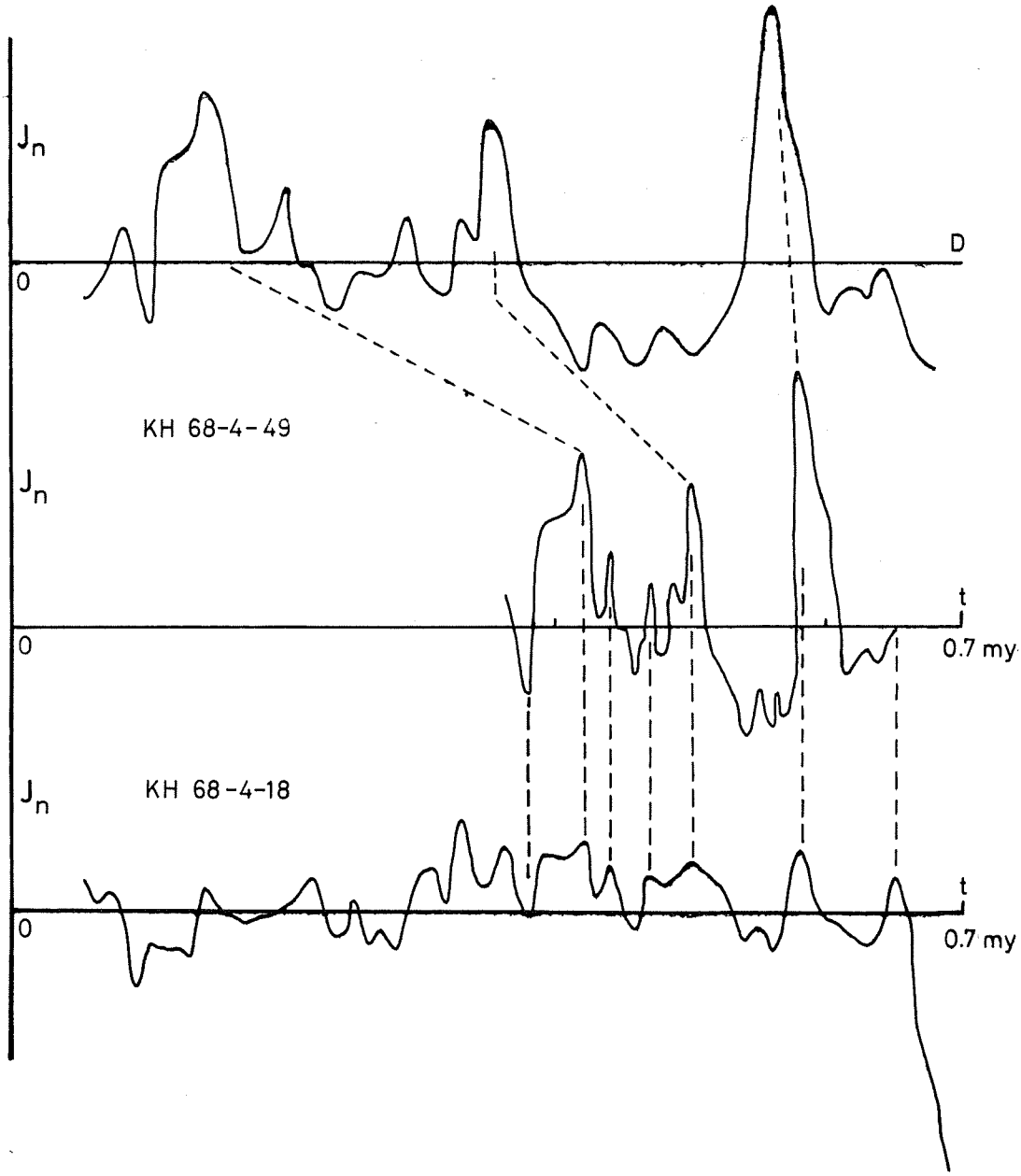

Fig.3 Correlation of the NRM intensity pattern of the cores KH68-4-18 and KH68-4-49 by a shift of the time axis of the latter.

PALEOMAGNETIC INVESTIGATION OF A WATER-LAID VOLCANIC ASH LAYER IN THE OSAKA GROUP

Masayuki TORII

Depertment of Geosciences, Faculty of Science,
Osaka city University, Sugimoto-cho, Osaka,558

Introduction

There are about forty water-laid volcanic ash layers in the Osaka Group, a typical Plio-Pleistocene series in Japan. These volcanic ash layers have been stuied in detail such as on paleomagnetism, absolute age determination with the fission track method by several investigators (Kawai, 1951; Ishida et al., 1969; Nishimura et al., 1970; Komyoike Research Group, 1971; Itihara et al., 1973), and so on.

The present report concerns with a volcanic ash layer which shows the rather unusual behaviors. The ash is named Kasuri volcanic ash layer, and has been studied as an efficient key-bed in the uppermost parts of the Osaka Group. The age determined with the fission track method is reported as 0.37±0.04 m.y. (Apatite) and 0.38±0.03 m.y. (Anthophilite) by Nishimura et al (1970).

Sampling and Measurements

Kasuri volcanic ash layer contains a lot of large amphiboles. The scattered amphiboles in the layer resemble in appearance to the so-called 'Kasuri' pattern that is common in Japanese cloth. The thickness of the layer is, ordinarily, about 10 cm or so. It is sandwiched between clay beds.

Because they are uncosolidated as yet and very fragile, it is difficult to obtain samples from the layer by means of usual sampling. By the same technique as Hirooka's (1971), they were coated by 'Plaster of Paris' prior to the removal. Next they were cut into cubes of 3.5 × 3.5 × 3.5 cm by using diamond cutter.

The remanent magentization of the samples were measured with an astatic magnetometer whose maximum sensitivity was 7×10^{-8}cgs emu/mm. Stability of the remanence was examined by the storage test and alternating field (AF) demagnetization method.

1) OG-20 (Fig. 1)

Sampling locality; Machikaneyama-cho, Toyonaka city
(34°47'53"N, 135°27'25"E)

A thick and fresh exposure of the ash layer crops out here as the results of the new costructions of a high way a few

years ago. The lower coarser part of the layer was about 5cm thick, including small pumice grains. The upper medium part was about 25 cm thick. Mean intensity of NRMs was 3×10^{-5}cgs/cc. This value is largest in the other ash layers in the Osaka Group. Directions of NRM suggests that the polarity of this site is normal. However, after about 240 days of storage, the intesity of the remanence was found to have decreased by 20∿30%, and directions also cosiderably deviated. A progressive AF demagnetization, therefore, was carried out. Most of the polarization changed except two samples obtained from coarser part, whose directions pointed also the abnomal ones.

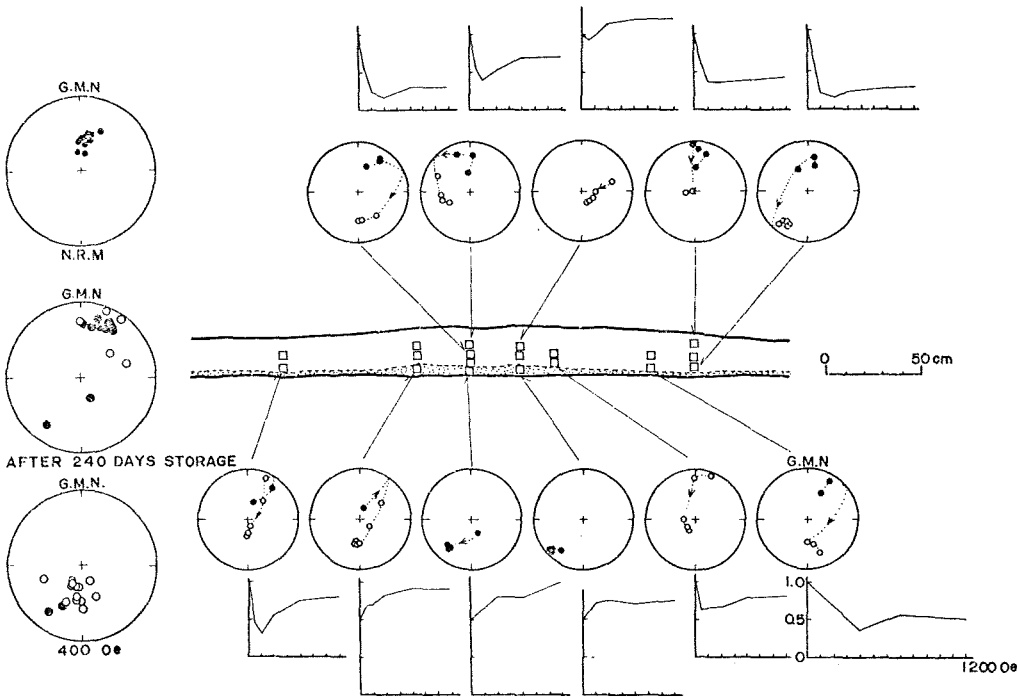

Fig. 1 OG-20
Schematic diagrams of the outcrop and results of the experiments. Directions of NRMs, after storage, and after AF cleaning at 400 Oe are shown at the left hand. Equal area projetion is used. Solid circles indicate positive inclination and open circles negative inclination. Results of progressive AF demagnetization on each sample were also plotted on Schmidt's net. Variations of intensities with a.c. peak demagnetiztion field are exhibited graphically. Each unit of abscissa is 100 Oe.

2) OG-55 (Fig. 2)

Sampling locality: Machikaneyama-cho, Toyonaka city
(same outcrop as OG-20)

To examine an influence of desiccation upon polarity change, the remanent magnetizations were measured soon after the fields collection. Mean intensity of NRMs was 2×10^{-5}cgs/cc. Although directions of NRMs were scattered, most of them showed reverse polarity after AF cleaning at 400 Oe except four samples which showed normal polarities. On further increasing the cleaning field four samples increased the intensities up to twice the original values. Although results obtained at OG-55 is not completely the same as those at OG-20, the two polarities may become same reverse direction after the cleaning.

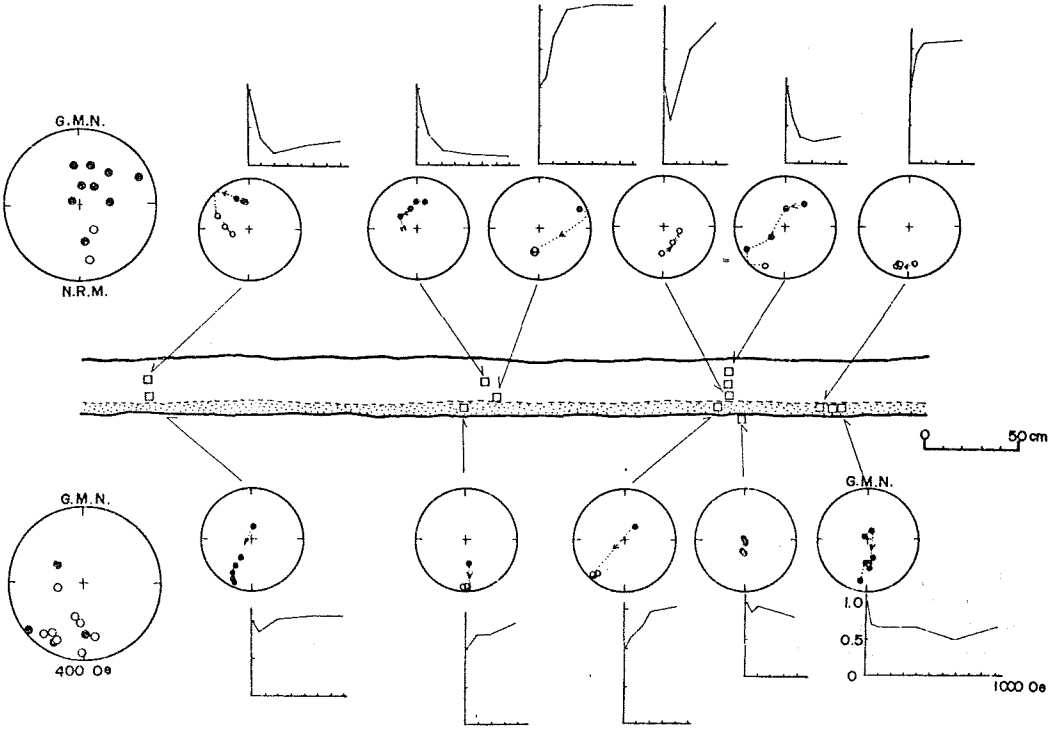

Fig. 2 OG-55
The way in which the obtained results are shown is the same as in Fig. 1.

3) OG-60 (Fig. 3)

Sampling locality: Machikaneyama-cho, Toyonaka city
(34°48'15"N, 135°27'32"E)

This outcrop being found about 700 m north of OG-20, is the same locality as that reported by Ishida et al (1969). The volcanic ash layer observed at this point was about 10cm thick and severely weathered. Mean intesity of NRMs was 2×10^{-6}cgs/cc. Both directions of NRMs and those after AF cleaning at 400 Oe were scattered, and normal. The remanence were rather unstable.

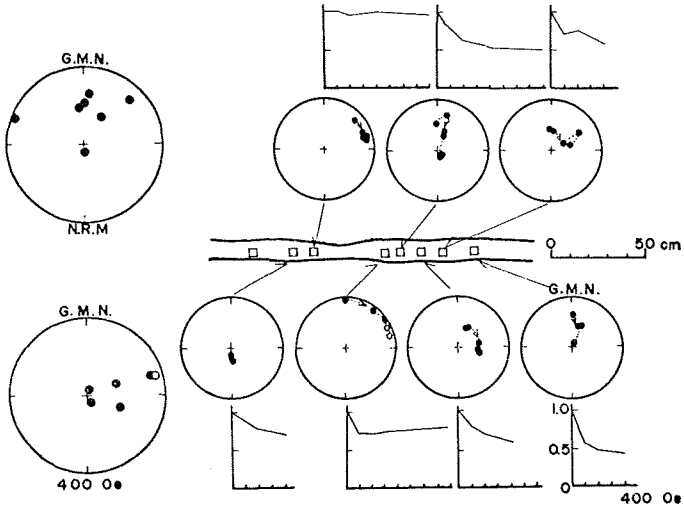

Fig. 3 OG-60

The way in which the obtained results are shown is the same as in Fig. 1.

4) OG-28 (Fig. 4)

Sampling locality: Fuseya-cho, Sakai city
(34°28'19"N, 135°27'56"E)

This site was about 37 km apparted from the above-mentioned sites. Thickness of the layer was less than 10 cm, and severely weathered with limonite staines. Mean intensity of NRMs was 1×10^{-6}cgs/cc. Samples were collected from the two parts of the outcrops found in a close vicinity of only 4 m. The results after AF cleaning was inconsistent with each other. Namely one group of samples changed their remanent vectors to reversal after cleaning and the other did not.

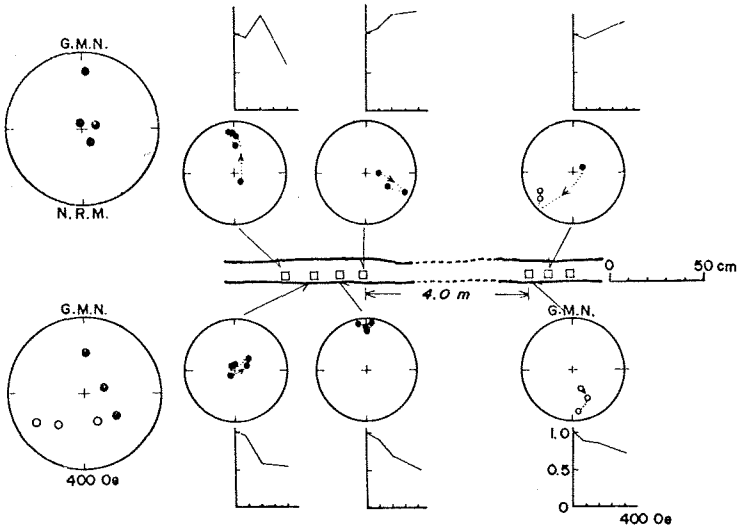

Fig. 4 OG-28

The way in which the obtained results are showm is the same as in Fig. 1.

Discussion

The volcanic ash layers in the Osaka Group were mostly water-laid. The remanent magnetism of them have been considered depositional remanent magnetization. But the mechanism and stability of the magnetization have not been sufficiently stutied except a few early works (Kawai, 1954; Kawai, 1955). We should not, therefore, easily regard the reverse polarity of Kasuri ash as that of the geomagnetism without further investigations.

On the other hand, AF cleaning test on many other volcanic ashes in the Osaka Group suggested that the large deviations of the remanent vector or polarity change, such as shown in Kasuri volcanic ash, was scarecely observed, and in ordinary case unstable components were removed by the AF cleaning till 400 Oe. (Torii, 1974)

Kasuri volcanic ash should erupt during Brunhes normal epoch, of which the age (0.37∿0.38 m.y.) was determined with the fission track method by Nishimura et al (1970). Recently, Bucha (1970), Wollin et al. (1971) and Kawai et al. (1972) reported independently the evidence of short geomagnetic polarity change at that time. The duration in which the reverse geomagnetic field persisted is approximately one tenth of that in which the normal fields cotinued in the Brunhes epoch. Consequently the probability of findig such reverse direction as Kasuri's from the Osaka Group is much larger that has been considered so far.

Furthermore, thermomagnetic and X-ray analysis together with microscopic observation have been undertaken with the separated magnetic minerals from Kasuri volcanic ash. Preliminaly results showed that magnetic minerals from OG-20 were titanomagnetite and those from OG-60 were titan-hematite. In this respect, further investigations also still have been required.

Acknowledgments

The author wishes to express his heartful thanks to Prof. N.Ikebe, Assistant Prof. M.Itihara and Mr. S.Yoshikawa, Osaka City University, for the valuable suggestions on the geological problems. The author is indebted to Prof. N.Kawai, Assistant Prof. K.Yaskawa and Dr. T.Nakajima, Osaka University, for the suggestions and discussions on the paleomagnetism.

References

Bucha, V. (1970) J. Geomag. Geoele. 22, 253.
Hirooka, K. (1971) Mem. Fac. Sci. Kyoto Univ. Ser. B 38, 167.
Isida, S., K.Maenaka and T.Yokoyama (1969) J. Geol. Soc. Japan 75, 183.
Itihara, M., T.Kamei, T.Mitsunashi, K.Suzuki and Y.Kuwano (1973) J. Geosci. Osaka City Univ. 16, 25.

Kawai, N. (1951) J. Geophys. Res. 56, 73.
(1954) J. Geomag. Geoele. 6, 208
(1955) Proc. Japan Acad. 31, 346
Kawai, N., K.Yaskawa, T.Nakajima, M.Torii and S.Horie (1972)
Proc. Japan Acad. 48, 186.
Komyoike Research Group. (1971) Earth Science 25, 201.(in Japanese)
Nishimura, S. and S.Sasajima (1970)
Earth Science 24, 222. (in Japanese)
Torii, M. (1974) thesis of master (in preperation)
Wollin, G., D.B.Ericson and W.B.Ryan (1971)
Earth Planet. Sci. Letters 12, 175.

PALEOMAGNETISM OF THE SAN JUAN VOLCANIC FIELD, COLORADO, U.S.A.

Hidefumi TANAKA and Masaru KONO

Geophysical Institute, University of Tokyo, Bunkyo-ku, Tokyo 113, Japan

Summary

The paleomagnetism of sixteen welded tuffs and lavas from the San Juan volcanic field of Oligocene and early Miocene age were studied. Most samples were quite stable to alternating field demagnetization and gave reliable paleomagnetic directions. The mean paleomagnetic pole position is at 76.1°N, 125.5°E with α_{95} of 9.0°. This is quite close to the mean pole obtained by Grommé and Mckee from Oligocene volcanic units of the western U.S.A.. Using the method of Doell, the angular dispersion of the virtual geomagnetic poles was calculated to be 18.9° with confidence limits of 14.9° and 25.9°, which is a little larger than that of the Quaternary paleomagnetic results.

Geology and Chronology

The San Juan Mountain is a large erosional remnant of a volcanic field of about 25,000 km² in the southwestern Colorado which once extended over much of the southern Rocky Moutains and adjacent areas in Oligocene and later times. The geological map of this area is shown in Fig.1 (Lipman et al., 1970). According to Lipman et al., the evolution of this volcanic field is devided into three periods.

(1) Early period (35 m.y. ~ 30 m.y.)
A large quantity of intermediate lavas and breccias —— mainly alkali andesite, rhyodacite, and mafic quartz latite —— were erupted from numerous scattered central volcanoes onto an eroded tectonically stable terrain.

(2) Middle period (30 m.y. ~ 25 m.y.)
Large quantity of ash flows —— quartz latite

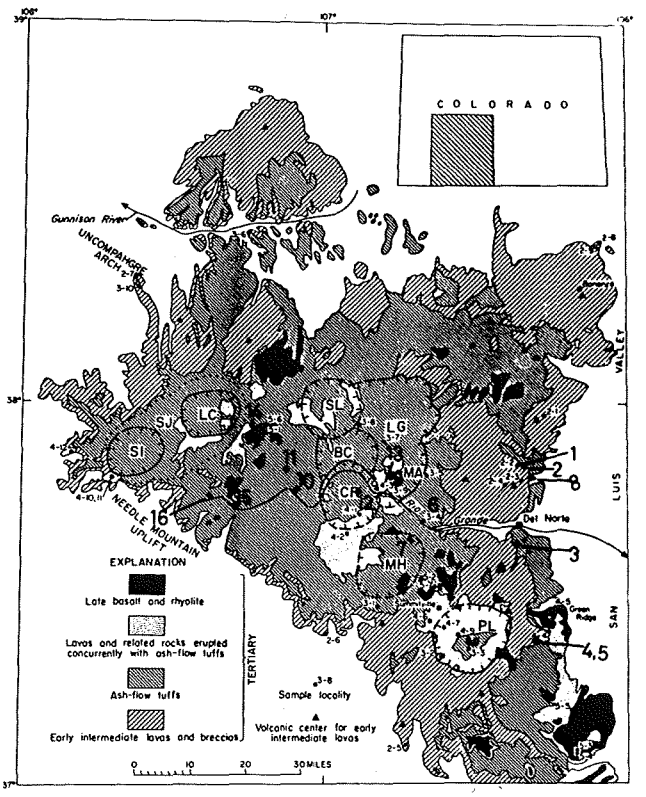

Fig.1 The generalized geological map of the San Juan volcanic field, Colorado (Lipman et al., 1970). The localities of our sampling sites are indicated by large numerals. Sampling site No.1 is for the unit SJ 1, etc..

and low-silica rhyolite——and intermediate lavas and associated rocks were erupted in this period.

(3) Late period (25 m.y.~ 5 m.y.)
Bimodal association of basalt and high-silica alkali rhyolite were erupted intermittently through the Miocene and Pliocene. The rate of eruption was much smaller than in Oligocene age.

Locations of sampling sites for our study are also shown in Fig.1. Fourteen out of sixteen cooling units we sampled belong to the middle period and most of them are welded tuffs.

Lipman et al. (1970) report many K-Ar ages determined mostly on various minerals separated from many formations in the San Juan volcanic field. Ten of the cooling units sampled in the present study have such K-Ar dates. The accuracy of these dates are quite high and in most cases errors do not exceed 1 m.y. By the stratigraphic control of many widely distributed ash flows, the ages of cooling units which are not dated radiometrically can also be assessed quite correctly.

Experimental Procedures

Eight or nine core samples 2.45 cm in diameter were taken from each cooling unit by means of an engine drill. All the core were oriented in situ by observing the azimuth of the sun through a specially made sun compass. Orientation errors were less than 0.5 degrees. Two or more specimens 2.3 cm long were cut from each core sample. One was used for stepwise alternating field (AF) demagnetization, while others were kept for other studies. Magnetization of specimens was measured by a spinner magnetometer.

Magnetic Minerals

Analyses of magnetic minerals have not been completed yet, but Curie temperatures were determined for eight units by thermomagnetic analyses carried out in vacuum of about 10^{-4} Torr and in a magnetic field of about 5 k Oe. In general, there seem to be two distinct types in thermomagnetic curves, i.e. (a) those with a single Curie point at about 550°C, and (b) those with two Curie points at about 300°C and 550°C indicating the coexistence of two phases of ferromagnetic minerals (Fig.2). However, identification of magnetic phases have not been carried out yet.

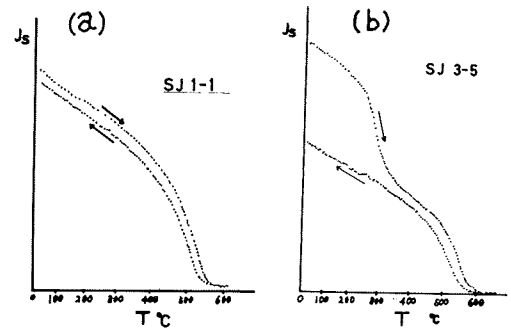

Fig.2 Examples of typical thermomagnetic curves

Alternating Field Demagnetization

Specimens from all the samples were demagnetized successively to peak alternating field of 50, 100, 200, 300, 400 Oe. All the specimens except from two units (SJ 1 and SJ 2) showed a good stability of NRM in AF demagnetization. Of these, eight units carried little unstable components of remanence, and six others had some secondary components which was demagnetized in fields ranging between 100 and 300 Oe (Fig.3). Typical examples of demagnetization curves are shown in Fig.4. In almost all specimens intensity of magnetization decreased

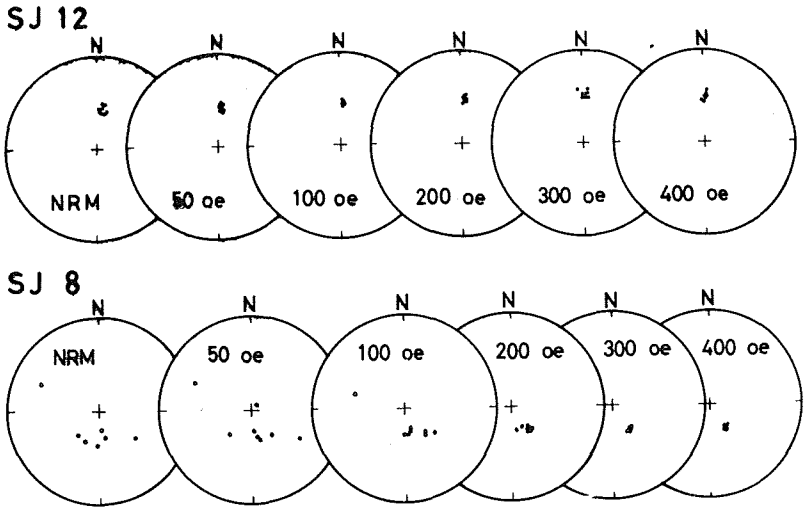

Fig.3 Examples of change in the direction of magnetization in the course of progressive AF demagnetization.

smoothly as the peak alternating field was increased.

Stable remanence of 20 ~ 80 % of the original NRM remained after the last step of 400 Oe. It seems due to viscous remanent magnetization (VRM) acquired in the present geomagnetic field that reversely magnetized unit SJ-6 shows an increase of magnetization at the step of 50 Oe. About eighty percent of reversely magnetized samples behave in such a manner. Fig.5 are histograms showing changes of intencity of magnetization and α_{95} in the course of progressive AF demagnetization.

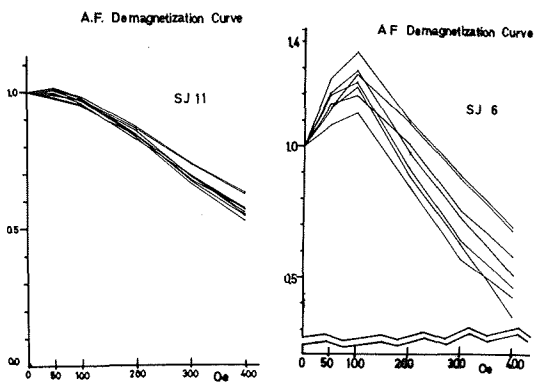

Fig.4 Examples of change of intensity of remanent magnetization of samples by AF demagnetization.

Paleomagnetic Directions

For each unit, direction of the primary component of NRM (also that of the paleomagnetic field) was determined as the mean direction of magnetization at a stage of AF demagnetization when the confidence angle α_{95} was minimum. The peak value of AF field that gave the stable remanent magnetization (stable RM) ranges between 100 Oe and 400 Oe according to different cooling units. Paleomagnetic directions and pole positions are summerized in Table 1. Virtual geomagnetic pole

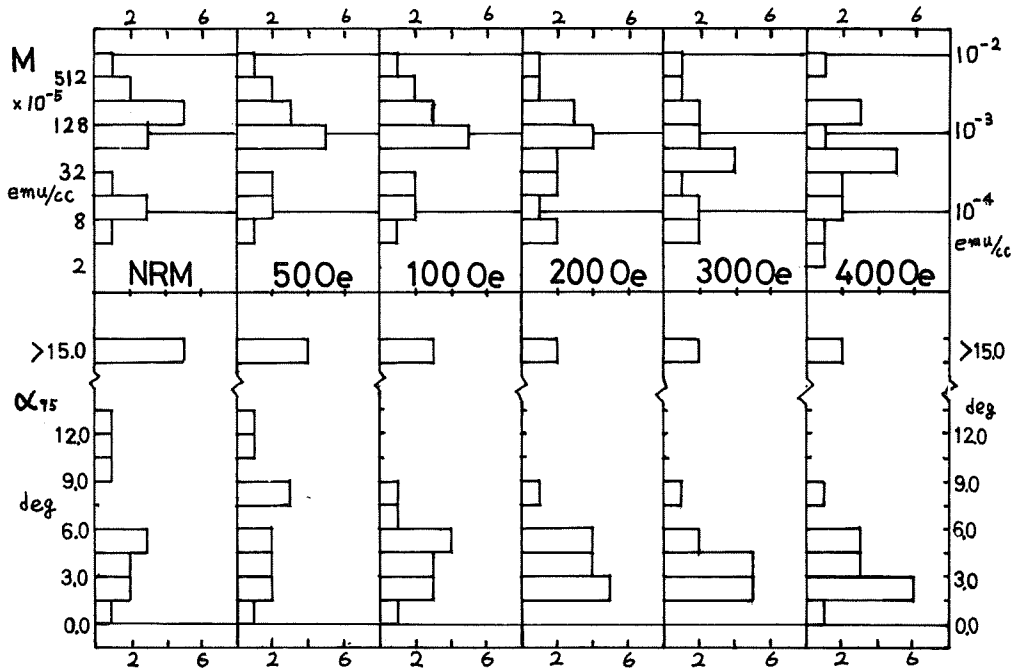

Fig.5 Histograms showing the change of mean magnetization (above) and α_{95} (below) by AF demagnetization.

(VGP) positions derived from the direction of stable RM are given in Table 1 and also shown in Fig.6(mean VGP position is indicated by white triangle).

It is interesting to compare the result of the present study with the other paleomagnetic results from North America in Oligocene. Three such Oligocene VGP's are also shown in Fig.6 (marked by black triangles). Two of these (B,C) are reported by Symons (1971b,1973) from Vancouver Island. He suggests a counter-clockwise rotation of about 20° of the Vancouver Island based on the paleomagnetic data for the pole C. He also states that the pole B may not represent a typical Oligocene pole as the secular variation may not be averaged out. Therefore, B and C may be excluded from the consideration of Oligocene VGP's. The mean VGP from the San Juan volcanic field (white triangle) is quite close to that from the western U.S.A. (marked as A) reported by Grommé and Mckee(1971). Both our data and data of Grommé and Mckee are generally concordant with the plate tectonic regime of North America.

We calculated the angular dispersion of secular variation(SV) using the expression by Doell(1970)

$$S=(N-1)^{-\frac{1}{2}}\left(\sum_{i=1}^{N}\delta_i^2\right)^{+\frac{1}{2}}$$

where δ_i is the angle between the i-th VGP and the mean pole position, and N is the number of poles. Three cooling units were excluded from this calculation because two of them(SJ 1,SJ 2) had large values of α_{95}(larger than ten degrees), and because VGP of the other(SJ 15) was near the equator and more than 45° apart from the mean pole position. The calculated dispersion for these thirteen units amounted to 18.9° with 95% confidence limits(Cox, 1969) of 14.9° and 25.9°.

Although statistically not significant, this value is a little larger than the dispersion expected from the model by Doell and Cox(1971) which is based on the rotation of the present non-dipole field and the 11° wobble of the main dipole.

Table 1. Paleomagnetic Directions and Pole Positions

	Sampling Sites		Age		NRM			Stable RM					VGP		
Unit	Lat,° N	Lon,° W	(m.y.)	N	I	D	α_{95}	AF	I	D	K	α_{95}	Lat,° N	Lon,° E	Formation
SJ 14	37.9	107.4	22.5	8	-50.4	171.0	5.7	400	-56.9	177.5	194	4.3	-88.0	335.6	Sunshine Creek Tuff
SJ 13	37.8	106.8	26.4	7	57.4	-24.1	5.2	400	53.4	-28.1	206	4.2	67.0	162.1	Fisher Quartz Latite
SJ 12	37.8	106.9		8	48.1	5.5	1.1	100	47.0	5.3	2660	1.1	79.4	46.7	Snowshoe Moutain Tuff
SJ 11	37.9	107.1		9	72.0	-5.6	3.9	400	69.8	-11.2	597	2.1	72.4	230.6	Nelson Moutain Tuff
SJ 10	37.8	107.1		8	-44.5	-117.0	50.	200	-26.7	160.4	425	2.7	-60.6	294.5	Wason Park Tuff
SJ 9	37.8	106.8	26.7	7	-33.1	173.3	9.2	400	-36.0	174.2	60	7.9	-71.5	270.6	Mammoth Moutain Tuff
SJ 8	37.7	106.3		8	-66.9	-176.6	27.	300	-59.2	142.9	1110	1.7	-61.3	359.6	Carpenter Ridge Tuff
SJ 7	37.6	106.8	27.8	7	7.2	-4.7	2.6	100	2.9	-4.1	630	2.4	53.7	80.2	Fish Canyon Tuff
SJ 15	37.7	107.3		8	-16.3	-101.3	12.	300	-25.6	-109.9	127	4.9	-23.9	163.8	Sapinero Mesa Tuff
SJ 6	37.7	106.7	28.2	8	-63.3	176.5	3.2	100	-61.0	-179.2	618	2.2	-85.7	80.7	Masonic Park Tuff
SJ 16	37.8	107.4	28.4	8	33.1	-18.7	2.0	400	31.2	-18.9	1307	1.5	63.2	117.2	Ute Ridge Tuff
SJ 5	37.3	106.3		7	-50.6	-160.1	22.	400	-37.3	164.9	717	2.3	-68.9	296.5	Treasure
SJ 4	37.3	106.3	29.8	8	41.0	-32.1	4.6	100	37.1	-34.6	211	3.8	55.8	144.4	Moutain
SJ 3	37.6	106.4		8	-32.7	176.5	11.	200	-50.6	-170.5	423	2.7	-80.0	199.7	Rhyolite
SJ 2	37.8	106.3	32.4	8	56.5	112.7	49.								Summer Coon Rhyolite
SJ 1	37.8	106.4	34.0	8	26.0	11.6	26.	300	23.9	4.5	6	26.	(normal)		La Garita Creek Rhyodacite

N : Number of samples(The number of samples of SJ 14 in the Stable RM is 7.).
I : Inclination of magnetization, downward positive, in degrees.
D : Eastward declination of magnetization in degrees.
K : Fisher's precision parameter.
α_{95}: Semiangle of cone of 95% confidence in degrees.
AF: Peak field value of AF field at which stable component is obtained.

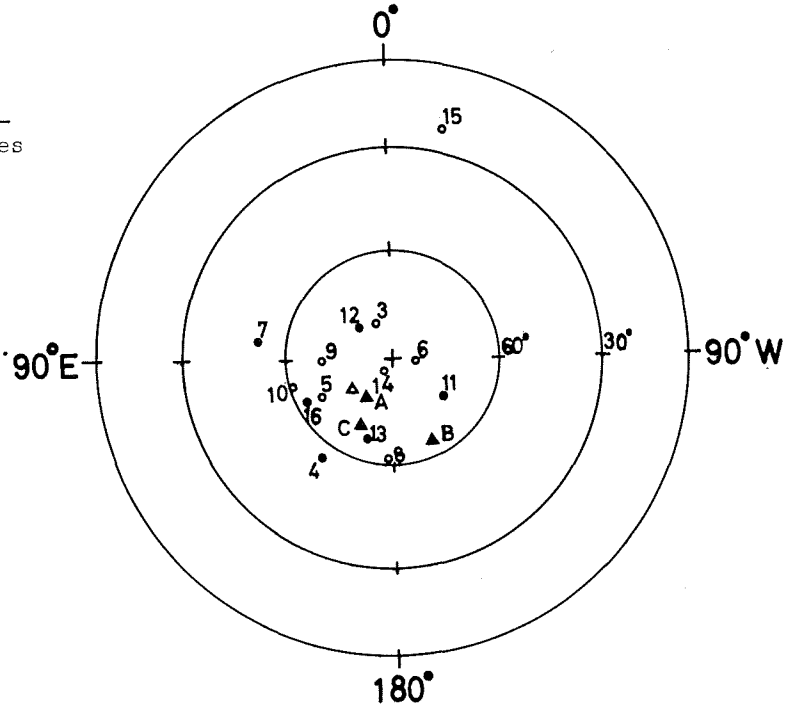

Fig.6
VGP's from the present study(marked by closed circles for normal, open circles for reverse and white triangle for the mean) and other results from the North America in Oligocene(marked by black triangles). A is the result by Gromme and Mckee, and B and C are by Symons.

This may be because of either or both of the two reasons, namely, (1) the SV in Oligocene was greater than that in the recent times,and (2) long period variation was considerably large , because we calculated the dispersion for a fairly long interval of eight million years. In order to test the second hypothesis, the angular dispersion of 9 units between SJ-13 and SJ-16(2 m.y.) is calculated. As the dispersion for these 9 units (20.1°,with cofidence limits of 15.2°and 29.8°) did not differ significantly from the previous value, it may be concluded that the SV in Oligocene was larger than that in the recent ages. Grommé and Mckee(1971) also report larger SV in Oligocene in the western U.S.A.. They obtained a value of 23.8° which is significantly greater than the dispersion at the same latitude expected from the model of Doell and Cox(1971).

Acknowledgement

Samples were collected while one of us(M.K.) stayed as a visiting fellow at CIRES, University of Colorado. We thank Richard Reynolds and Sumiko Kono for the help in sampling. We are also indebted to Peter Lipman and Thomas Steven of U.S. Geological Survey, Denver, for the selection of sampling sites and identification of rocks.

References

Cox, A. (1969) Roy. Astron. Soc. Geophys. J. 17, 545
Doell, R.R. (1970) Earth Planet. Sci. Letters 8 , 352
Doell, R.R. and A. Cox (1971) Science 171, 248
Grommé, C.S. and E.H.Mckee (1971) Eos Trans. AGU 52, 187
Lipman,P.W.,T.A.Steven,and H.H.Mehnert(1970) Geol. Soc. America Bull. 81, 2329
Symons, D.T.A. (1971b) Geol. Surv. Can. Pap., 71-24, 1
Symons, D.T.A. (1973) J. Geophys. Res. 78, 5100

DRIFT OF SOUTHWEST JAPAN RELATIVE TO SOUTH KOREA SINCE LATE MESOZOIC

—A palaeomagnetic approach to the origin of the Japan Sea—

Katsumi YASKAWA

Department of Physics, Faculty of Engineering Science,
Osaka University, Toyonaka

1 Introduction

In his famous book Holmes (1965) mentioned that the Japan Sea was originated in concequence of the southward or southeastward drift of Japan, referring Carey's speculative figure (1958). The same idea concerning to the origin of the Japan Sea was mentioned by a few investigators, that is, Terada (1934) on the basis of the topographical analysis of the bottom of the Japan Sea, Yasui et al. (1968) Matsuda and Uyeda (1971) Takeuchi (1971) to give an explanation to high heat flow region in the Japan Sea, Ozima et al. (1972) using their data of K-Ar and Rb-St dating and Isezaki et al. (1973) analysing magnetic anomaly.

It is wellknown fact that the palaeomagnetic results from the continents revived Wegener's hypothesis of continental drift. In this paper the drift of the Southwest Japan will be discussed since Cretaceous using all the palaeomagnetic data of the rocks in this area reported to date.

2 Mean directions of NRM and Palaeolatitudes

Among the many results of palaeomagnetic investigation of Southwest Japan, the followings were not adopted for this calculation: (a) Such a result that Fisher's 5 % error angle of natural remanent magnetization (NRM) is greater than 20 degree at a site. (b) Such a result that the collecting site of specimens is located outside of the following area; north of the Median Tectonic Line and Matsuyama-Imari line, south of the shore line of Southwest Japan and west of the east boundary of Kyoto, Shiga and Mie Prefectures.

It would rather be easy to obtain the latitude from the observation of geomagnetic inclination at a point, if the geomagnetic field were due to a pure geocentric dipole whose axis was parallel to the earth's rotational axis. The correct latitude, however, cannot be expected from a single measurement of the geomagnetic field, because the geomagnetic poles have been drifting around the geographic poles and besides geomagnetic field is not a complete dipole field. To get the correct latitude, it is necessary to take an average of the direction of geomagnetic field over the longer duration than the period of its secular variation and over the area wide enough to average out the local field anomaly.

All the palaeomagnetic results in Southwest Japan were classified into four ages, i.e. Cretaceous, Paleogene, Miocene and Pliocene-Pleistocene, and an attempt was made to calculate the latitude in this area by taking an average of the direction of magnetization over each age as the following scheme: The area concerned was divided into squares by the longitude and the latitude every half degree, and calculated the mean direction of NRM for each square. The virtual pole position was calculated in the usual method with the mean direction of each square thus obtained, using the lattitude and longitude at the center of the square (Table 1). From these virtual poles, the number of which was as many squares belonging to each age, a Fisher's mean palaeopole was obtained for each age (Table 2 and Fig. 1). The palaeolatitude at about the center of this area (134°E, 35°N) was easily calculated for each age using the data of Table 2, which was also tabulated in Table 2.

Table 1

Age	Center of square		Mean direct. of NRM		Palaeopole	
	Long.(°E)	Lat.(°N)	Dec.(°E)	Inc.(°D)	Long.(°E)	Lat.(°N)
Cretaceous	131.0	34.0	54	57	-160	47
	131.0	34.5	49	69	178	51
	131.5	34.0	61	60	-166	42
	131.5	34.5	1	69	134	72
	132.0	34.5	34	38	-123	58
	132.5	35.0	54	59	-160	48
	133.0	34.5	80	53	-161	26
	133.5	35.0	64	54	-156	38
	134.0	35.0	-6	42	-19	78
	134.5	35.0	46	53	-147	52
	135.0	34.5	65	55	-156	38
	135.5	35.0	59	61	-162	44
Paleogene	131.0	34.5	36	59	-160	61
	132.0	35.0	38	36	-124	53
	132.5	35.0	-21	55	50	73
	134.5	35.0	13	61	-174	78
	135.0	34.5	40	50	-140	56
Miocene	132.5	33.5	-25	37	19	64
	132.5	35.5	11	58	-161	81
	133.0	33.5	38	61	-164	59
	133.0	34.0	-5	50	7	85
	133.0	35.5	-14	52	33	78
	134.0	34.5	8	55	-145	83
	134.0	35.5	44	36	-126	49
	134.5	35.5	2	54	-111	88
	135.5	34.5	-26	42	-117	65
	136.0	34.5	72	64	-167	35
	131.0	34.5	3	49	-80	85
	133.0	35.5	5	53	-111	86
	133.5	35.5	0	54	-73	89

Pliocene & Pleistocene	134.0	35.5	5	48	-82	82
	135.0	35.5	21	41	-107	69
	135.0	34.5	-11	45	8	78
	135.5	34.5	-16	45	19	74
	135.5	35.0	2	46	-59	82
	136.0	35.0	5	53	-121	85
	136.5	35.0	-3	45	-27	82

Table 2

Age	Mean palaeopole		Palaeolatitude of SW Jpapan
Cretaceous	-159°E	53°N	41°N
Paleogene	-147	72	36
Miocene	-136	77	34
Pliocene-Pleistocene	-56	85	30
Present	0	90	35

3 Discussion

Only a few reliable palaeomagnetic results were reported from South Korea as shown in Table 3 (Kienzle and Scharon, 1966). The palaeopole for the Cretaceous was calculated from the data in Table 3 as at 140.6 degree west and 73.9 degree north. The palaeolatitude in the Cretaceous is calculated as 34 degree north at the mean site of South Korean sampling sites (128.6°E, 35.7°N). This value is almost 7 degree lower than that at the center of Southwest Japan.

Table 3

Age	Sampling site		Direction of NRM		Palaeopole	
	Long.(°E)	Lat.(°N)	Dec.(°E)	Inc.(°D)	Long.	Lat.
Creta.	127.5	35.9	14.6	46.2		
	128.7	35.8	21.4	39.4		
	128.8	35.2	14.9	54.0		
	128.9	35.4	42.5	62.0		
	129.3	36.2	18.5	59.8		
Mean	128.6	35.7	19.5	53.3	140.6°W	73.9°N

To obtain the difference of palaeolatitude between South Korea and Southwest Japan at each age, it is necessary to have the palaeomagnetic data for the other ages than the Cretaceous, but unfortunately no other reliable data than in Table 3 has been reported. As can be clearly seen in Table 2, the palaeolatitude in Southwest Japan had a tendency

of decreasing untile the Pliocene-Pleistocene and then suddenly changed to the opposite direction, i.e. increasing the latitude to the present value. The variation of latitude reflects the effect of the polar wondering and also that of the drift of land, unless there was tilting of the land.

It is difficult to suppose that the land block, which had a certain extent and had been drifting to a direction, changed its direction all of a sudden to the opposite direction. On the contraly, it seems to be naturaly acceptable that the drift of Southwest Japan may have been kept constant velocity and so unchanged its original direction, and the sudden change of direction, such as shown in Table 2, may have been due to a polar wondering as shown in fig. 1 with a dotted line. Then, it leads us to the conclusion that Southwest Japan, having situated at 7 degree higher latitude than South Korea in the Cretaceous, has drifted southward to the present position. The original position of Southwest Japan in the Cretaceous is represented in Fig. 2, referring the comment of Ichikawa (1972) from the view point of geological structure of the both land blocks.

Of course, considering the fact that from palaeomagnetic data it is impossible to determine the longitude at the past, we can only say that the representative point of Southwest Japan (134°E,35°N) in the Cretaceous could be at any point on the line A in Fig. 2 which was drawn as the latitude 41 degree north for the Cretaceous Korean pole.

References

Carey, S. W. (1958) Symp. Continental Drift, hobert, 117.
Holmes, A. (1965) Principles of Physical Geology, Thomas Nelson, 1134.
Ichikawa, K. (1972) Kagaku 42, 630.
Isezaki, N., S. Uyeda and M. Yasui (1973) IAGA Bull. 34, 259.
Kienzle, J. and L. scharon (1966) J. Geomag. Geoelectr. 18, 413.
Matsuda, T. and S. Uyeda (1971) Tectonophys. 11, 5.
Ozima, M., I. Kaneoka and N. Ueno (1972) Kagaku 42, 350.
Takeuchi, H. (1971) Kagaku 41, 687.
Terada, T. (1934) Bull. Earthq. Res. Inst. 12, 650.
Yasui, M. T. Kishi, T. Watanabe and S. Uyeda (1968) Geophys. Monograph 12, 3.

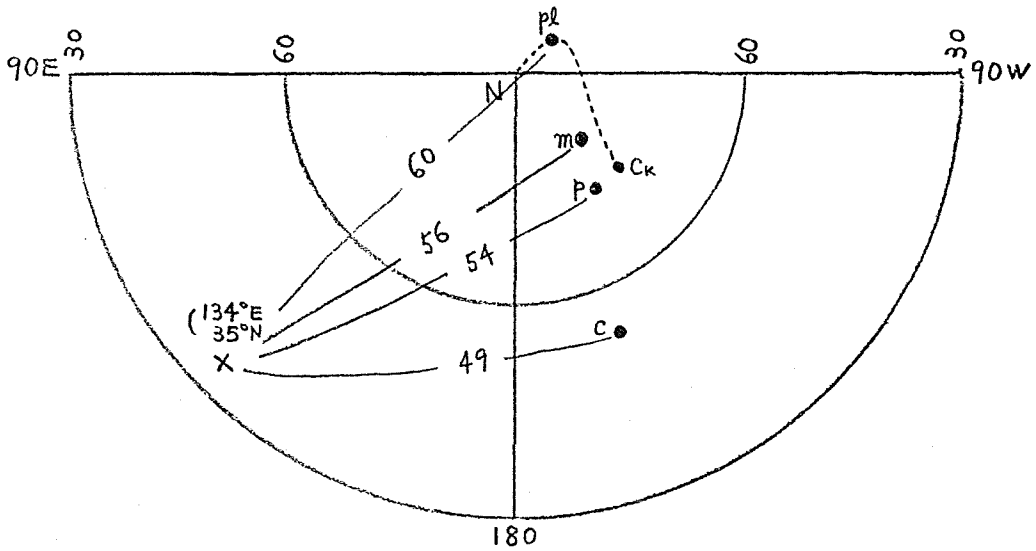

Fig. 1

Palaeopoles since Cretaceous obtained from all the palaeomagnetic data of Southwest Japan. Dotted line shows a possible path of polar wondering.
c: Cretaceous, p: Palaeogene,
m: Miocene, pl: Pliocene-Pleistocene,
c_k: Cretaceous pole obtained from South Korea.

Fig. 2

A possible reconstruction of
Cretaceous SW Japan.
A: Latitude 41°N for the Cretaceous
pole obtained from South Korea.
K: (128.6°E, 35.7°N)
J: (134°E, 35°N)

GEOMAGNETIC PALEOINTENSITIES IN THE CENOZOIC

Masaru KONO

Geophysical Institute, University of Tokyo, Bunkyo-ku, Tokyo 113, Japan.

1. Paleointensity Methods

Paleointensity methods used on TRM-bearing materials such as baked earths or igneous rocks can roughly be divided into five categories; they are, (i) NRM method based on the comparison of NRM intensities among rocks formed under similar conditions, which was recently applied very extensively to the Tertiary lavas of Iceland by Dagley and Wilson (1971), (ii) Königsberger's (1938) method of total NRM/TRM ratios, (iii) van Zijl et al.'s (1962) method of ratios of partial NRM to partial TRM with the same coercivities, (iv) Wilson's (1961) method of partial NRM to partial TRM with the same blocking temperatures, and (v) the Thelliers' method (Thellier and Thellier, 1959) using the double-heating technique.

All of these methods are based on the linearity of TRM (or partial TRM) in a weak magnetic field. But the reliability of data is considerably different among these methods. We shall not discuss the NRM method further, since this method is intended to give statistical measures of fluctuations rather than the absolute values of paleointensities.

The most important sources of errors in paleointensity experiments other than the non-linearity of TRM are, (i) the VRM effect, or the existence of secondary component of magnetization superposed on the primary NRM, (ii) the natural alteration effect, such as maghemitization of NRM-bearing titanomagnetites taking place in a prolonged time at low temperatures in nature (Ozima, 1971), and (iii) laboratory chemical change effect, or oxidation or reduction of the ferromagnetic minerals caused by heatings in a laboratory. Spontaneous decay of NRM may be included in (i) by considering a VRM component directed opposite to the NRM.

Data obtained by Königsberger's method are liable to large errors as it does not take these factors into account. The VRM effect can be minimized in van Zijl's or Wilson's methods by using partial NRM's and TRM's with higher coercivities or blocking temperatures. Since titanomaghemites are extremely unstable to heat treatments, it is relatively easy to distinguish and discard such naturally altered samples if comparison is made between the coercivity or blocking temperature spectra of NRM and TRM rather than between the single partial NRM and TRM. Thus it may be said that these two methods are safe from the VRM and the alteration effects. However, NRM/TRM ratios are obtained in these methods only after a sample is heated to a temperature higher than the Curie point. If the TRM capacity of a sample is increased or decreased by heatings in a laboratory without much change in the coercivity or blocking temperature spectra of TRM, the results by these two methods are erroneous and yet give one an impression of reliability because of the internal consistency of the data.

The Thellier's method, on the other hand, employs two heatings to a

same temperature T to determine the NRM component with blocking temperatures T_B higher than T and the TRM component with T_B less than T (see Fig. 1). The temperature T is successively raised until the Curie temperature T_c is reached, but the NRM/TRM ratios can be determined even while T is lower than T_c from the slope of the linear relation in the Arai's diagram (NRM-TRM diagram). The VRM and the chemical change effects appear in the NRM-TRM diagrams as deviations from the ideal linear relations at low and high temperatures, respectively, while the altered samples will not show any linear relations between the NRM and TRM components. Only the data obtained by the Thelliers' method are therefore free from errors caused by the VRM, natural alteration, and laboratory chemical change effects.

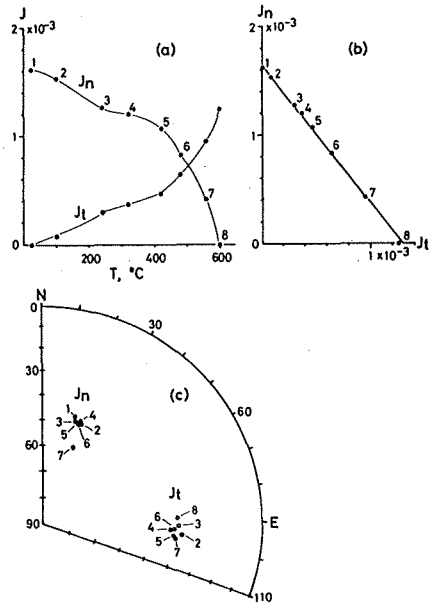

Fig. 1. An example of a nearly ideal result from the Thelliers' method (sample: recent pyroclastic rock from Mt. Asama). (a) decay and acquisition of NRM(J_n) and TRM (J_t). (b) Arai diagram. (c) Change of magnetization directions at various temperatures.

Many people tried to modify van Zijl's and Wilson's methods of paleointensity determination by adding measurements of some of the magnetic properties before and after the heating. The quantities measured are such as saturation magnetization J_s, susceptibility X, saturation IRM, and so on. (See, e.g., Symons and Schwarz, 1970; McElhinny and Evans, 1968; York et al., 1971). The idea is that changes in TRM characteristics may be monitored by changes in other magnetic properties of the same rock. Carmichael (1967) even used the ratios of saturation IRM before and after heating to modify the experimental NRM/TRM ratios to obtain the paleointensity. But such treatments are by no means sufficient. In fact, a change in TRMcharacteristics is usually not directly related to the changes in J_s, X, or saturation IRM. It is often noticed that if changes were induced by heating in air, most volcanic rocks show more pronounced changes in TRM capacity than in other magnetic properties such as J_s.

2. Representation of Paleointensity Data

If we take the International Geomagnetic Reference Field at 1965.0 (IGRF65) as representative of the present geomagnetic field, we see that the field intensities on the surface of the earth has a rather broad spectrum as shown in Fig. 2a. The dispersion, of course, is caused by both the dipole and the non-dipole components of the IGRF65. However, if we refer to Fig. 3a, we may safely conclude that the contribution of the non-dipole components to the dispersion of field intensities is small compared to that of the dipole component. Fig. 3a shows that the mean field intensity at each latitude circle (circles) is quite close to the intensity expected from an axial, centered

dipole of magnitude 8 x 10^{25} gauss cm^3 (broken line). The standard deviation around each latitude mean (vertical bars) is considerably larger in the southern hemisphere than in the northern hemisphere, indicating the relative magnitudes of non-dipole field in the IGRF65 in both hemispheres. The fit of the latitude mean values to the dipole scheme may be made better by taking the geomagnetic latitudes and the inclined dipole instead of the geographic latitudes and the axial dipole, respectively.

On the other hand, if we compute intensities of dipoles at the center of

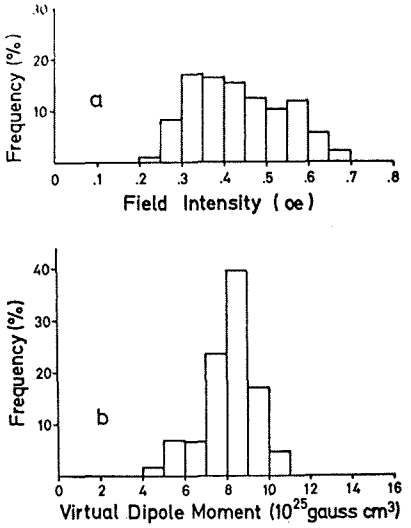

Fig. 2. Histograms of (a) field intensities and (b) the virtual dipole moments(VDM) on the surface of the earth of the IGRF65.

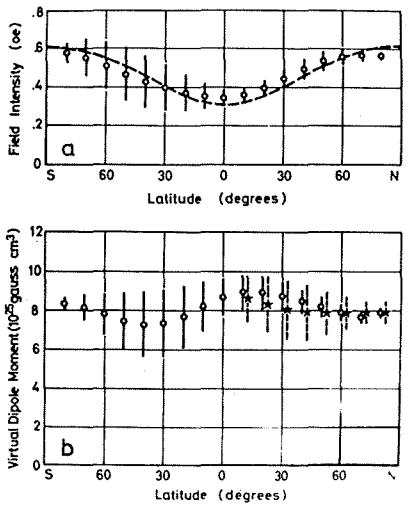

Fig. 3. Latitude means with standard deviations (circles and bars) of (a) the field intensity and (b) the VDM. The broken line in (a) is the values expected from the axial dipole model. Stars and broken bars are the mean and standard deviations for both of the hemispheres.

the earth which would produce the field intensity F, the inclination I, and the declination D of IGRF65 at individual point on the surface of the earth by the dipole formula

$$VDM = \tfrac{1}{2}Fr^3 (1 + 3 \cos^2 I)^{\frac{1}{2}}$$

such moments have a much more peaked distribution confined to a narrower range and of the shape similar to the Gaussian distribution (Fig. 2b). We shall call such a dipole defined at one point by F and I a virtual dipole moment (VDM).

The latitude mean of VDM changes only in the range of $\pm$ 10 % (Fig. 3b) compared to more than $\pm$ 30 % for the field intensity F, and moreover the standard deviation from the latitude mean is almost always smaller for the VDM than for F. These results indicate that the VDM can be a good method of

representation of paleointensity data if the paleomagnetic field was made of dipole and non-dipole components of which the relative importance and the latitude dependence are similar to those of the present geomagnetic field. But the paleosecular variation studies show that the situation was exactly so for at least several million years before present. Doell and Cox (1971 and many other related papers) showed that the values of angular dispersions of the paleomagnetic data of the upper Pliocene and Pleistocene from many places in the world can be accounted for by a model composed of an wobbling, inclined dipole and a non-dipole field which is drifting westwards. The relative magnitudes of the dipole and non-dipole fields are thought to be the same as that of the present geomagnetic field.

Although statistically insufficient, paleomagnetic data from the older Cenozoic also suggest a similar nature of the magnetic field if the possible movements of the landmasses are taken into account. We are therefore entitled to use the VDM representation of paleointensity data. A direct comparison is possible between the data of different ages and places, once we adopt the dipole hypothesis.

3. Cenozoic Paleointensity Data

Fig. 4 shows frequency histograms of the Cenozoic paleointensity data obtained by various authors by the Thelliers' method. These include data from normal or reversed polarities as well as those from transitional periods (black). Three points call our attention. The first is that the average values of VDM and their dispersions for individual subperiods except the Brunhes normal epoch are almost the same. The second is that the average paleointensity for the Brunhes epoch was about 50 % larger than the averages of other periods. And the third is that the intensity was substantially smaller when the geomagnetic field was either reversing or undergoing an excursion.

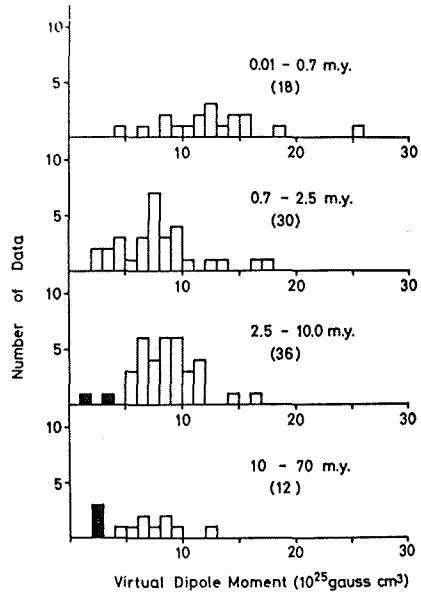

Fig. 4. Histogram of paleointensity data obtained by the Thelliers' method. White portion is for a normal or reversed data, black for data of intermediate polarity. Numbers in brackets indicate the tatal number of data for each interval. Data are obtained from Kono (1971, 1974) and Coe (1967).

If we combine the data for the last 10 m.y. using appropriate weights to make the sampling density uniform in this period, the resulting histogram of VDM's closely resemble a normal curve.(Kono, 1971). The mean and the standard deviation of this distribution is 8.9×10^{25} gauss cm^3 and 3.4×10^{25} gauss cm^3 or 38 % of the mean, respectively. Since the standard deviation of the experimental errors in the Thelliers' method is usually about 10 % and that due to the non-dipole field is

typically about 15 % (see Fig. 3), the standard deviation of about 30 % or more should be accounted for by the change in the dipole intensity itself in this period.

It may be premature to draw serious conclusions from small number of data, but it seems that the VDM has been not much different from the present value of 8.0×10^{25} gauss cm^3 throughout the Cenozoic if we are interested only in long-range averages of a few million years or more.

4. Discussion

Summarizing the paleointensity data and also other paleomagnetic information for the Cenozoic, we obtain an image of a binary structure of the geomagnetic field in this period. That means, except a small fraction of time when the field was reversing or in excursion, the geomagnetic field has been in either of the normal or reversed dipolar states with nearly the same field intensity (when averaged over sufficiently long time interval).

This picture is quite different from that of Smith (1967), whose compilation is based mostly on paleointensity data obtained by methods other than the Thelliers'. While Smith suggests a steady increase in the dipole strength for the last 400 m.y. and that the present day intensity is much stronger compared to the older periods, including the Tertiary, our compilation suggests an almost flat curve at least for the Cenozoic. It is quite conceivable that Smith's data give systematically low paleointensities because of the chemical change of ferromagnetic minerals in the heating experiments. As discussed earlier, changes in TRM capacity of volcanic rocks by heating in air are predominantly to increase the capacity. It may be concluded that such summary based on data obtained by less reliable methods should not be toomuch trusted.

Acknowledgments

This study was initiated while I kept a visiting fellowship at Cooperative Institute for Research in Environmental Sciences, University of Colorado/ National Oceanic and Atmospheric Administration (NOAA), Boulder, Colorado, U. S. A.

Partial financial support from Kudo Foundation is gratefully acknowledged.

References

Carmichael, C. M. (1967) Earth Planet. Sci. Lett. 3, 351.
Coe, R. S. (1967) J. Geophys. Res. 79, 3247.
Dagley, P. and R. L. Wilson (1971) Nature Phys. Sci. 232, 16.
Doell, R. R. and A. Cox, (1971) Science 171, 248.
Königsberger, J. G. (1938) Terr. Mag. Atmos. Elect. 43, 119 and 299.
Kono, M. (1971) Earth Planet. Sci. Lett. 11, 10.
Kono, M. (1974) J. Geophys. Res. 79, in press.
McElhinny, M. W. and M. E. Evans (1968) Phys. Earth Planet. Inter. 1, 485.
Ozima, M. (1971) Earth Planet. Sci. Lett. 13, 1.
Smith, P. J. (1967) Geophys. J. 12, 321.
Symons, D. T. A. and E. J. Schwarz (1970) Canad. J. Earth Sci. 7, 176.
Thellier, E. and O. Thellier (1959)Ann. Géophys. 15, 285.
Van Zijl, J. S. V., K. W. T. Graham and A. L. Hales (1962) Geophys. J. 7, 23 and 169.
Wilson, R. L. (1961) Geophys. J. 5, 45.
York, D., D. W. Strangway and E. E. Larson (1971) Earth Planet. Sci. Lett. 11, 333.

AN ATTEMPT OF PALEOINTENSITY DETERMINATION ON PERMIAN PORPHYLLITES AND TERTIARY GRANODIORITES

Masaru KONO[1] and Nazario PAVONI[2]

1) Geophysical Institute, University of Tokyo, Bunkyo-ku, Tokyo, Japan
2) Institute fur Geophysik der ETH, Postfach 266, CH-8049, Zurich, Switzerland

1. Introduction

The Thelliers' method (Thellier and Thellier, 1959) was applied to six samples collected from Switzerland. Preliminary thermomagnetic analyses show that these rocks contain ferromagnetic minerals which have Curie points near that of magnetite. Three of them belong to the Permian age and three to the Triassic (Table 1).

Table 1 Samples

Sample No.	Rock Type	Age	Locality
P11, P13, P20	Porphyllite	Permian	Lugano area, Switzerland
A14	Granodiorite	Triassic	"

The samples were heated in a step of 100°C to progressively higher temperatures in air in the presence of the geomagnetic field (0.46 oe in Kakioka Laboratory). NRM and TRM components were obtained from the vector sum and difference of the two measurements of remanent magnetization after the heatings to the same temperatures. These experimental procedures are the same as described in Kono and Nagata (1968).

2. Results

Fig. 1 shows the changes in the direction of the NRM components by thermal demagnetization of the Thelliers' method. Samples P11 and P13 are quite stable to thermal demagnetization and the direction of the NRM component does not change appreciably to 500°C. Other samples are not so stable. In the samples P20 and A14FA, changes in the NRM directions are about 40° while changes of almost 180° were observed for AF14FA and AF14FB. This indicates a predominance(for samples AF14FA and AF14FB) or at least a partial existence (for P20 and A14EB) of soft magnetization in the NRM of the four samples.

Decay of NRM by thermal demagnetization and acquisition of partial TRM at each temperature in the Thelliers' experiment is illustrated in Fig. 2. Obviously the greater part of the partial TRM in each sample is acquired between 500 and 600°C suggesting a sharp peak in the blocking

temperature spectrum . The ferromagnetic minerals may have under gone some chemical changes with an increase in TRM capacities due to heating to 600° C in air. But even if we suppose that the original

Fig. 1

Larger circles are the original NRM directions, and smaller circles are for NRM components at 1 0°, 200° 300°, 400° and 500°C in thermal demagnetization. The position of the original NRMs in the diagram is arbitrary.
Equal area Projection.

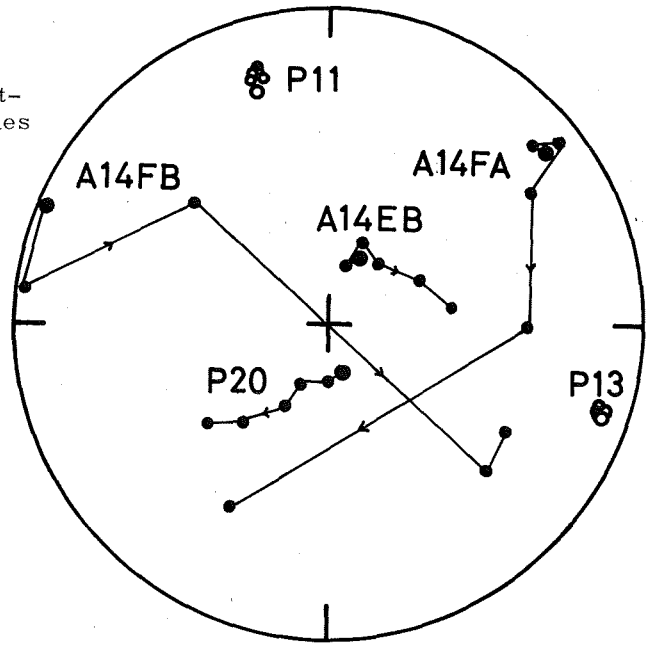

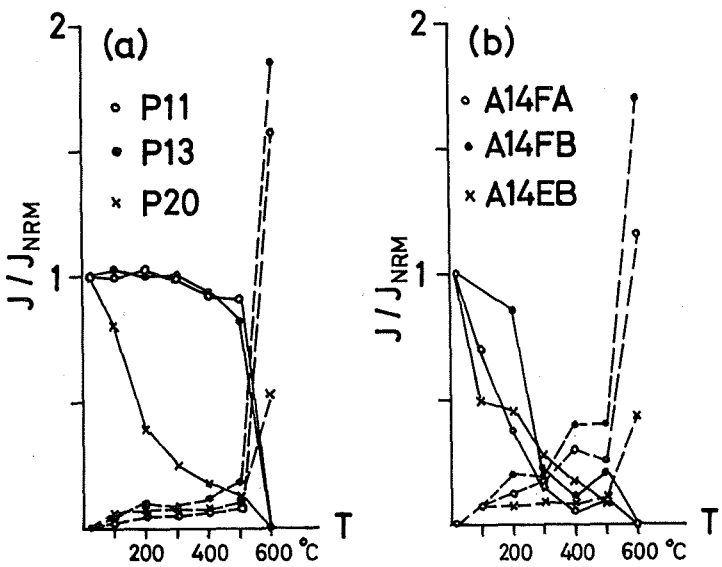

Fig. 2

Decay of NRM component (solid lines) and acquisition of partial TRM component (Broken lines), at each stage of the Thelliers' method.
(a) Permian porphyllite samples.
(b) Triassic granodiorite samples.

TRM capacity at 600°C is only 1/3 of what is actually observed, (this may be an underestimate, see Fig. 3) more than half of the TRM should have been acquired in the temperature interval 500° - 600°C. Therefore, if the NRM in these samples is of thermoremanent origin, we should expect in thermal demagnetization of NRM at first a gradual decrease of magnetization until 500°C and a big decrease in the interval 500°C - 600°C. The demagnetization curves for P11 and P13 shows this is really so. However, NRM components decreases rapidly at low temperatures in other samples. By comparison of Figs. 1 and 2, it can be concluded that the NRM's of P11 and P13 are of TRM origin, while those of the other samples are predominantly secondary soft magnetizations.

The Arai diagram (NRM-TRM diagram) for P11 and P13 is shown in Fig. 3. For the sample P11, the experimental points except for 600°C cluster close to the NRM point and it is difficult to obtain a linear relation between NRM and TRM. For the sample P13, on the other hand, the point corresponding to 100, 200, 300, 400 and 500°C align on a straight line with a gradient of -1.52. The deviation of the NRM point may indicate the

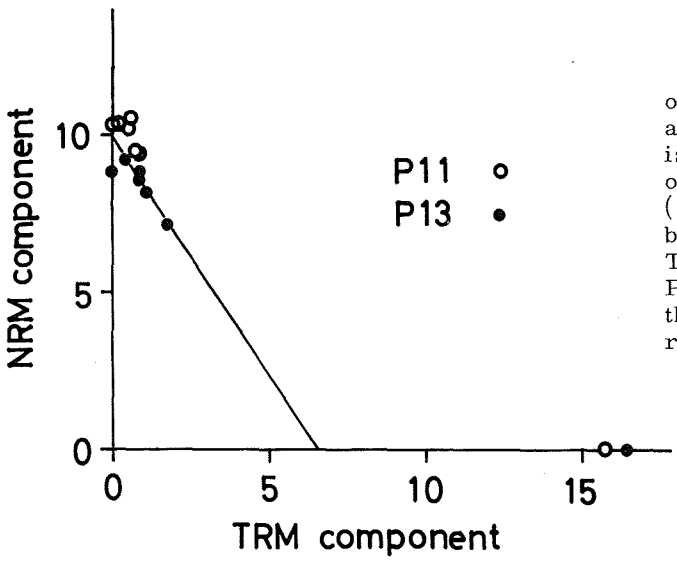

Fig. 3

NRM-TRM diagram of the samples P11 and P13. Solid line is the best estimate of the linear relation (gradient = -1.52) between the NRM and TRM components of P13 obtained from the points in the range 100 - 500°C.

superposition of VRM component with low blocking temperatures. The deviation of 600°C point (on the TRM axis) may be a result of increase in TRM capacity. It is interesting to note that the points for P11 (except that for 600°C) seem to align on nearly the same regression line.

3. Discussion and Conclusion

Six samples from Switzerland were treated by the Thelliers method. Of these, three Triassic granodiorite and one Permian porphyllite samples had NRM predominantly of soft, secondary magnetization. Samples P11 and P13 of Permian porphyllite had NRM of TRM origin. Although the points for 600°C of both samples deviate greatly from the probable linear line

formed by the points between 100° and 500°C, this may indicate an increase of TRM capacity by heating to 600°C. If we adopt the linear line for the sample P13 to be indicative of the geomagnetic field at the time the rock was formed, the paleointensity was 0.70 oe. Other pertinent data for P11 and P13 are summarized in Table 2.

Table 2

Sample	Incl. I deg.down	Decl. D deg. east	NRM/TRM	-b	F oe
P11	-36.8	235.4	.65	-	
P13	41.6	302.1	.539	1.52	.70

References

Kono, M. and T. Nagata (1968) J. Geomag. Geoelect. 20, 211.
Thellier, E. and O. Thellier (1959) Ann. Géophys. 15, 285.

SHIN'ETSU-BOZU ZONE, THE BOUNDARY AREA BETWEEN NORTHEAST AND SOUTHWEST JAPAN

Noboru YAMASHITA

Department of Geology, Faculty of Science, Shinshu University
Asahi-machi, Matsumoto-shi, Nagano-ken

1. Introductory Remarks

Naumann's Fossa Magna, though defined well in the west by the Itoigawa-Shizuoka Tectonic Line, is vague and ambiguous in the east. Kobayashi's Kwanto Tectonic Line or Mochizuki's Tonegawa Tectonic Line, however it is burried deep beneath the younger sediments, is not thoroughgoing, because its northwestern extension has never been pointed out by any scientist. Various basement rocks narrowly exposed or barely detected in certain boreholes of this area and also the overlying younger sediments have hitherto been unaccountable or confusing from the viewpoint of geotectonics. These complexities and ambiguities are explained more reasonably by the writer's Shin'etsu-Bozu Zone and the Kashiwazaki-Choshi Tectonic Line.

2. Historical Review of Geotectonic Studies of the Area

The name of the Fossa Magna was proposed by Naumann(1893) who made several times of geological excursion in this area(Fig.1). He was impressed with the N-S trending Yatsugatake Volcanic Chain which ran at right angles with the E-W trending Kanto (Kwanto) Mountainland to the east. He emphasized the peculiar, transverse zone of the Fossa Magna that divided the Japan Arc into Northeast and Southwest Japan. He regarded the Fossa Magna as a result of collision of the southeastward drifting Japan Arc with the Shichito Arc in front.

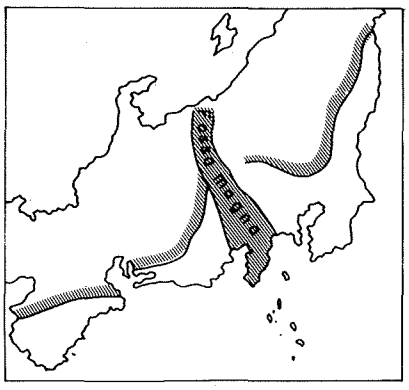

Fig.1 Fossa Magna of Naumann

Harada(1888), one of the followers of then influential Suess, gave the name of the Fuji Zone to the same area as that of the Fossa Magna, and regarded it as an example of "Scharung". In other words, he considered Northeast and Southwest Japan as two, simultaneous but independent mountain systems. Northeast Japan, according to Harada, is the southern extension of the Sachalin System, while Southwest Japan belongs to the Chinese System.

Ogawa(1899) had advantages to get much data and experience of geological survey. He presented a new name of the Central Japan Transverse Rift Zone for that area. His most important contribution was that he pointed out the age of the Rift Zone to be Palaeogene. He noticed that the oldest rocks filling up the Rift Zone were the Neogene, while the youngest of the separated rocks in the Akaishi and Kanto Mountainlands were the Cretaceous.

This estimation of age, though later corrected to be post-Palaeogene and pre-Neogene, was one of the results of the comprehensive survey commanded by the Geological Survey of Japan. About fifty of one hundred sheets of geological map in scale 1:200,000 had been published at that time of Ogawa's paper.

The Itoigawa-Shizuoka Tectonic Line was named by Yabe in 1918. The Neogene sediments in the Fossa Magna especially in its northern part were studied and compiled for the first time by Homma(1931). We owe to him such standard stratigraphic names as the Moriya, Uchimura, Bessho, Aoki, Ogawa and Shigarami Formations, that are still in current use. His opinion on the origin of the Fossa Magna is interesting, though it seems to have been taken as curious or rather odd. He considered that the Fossa Magna was formed by depression of the area after the preceding upwarping, and that the simatic crust was exposed to be covered later with the Neogene sediments.

Kobayashi(1941) noticed the remarkable difference in structural trend between the Kanto Mountainland in the southwest and the Ashio, Yamizo and Abukuma Mountainlands in the northeast, and proposed the Kwanto Tectonic Line for the supposed boundary line in between (Fig.2). Since the Kanto Mountainland belongs to the Outer Zone of Southwest Japan, he took the tectonic line to be also the boundary between Northeast and Southwest Japan. At the same time, he commented that the boundary was applicable only to the pre-Neogene geology, while the Itoigawa-Shizuoka Tectonic Line should be taken as the Northeast-Southwest boundary for the Neogene and Quaternary geology. Mochizuki(1950) used the name of the Tonegawa Tectonic Line, but it is essentially the same as the Kwanto Tectonic Line.

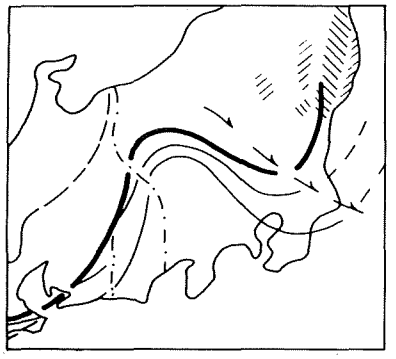

Fig.2 Kwanto Tectonic Line of Kobayashi(arrows)

After the World War II geological investigation of the Japanese Islands developed generally and rapidly, and new important data concerning the basement of the Kanto Plain were obtained. It enabled Ishii(1962) to depict, though somewhat inconclusively, the Median Tectonic Line and the Mikabu Line beneath the younger sediments of the Kanto Plain. Later in 1968 Isomi and Kawada also presented a tectonic map of this area. Their illustrations are reproduced to avoid tedious introductions(Figs.3 & 4).

3. The Kashiwazaki-Choshi Tectonic Line as the Southern Limit of Northeast Japan

In 1964 the writer, consulting then existing data, distinguished, in the southern half of Northeast Japan, several, meridional zones of horsts and grabens separated from each other by remarkable tectonic lines. And he realized that the Kwanto Tectonic Line marked the southern limit of Northeast Japan characterized by the meridional zones. In this point of view the Niigata Oil Field was one of the meridional zones that had sunk to receive Neogene and Quaternary sediments. The apparent continui-

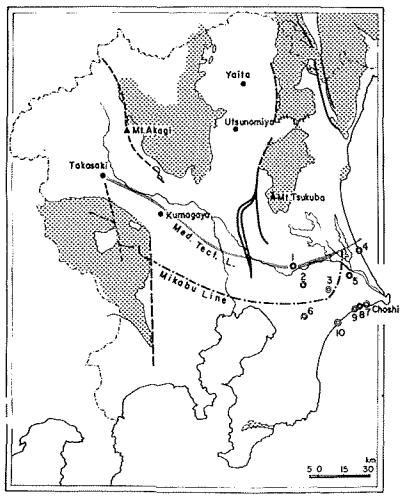

Fig.3 Basement structure of the Kanto area(Ishii, 1962)

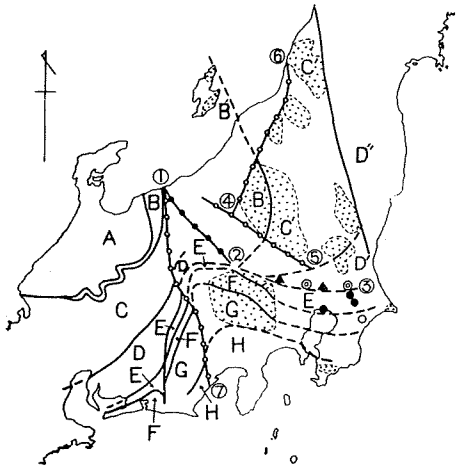

Fig.4 Basement structure on both sides of the Fossa Magna (Isomi et Kawada, 1968)

ty of the younger sediments of the Niigata Oil Field and those of the northern Fossa Magna had long dazzled the eyes of geologists, and had concealed the boundary line between the two provinces. Thus the Kwanto Tectonic Line was extended to pass somewhere around Kashiwazaki, and was renamed the Kashiwazaki-Choshi Tectonic Line(Yamashita, 1970). Consequently the difference of the younger sediments between the two provinces in rock facies, structural features and oil production emerged, and the tectonic line itself came out of the depths in the form of ultramafic rocks from the bottom of boreholes(Inoma, 1971).

The Kashiwazaki-Choshi Tectonic Line marks not only the southern limit of Northeast Japan, but also the limit of another province to the south, i.e. the Shin'etsu-Bozu Zone, which, in turn, is limited in the west by the well-known Itoigawa-Shizuoka Tectonic Line. The complexities and ambiguities are confined almost within the Shin'etsu-Bozu Zone, and are not conspicuous beyond the limits.

4. Data Concerning the Basement of the Shin'etsu-Bozu Zone

The Shin'etsu-Bozu Zone is a subsided area filled with the Neogene and Quaternary sediments and volcanics. There,as is usual in Japan, a remarkable unconformity is widespread beneath the Neogene sequence. Therefore the Kanto Mountainland consisting mainly of pre-Neogene rocks is just like an island above the sea of younger sediments and volcanics. Other examples of similar mode of occurrence are as follows.

A narrow belt of Palaeogene formations makes the Mineoka Mountains in southern Boso Peninsula. The rock facies of the Palaeogene is quite indistinguishable from that of the correlative Setogawa Formation in the southern Akaishi Mountainland. The small Matsuyama Hills immediately to the east of the Kanto

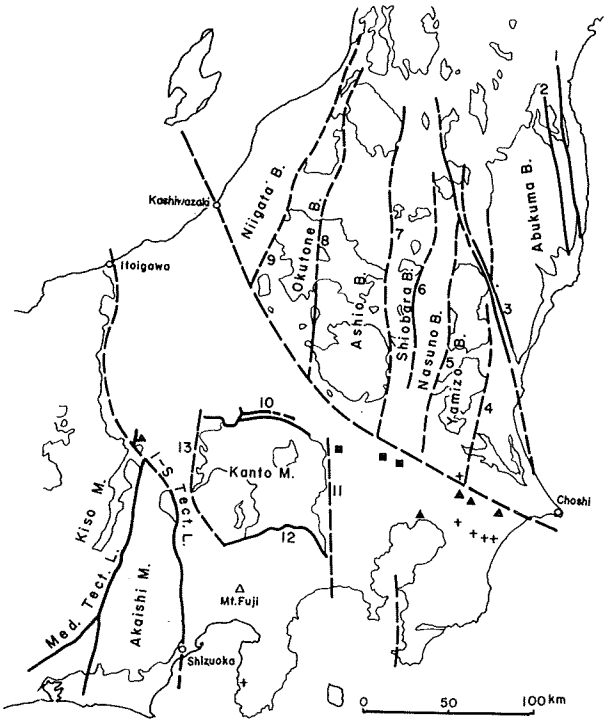

Fig.5 Shin'etsu-Bozu Zone and the meridional belts of southern Northeast Japan (Yamashita, 1970)

1: Iwanuma-Hisanohama Line
2: Hatagawa Sheared Zone
3: Tanagura Sheared Zone
4: Daigo-Ishioka Line
5: Shirakawa-Moka Line
6: Yaita-Utsunomiya Line
7: Kanuma-Tochigi Line
8: Katashina Tectonic Zone
9: Shibata-Koide Line
10: Shimonita Tectonic Zone
11: Hachioji Line
12: Tonoki-Aikawa Line
13: Iwamurata-Wakamiko Line

▲: crystalline schists
■: gneisses
+: clastic sediments

Mountainland are important, for there are gneisses that are unknown in the adjacent Kanto Mountainland.

Near the west margin of and still inside the Shin'etsu-Bozu Zone crystalline schists belonging to the Sambagawa Metamorphic Rocks are exposed in the Yokokawa Valley to the northwest of Lake Suwa. The western margin of this exposure is meridionally straight(Yoshino, 1973, MS), and represents the extension of the Median Tectonic Line. The Line is offset in relation to that in the Akaishi Mountainland about 10 km northwestward along the NW-SE trending Itoigawa-Shizuoka Tectonic Line. In this connection, another section of the Median Tectonic Line was recognized recently by the writer and his colleagues along the northern margin of the Kanto Mountainland. Here, it is represented by a fault along the southern side of the Shimonita Tectonic Zone (Arai et al., 1966).

Data from boreholes of this area are shown in Figure 5 by symbols.

5. Relation Between Northeast and Southwest Japan

In the southern half of the Shin'etsu-Bozu Zone the island-like exposures of older rocks and the rock specimens from the deep boreholes make it possible to draw a sketch of the basement structure. Among the data from boreholes the most reliable are the crystalline schists that are regarded as of the Sambagawa Belt. They are distinct from others and are not confusing. Such

clastic sediments, however, as sandstones and slates are often misleading for discrimination of formations and ages. Palaeozoic and Mesozoic rocks, in many cases, are hardly distinguished from each other even at exposures on land surface.

The gneisses from boreholes of Kasukabe and Matsubuse together with those of the Matsuyama Hills are interesting. Their positions to the north of the inferred Sambagawa Belt suggest that they belong to the Ryoke Metamorphic Belt, which, in Southwest Japan, is characterized by gneisses and granites, and bordered on the south by the Sambagawa Belt. But the petrographic characters of the gneisses from the Matsuyama-Kasukabe-Matsubuse area are somewhat different. Moreover, the metamorphic grade of the Ryoke Belt in the Kiso Mountainland lowers toward northeast, and the rocks there are represented by hornfelsic slates. It suggests that the gneisses of the Ryoke Belt and those of the Matsuyama-Kasukabe-Matsubuse area are not continuous.

The Abukuma Belt of southern Northeast Japan is characterized also by gneisses and granites. Accordingly the writer once grouped the Ryoke and Abukuma Belts into the Honshu Axial Plutonic and Metamorphic Belt(Yamashita, 1957), which was characterized by high-temperature and low-pressure conditions of metamorphism. Certain differences in geology and petrography, however, are also recognized between the two Belts. The gneisses of the Matsuyama-Kasukabe-Matsubuse area are different from those of the Ryoke and Abukuma Belts. The writer is now of the opinion that they are the links between the Ryoke and Abukuma Belts that are related with but different from each other.

In any case, the structural belts of Southwest Japan are traced, though not convincingly, to the area of the Kanto Plain by way of the Kanto Mountainland. But none of them goes over the Kashiwazaki-Choshi Tectonic Line, except the Axial Belt of the Ryoke and Abukuma Belts.

In the northern half of the Shin'etsu-Bozu Zone no data of the basement rocks are available from boreholes except the ultramafic rocks near Kashiwazaki. But the relation between Northeast and Southwest Japan across the Shin'etsu-Bozu Zone is more evident than in the southern area. The evidence is sufficient in the Okutone Belt at the southwestern corner of Northeast Japan.

The Joetsu Metamorphic Rocks(Hayama et al., 1969) that have largely been replaced by granites of the Okutone Belt are composed of green schists, and are correlated undoubtedly to the Sangun Metamorphic Rocks of Southwest Japan, of which the easternmost exposures are found in the southwest of Itoigawa. The lower Jurassic Iwamuro Formation of the Okutone Belt is identical with the Kuruma Formation to the south of Itoigawa in its rock facies and fossil contents. The lower Cretaceous Tokurazawa Formation of the Okutone Belt is a series of lake deposits with fossils of Corbicula tetoriensis, a fresh-water bivalve, and is an unmistakable equivalent of the Tetori Group in the Hida Plateau. Thick and extensive acidic volcanics with welded tuffs of late Mesozoic to early Cainozoic ages are generally found in the inner side area of Southwest Japan, while correlatives are known in the southern part of the Ashio and Shiobara Belts of Northeast Japan.

Such correlative formations as enumerated above on both sides of the Shin'etsu-Bozu Zone relate eloquently the original continuity of Northeast and Southwest Japan that are now separated.

6. Concluding Remarks

From the above lines it is clear that the Shin'etsu-Bozu Zone is a unique province that should be distinguished from either of Northeast and Southwest Japan, and is a boundary area between them. Also it is evident that Northeast and Southwest Japan had been continuous but somewhat different from each other during the long history from late Palaeozoic to early Cainozoic. It means that conditions had been prepared long since for the birth of the Shin'etsu-Bozu Zone.

The Shin'etsu-Bozu Zone, though not commented in this paper, represents also the intersecting area of two island arcs, i.e. the Honshu Arc and the Shichito-Mariana Arc. The latter, as discussed in another paper to be published soon, has also a long history of development beginning at an age not later than Eocene (early Cainozoic).

References

Arai, F. et al. (1966) Earth Sci. No.83, 8.
Harada, T. (1888) Versuch einer Geotektonischen Gliederung der Japanschen Inseln.
Hayama, Y. et al. (1969) Mem. Geol. Soc. Japan No.4, 61.
Homma, F. (1931) Geology of Central Shinano Province.
Inoma, A. (1971) J. Geol. Soc. Japan 77, 757.
Ishii, M. (1962) J. Japan. Ass. Petrol. Geol. 27, 405.
Isomi, H. et Kawada, K. (1968) Fossa Magna 4.
Kobayashi, T. (1941) J. Fac. Sci., Imp. Univ. Tokyo II, 5, 219.
Mochizuki, K. (1950) J. Geol. Soc. Japan 56, 285.
Naumann, E. (1893) Petermanns Mittheil Ergaenzungsheft Nr.108.
Ogawa, T. (1899) J. Geogr. Soc. Tokyo 11.
Yabe, H. (1918) Modern Sci.(Gendai no Kagaku) 6, 147.
Yamashita, N. (1957) Geosci. Ser. Ass. Geol. Collab. Japan No.10.
Yamashita, N. (1970) Island Arcs and Oceans 179.

K-Ar AGES OF SIX DSDP LEG17 SAMPLES

Kazuo SAITO and Minoru OZIMA

Geophysical Institute, University of Tokyo
Bunkyo-ku Tokyo

1.Introduction

Six samples of DSDP Leg17 were dated by conventional K-Ar dating method. Location of the sampling sites and others are shown in Table 1 and Figure 1.

The absolute age of these samples are interesting from following reasons. First, since the sampling site of the sample DSDP-165 is close to the Line islands, the comparison of the age with those of the islands would offer unique test to examine the hypothesis of hotspot origin of these islands posturated by Morgan (1972). Second, since geomagnetic anomaly lineations around these sampling sites have not been well observed, the K-Ar dating of submarine rocks would be an only way to determine the absolute age of the ocean floor. Recently Larson and Chase (1972) reported the geomagnetic anomaly lineations near this region, but lineation pattern around this region are so complicated that simple extrapolation of the lineation does not resolve the geochronological structure of the ocean floor.

2.Results

DSDP-167-a and -b are obtained from the same drilled core at different levels.DSDP-167-c is from the same hole as DSDP-167-a and -b, but from a different core. It is remarkable that in spite of the large differences in their K content, the K-Ar ages show good concordance. The large difference in the K content may indicate that these samples are from different lava flows. However, concordant K-Ar ages strongly suggest that these samples are contenporaneous, the age being about 100 m.y. However,the K-Ar age is much younger than the fossil age of the overlying sediments. This discrepancy cannot be explained either by argon loss or secondary K fixation (Ozima and Saito), since it would be too fortuitous that the samples of very different K content show such an excellent concordance in K-Ar ages. The discrepancy may be explained if either 1) the basalt is intrusion or 2) the overlying sediments were reworked.

Both samples DSDP-165 and -170 show the similar discrepancy with the fossil age. However, because of a single analysis, it is difficult to judje whether this discrepancy is due to argon loss or to other causes.

The K-Ar age of DSDP-169 shows an order of magnitude younger than the fossil age. Thermomagnetic analysis of this sample (Joshima, private communication, 1973) shows an almost reversible thermomagnetic curve indicating that the ferromagnetic constituents are essentially titanomagnetites. The latter observation does imply that the sample DSDP-169 may not be as old as hundred million years suggested by the fossil age (Ozima and Joshima, submitted to Nature)

3.Conclusions

K-Ar ages of DSDP-165, -167, -169 and -170 presented here are much younger than the ages which would be expected by a simple extrapolation of a chronological pattern of the oceanic crust on the basis of the magnetic anomaly lineation pattern proposed by Larson and Chase (1972). These K-Ar ages are also younger than the fossil ages. The discrepancy may be explained as argon loss in the core of DSDP-165 and -170. However, as the data of DSDP-167 and -169 strongly suggest, it is possible that the part of the ocean crust is really as toung as indicated by the K-Ar ages. Further examination of the samples by means of ^{40}Ar-^{39}Ar method is now being in progress.

Acknowledgement

We are grateful to Scrpps Institute of Oceanography for DSDP samples. The K analysis were made by Mr.S.Zashu of Geophysical Institute, University of Tokyo.

References

Geotimes (1971) September, 12.
Larson,R.L.and C.G.Chase (1972) Geol. Soc. Amer. Bull. 83,3627.
Larson,R.L.and W.C.Pitman (1972) Geol. Soc. Amer. Bull. 83,3645.
Morgan,W.J. (1972) Bull. Amer. Assoc. Pet. Geologist 56,203.
Ozima,M.and K.Saito (1973) Earth Planet. Sci. Lett. 20,77.

Table 1

SAMPLE	LOCATION	DEPTH(m)	%K	Ar(10^{-10}) (mol/g)	%Air Ar	K-Ar AGE (m.y.)	FOSSIL AGE
DSDP-165	8°10.7′N 164°51.6′W	5053	1.79	2.16	48.6	67.0	LATE CRETACEOUS
DSDP-167 -a	7°04.1′N 176°49.5′W	3176	0.14	0.270	89.8	105.2	JUR(?) EARLY CRETACEOUS
-b			0.49	0.901	39.8	104.7	
-c			0.77	1.41	36.7	99.4	
DSDP-169	10°40.2′N 173°33.0′E	5415	0.37	0.100	95.0	15.1	EARLY CRETACEOUS
DSDP-170	11°48.0′N 177°37.0′E	5792	0.57	0.707	60.7	69.6	EARLY CRETACEOUS

* The data of location, depth and fossil age are taken from Geotimes (September 1971).

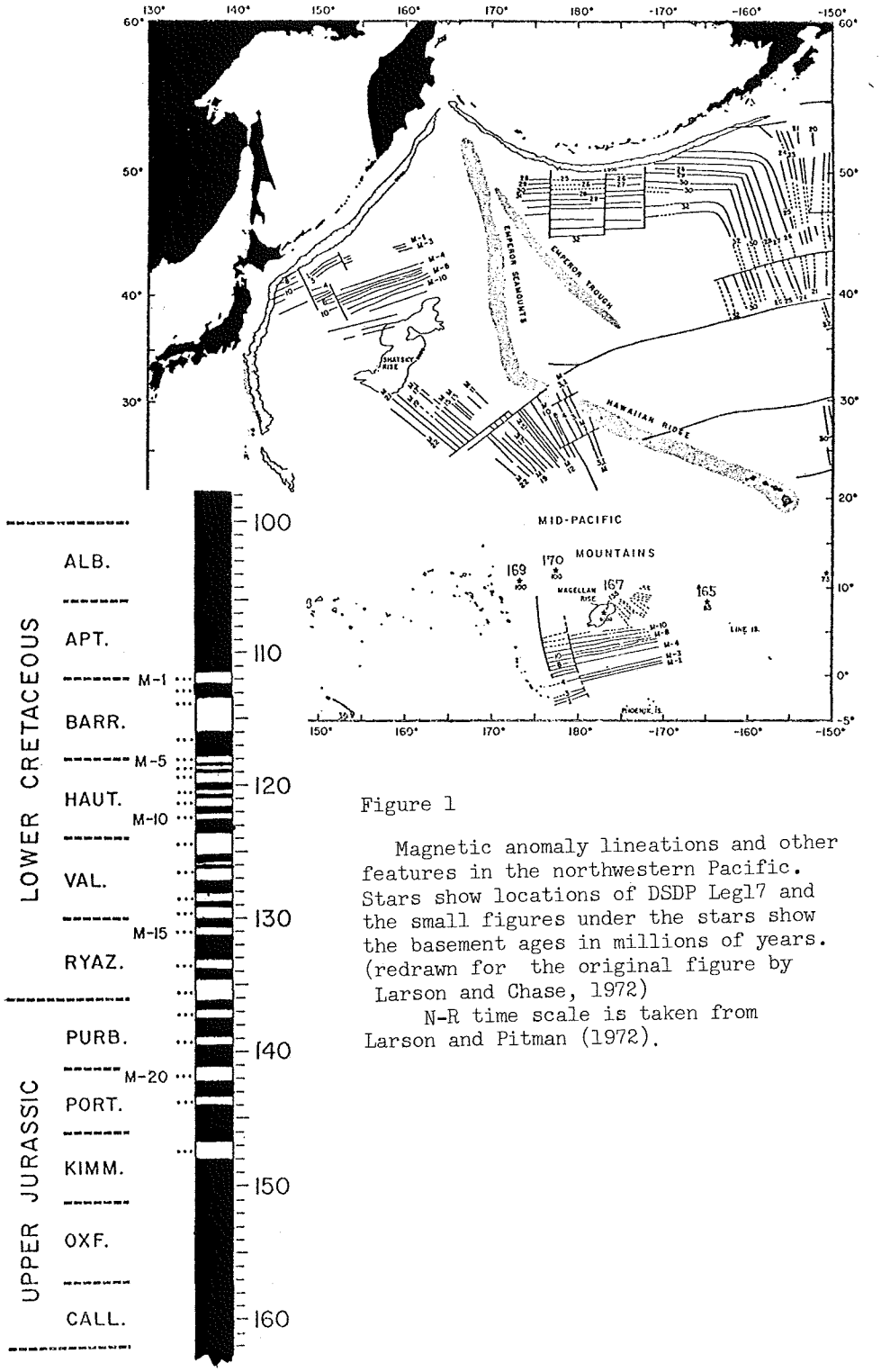

Figure 1

Magnetic anomaly lineations and other features in the northwestern Pacific. Stars show locations of DSDP Leg17 and the small figures under the stars show the basement ages in millions of years. (redrawn for the original figure by Larson and Chase, 1972)

N-R time scale is taken from Larson and Pitman (1972).

ANOMALOUSLY HIGH ($^{87}Sr/^{86}Sr$) RATIO FROM MID-ATLANTIC RIDGE BASALT

Jun-ichi MATSUDA, Sigeo ZASHU, and Minoru OZIMA

Geophysical Institute, University of Tokyo

1. Introduction

It is generally recognized that oceanic basalts yield important informations of mantle materials, because they come directly from the mantle and are generally less contaminated with sialic crustal materials because of the thin oceanic crust. Chemical and isotopic studies have been carried out on these rocks by many authors. (Engel et al., 1965; Gast, 1968; Peterman & Hedge, 1971; etc.) Oceanic basalts may be divided into two groups, that is, ridge basalts and oceanic-island basalts. Ridge basalts are distinguished from oceanic-island basalts in the following respects.

(1) Ridge basalts are more depleted in trace elements than oceanic-island basalts. The depletion is larger for elements with larger ionic radius. (Gast, 1968)

(2) ($^{87}Sr/^{86}Sr$) ratios of ridge basalts range from 0.7010 to 0.7030 having a mean value of 0.7026, whereas ($^{87}Sr/^{86}Sr$) ratios of oceanic-island basalts range from 0.7030 to 0.7060 with a mean value of 0.7038. (Peterman & Hedge, 1971)

Briefly speaking, ridge basalts are generally characterized by both low ($^{87}Sr/^{86}Sr$) ratio and high K/Rb ratio (Hart, 1970). In this paper we report the sample which has anomalously high ($^{87}Sr/^{86}Sr$) ratio and low K/Rb ratio.

2. Samples

AM50 is one of the basalt boulder dredged from the Mid-Atlantic Ridge near 30°N latitude during Atlantis expedition in 1947 (Fig. 1). This sample was provided by Dr. A. Miyashiro, New York State University. Dredging site for sample is shown in Table 1 (Miyashiro, 1969).

Latitude (N)	Longitude (W)	Depth (m)	Note
30°01'	42°04'	4,280	Floor of Junction of Median Valley with Atlantis fracture zone

Table 1 Dredging site of AM50 (Miyashiro 1969)

Since it is within a few tens of kilometers from a ridge, one would assume that it must be very young. However, U-He age is 30±15 m.y. (Kulp, 1953) and fossil age is of lower Miocene (Saito et al., 1966).

Fig. 1 Sample locations

○ AM50 (this paper)
● Alpine-type peridotite (Bonatti et al., 1970)

Recently K-Ar and ^{40}Ar-^{39}Ar age determinations were made on this sample (Ozima & Saito. 1973). K-Ar method gives 198 m.y., whereas ^{40}Ar-^{39}Ar method gives 100 m.y.. The fact that such an old age was observed for rock from the Mid-Atlantic Ridge is very puzzling.

3. Experiment and results

The sample was cut into three specimens, namely, the innermost part, the inner part, and the outer part. These are denoted as AM50I, and II, and III respectively. The ($^{87}Sr/^{86}Sr$) ratio of seawater is about 0.7093. Therefore, if the initial ($^{87}Sr/^{86}Sr$) ratio of AM50 is about 0.7026 (the mean value for ridge basalts) and the sample was contaminated with seawater Sr, we expect to observe that the ($^{87}Sr/^{86}Sr$) ratio of outer part is higher than that of inner part.

However, the results are not as we expected. (Table 2)

Sample	($^{87}Sr/^{86}Sr$)	K (ppm)	Rb (ppm)	Sr (ppm)	K/Rb	Rb/Sr
AM50I	0.7206±0.0004	7040				
" II	0.7210±0.0002	7200	33.8	488	213	0.07
" III	0.7207±0.0001	7760				
Average	0.7208±0.0002	7333				
AM 1	0.7018±0.0001					
AM 5	0.7021±0.0002					

Table 2 ($^{87}Sr/^{86}Sr$), K, Rb, Sr, K/Rb and Rb/Sr of AM50, and ($^{87}Sr/^{86}Sr$) of AM 1 and AM 5

In this table, measurements are made twice for each specimen and the error is the difference between the mean value and the measured values. AM50 has an anomalously high ($^{87}Sr/^{86}Sr$) ratio of 0.7208 which is higher than that of seawater. Hence, we conclude that there is no effect of seawater Sr contamination. Table 2 includes the results for two other dredged samples AM 1 and AM 5 from the same location. In contrast to AM50, they have low ($^{87}Sr/^{86}Sr$) ratios of ordinary ridge basalts.

We measured Rb and Sr contents with an isotope dilution technique, and K content with a flame photometer for AM50II. Although Rb and Sr

contents are rather high, the Rb/Sr ratio is not so high. Using the Sr isotopic ratio development equation

$$(^{87}Sr/^{86}Sr) = (^{87}Sr/^{86}Sr)_o + (Rb/Sr)\ k\lambda t$$

in which k = 2.8936 and $\lambda = 1.39 \times 10^{-11}$ and substituting t = 100 m.y. (^{40}Ar-^{39}Ar age), we can find that the change in ($^{87}Sr/^{86}Sr$) ratio is only 0.0003 during this period. Hence, the observed ($^{87}Sr/^{86}Sr$) ratio of 0.7208 cannot be explained by the aging effect due to the decay of ^{87}Rb in this sample.

K/Rb ratio of AM50 (K/Rb = 213) is rather low. This means that AM50 is not so depleted in Rb compared with K. In this respect AM50 is different from ordinary ridge basalts which are characterized by large depletion in large ion elements.

Among oceanic basalts, alkaline basalts are known to have generally higher values of ($^{87}Sr/^{86}Sr$) than those of tholeiites. (Peterman & Hedge, 1971) However, even for a oceanic alkaline basalts, such a high ratio as 0.7208 has not been reported.

4. Discussion and conclusion

Such an anomalously high ($^{87}Sr/^{86}Sr$) ratio is also obtained for ultramafic rocks from the Mid-Atlantic Ridge which are dredged at near 0°N (Fig. 1). These rocks are peridotites and the highest ($^{87}Sr/^{86}Sr$) ratio is 0.7227 (Bonatti et al., 1970). Their high ($^{87}Sr/^{86}Sr$) ratios are within the range of values found in alpine-type peridotites from the continents. Therefore, Bonatti concluded that either a continuous layer or large blocks of ancient, residual, alpine-type peridotite, hitherto believed to be typically sub-continental, must exist at least in the equatorial Atlantic. (Bonatti, 1971) The origin of high ($^{87}Sr/^{86}Sr$) ratio of alpine-type peridotites is very difficult problem in itself. AM50 is different from alpine-type peridotite in rock type and the Rb and Sr contents in the former are much higher than those of the latter. Therefore, we cannot discuss the origin of high ($^{87}Sr/^{86}Sr$) ratio of AM50 in the same way as that of alpine-type peridotite.

However, the existance of ridge basalt with such a high ($^{87}Sr/^{86}Sr$) ratio and low K/Rb ratio is difficult to understand, if one assume that the sample come from upper mantle region. These data suggest that AM50 is not derived from the same parent materials as that for ordinary ridge basalts. Hence, we think that AM50 is originated in continental crustal area and the high ($^{87}Sr/^{86}Sr$) ratio represents that of sialic crustal materials. This sample may be one of the continental crustal fragment materials which are left behind in its original situation as Bonatti thought about the alpine-type peridotites. But we need not to think that large blocks are left behind. We would like only to say it may be not so strange to find one or two samples in Mid-Atlantic Ridge where the continent (Pangaea) was located in the past time.

But, even though this sample originated in continental crustal area, we would not be able to account completely for the mechanism to

make such a basalt of high ($^{87}Sr/^{86}Sr$) ratio as 0.7208. Antarctic and Tasmanian dolerites are known to have high ($^{87}Sr/^{86}Sr$) ratios in continental basaltic rocks. Their ratios range from about 0.7080 to 0.718, and average 0.712, but their average Sr content of only about 130 ppm is unusually low for continental basaltic rocks. This low Sr content suggests that they have been contaminated. The Sr content of AM50 is so large that the contamination, if any, must require large amount of sialic materials.

Acknowledgement

We thank Dr. A. Miyashiro, New York State University, for samples.

References

Bonatti, E., Honnorez, J., Ferrara, G., (1970 Earth Planet. Sci. Lett. 9, 247.
Bonatti, E., (1971) J., Geophys. Res. 76, 3825
Carr, D. R., Kulp, J. L., (1953) Bull. Geol. Soc. Amer. 64, 253
Engel, A. E. J., Engel, C. G., Havens, R. G., (1965) Geol. Soc. Am. Bull. 76, 719
Gast, P. W., (1968) Geochim. Cosmochim. Acta 32, 1057
Hart, S. R., (1970) Carnegie Inst. Wash. Yearbook 70 353
Ozima, M., Saito, K., (1973) Earth Planet. Sci. Lett. 20,77
Peterman, Z. E., Hedge, C. E., (1971) Geol. Soc. Am. Bull 82,493
Saito, T., Ewing, M., Burckle, L. H., (1966) Science 151, 1075

THE ARGON-40/ARGON-36 RATIO IN THE EARTH'S INTERIOR

Ichiro KANEOKA

Max-Planck-Institut für Kernphysik, Heidelberg, Germany
and Geophysical Institute, University of Tokyo, Tokyo*

* Present address

1. Introduction

In connection with the evolution of the earth's atmosphere, it is very important to know the Ar-40/Ar-36 ratio in the earth's interior. Experiments have indicated that some part of Ar-36 is tightly trapped in the rocks (e.g. Mussett and Dalrymple, 1968). Hence it is probable that at least some part of Ar-36 is incorporated into the rock during the rock formation.

Excess Ar in submarine basalts may reflect the Ar-40/Ar-36 ratio in the magma source. Adopting the hypothesis, Ozima and Kudo (1972) have developed an earth's atmoshere evolution model. However we cannot neglect the possibility of atmosheric Ar contamination for these samples, resulting in reducing the apparent Ar-40/Ar-36 ratio. Furthermore, no blank corrections are applied in these measurements. Hence we should regard the values as a minimum of the Ar-40/Ar-36 ratio in the magma source.

On the other hand, the Ar-40/Ar-39 method allows us to separate the radiogenic Ar-40 from the excess Ar-40 (Kaneoka, 1973). By applying the stepwise heating, it is very interesting to study the high temperature components of the excess Ar-40 and Ar-36.

2. The excess Ar-40 in the ultramafic xenoliths from the Kola Peninsula

Ultramafic rocks from the Kola Peninsula show very high K-Ar ages of 4-10 b.y. (e.g. Gerling et al., 1962; Kirsten and Gentner, 1966; Kirsten and Müller, 1967), suggesting the existence of large quantities of excess Ar. Several xenolithic ultramafic rocks from this area were studied by the Ar-40/Ar-39 method. These samples were studied before by the conventional K-Ar method and by diffusion experiments, which also indicated the existence of large amounts of excess Ar in these rocks (Kirsten and Gentner, 1966; Kirsten and Müller, 1967). The rock types and the sampling localities are shown in Table 1.

Table 1

Sample No.	Rock Type	Locality
4702B (W.R.)	Peridotite	Montsche Tundra, Kola Peninsula
4702B (MAG)	do	do
601 (W.R.)	Lherzolite	do
4743B (W.R.)	Peridotite	Nittis, Kola Peninsula
4719 (W.R.)	do	do
4720 (W.R.)	do	Montsche Tundra, Kola Peninsula

N.B. W.R.: whole rock, MAG: magnetic fraction.

These samples were irradiated with fast neutron in the core of the Karlsruhe FR2 reactor for three weeks, resulting in the integrated fast neutron flux of about 4.8×10^{18} n/cm^2. For these samples, the stepwise heating was applied and Ar isotopes were measured by a Nier-type massspectrometer. After blank and Ca and K -derived Ar corrections, the Ar-40/Ar-39 ages were calculated for each temperature fraction. All samples show abnormaly high Ar-40/Ar-39 ratios at low and high temperatures. The lowest Ar-40/Ar-39 ratio was consistently observed at intermediate temperatures (900-1100°C), indicating an apparent age of 2.8-3.1 b.y.; however this may not indicate the formation age (Fig. 1).

The quantity of excess Ar-40 was estimated at each temperature fraction, adopting ages inferred from the published Rb-Sr ages (2-3 b.y., Lippolt and Wasserburg, 1973) or the minimum Ar-40/Ar-39 ages. Excess Ar-40 is revealed to be abundantly trapped both in mineral lattices and non-retentive trapping sites, but the trapping sites are different from those of in-situ radiogenic Ar-40 (Fig. 2). The high temperature component of excess Ar-40 is considered to represent Ar dissolved during mineral formation in the upper mantle or the lower crust.

If there exists some Ar-36 in the magma source, it is natural that it is also trapped in minerals with coexisting Ar-40. Hence a correlation is expected between the amount of excess Ar-40 and that of Ar-36. In effect, the correlation exists for samples 4743B(W.R.) and 4720(W.R.) for the high temperature fractions (above 1000°C) (Fig. 3). It is important to note that only the high temperature componenet of excess Ar-40 show a correlation with Ar-36. No correlation is observed between the Ar-36 and the radiogenic Ar-40. From this correlation, we can estimate the approximate Ar-40/Ar-36 ratio when the rock was formed. For sample 4743B, the ratio ranges from 5000 to 9500 and for sample 4720 it ranges from 10000 to 17000. For samples 4702B and 4719(W.R.), a similar tendency is observed, though less clear than for 4743B and 4720. The excess Ar-40/Ar-36 ratio of 35000±8000 is assigned to sample 4702B(W.R.), 14000±4000 to sample 4719 and about 22000 to sample 4702B(MAG) for their high temperature fractions. Sample 601 shows no correlation. The amount of excess Ar-40 and Ar-36 in sample 601 is much less than in the other samples. Corrections are large for the 1500°C and 1700°C fractions. Hence it is difficult to get reliable results from this sample.

We conclude that the Ar-40/Ar-36 ratio in the sample source ranged from 5000 to 35000. Furthermore, the initial Sr-87/Sr-86 ratios have been reported for some samples (0.7035±0.0008 for sample 4702B, 0.7015 ±0.0012 for sample 601 and 0.706-0.708 for sample 4743B, Lippolt and Wasserburg, 1973). Hence sample 4743B might be of crust origin or seriously contaminated by the crustal material. If we exclude it, the ratio ranges from 10000 to 35000 for samples of probable the upper mantle or the lower crust origin.

3. The Ar-40/Ar-36 ratio in the earth's interior

As shown above, in spite of large errors, it is remarkable that we observe such high excess Ar-40/Ar-36 ratios in the rocks of probable the upper mantle or the lower crust origin. If we consider the fact that these rocks were formed 2 or 3 b.y. ago, the present Ar-40/Ar-36 ratio in the upper mantle or the lower crust may be larger. The large variance in the measured ratio may be partly due to the difference in the formation age of these rocks, but may reflect the large inhomogeneity

of the ratio in the upper mantle or the lower crust itself.

From the published data, we can estimate the excess Ar-40/Ar-36 ratio. Since the Ar-36 always includes the secondary component, we should regard the ratio as the minimum value. The peridotites from the Kola Peninsula show high ratios up to about 36000 (Kirsten and Müller, 1967). A hypersthene in the Stillwater complex (age: 2.7 b.y.) shows a ratio of about 15000 (Schwartzman, 1971). A phlogopite in the Kimberlite (age: 60 m.y.) shows also a high ratio (more than 16000, Kirsten, 1964). A diopside from the Salt Lake Crater (age: less than 1 m.y.) indicates a value of 7500 (Funkhouser and Naughton, 1968). Similar estimation is possible for the excess Ar in submarine rocks. The ratio scatters from nearly zero to about 10000 (Dalrymple and Moore, 1968; Fisher, 1970), which probably reflects the difference of the circumstances of the rock formation and the experimental conditions.

For crustal materials, it is reported that beryl contains large amounts of excess Ar. The excess Ar-40/Ar-36 ratio in a beryl exceeds 100000 (Damon and Kulp, 1958). Studies on natural gases that emanate from wells and fumaroles have shown that the argon in many of these gases is highly radiogenic and even the Ar-40/Ar-36 ratio of 34000 have been reported (Boato et al., 1952; Ferrara et al., 1963; Zartman et al., 1961; Wasserburg et al., 1963). Although the ratio in natural gases probably reflects the value of crustal material and the gas might be contaminated with the atmosphere, this high ratio also suggests the possibility of the high value of the Ar-40/Ar-36 ratio in the earth's interior.

From these considerations, we conclude that the Ar-40/Ar-36 ratio in the earth's interior probably exceeds 10000, though the value may be rather inhomogeneous in the earth's interior. The excess Ar-40/Ar-36 ratio observed in submarine basalts is probably lowered due to the contamination. Furthermore, the high value in the excess Ar-40/Ar-36 ratio for rocks formed 2 or 3 b.y. ago suggests that most Ar-36 was degassed in the earlier stages of the earth's evolution.

References

Boato, G., Careri, G., and Santangelo, M. (1952) Nuovo Cimento, ser. 9, 9, 44.
Dalrymple, G. B., and J. G. Moore (1968) Science 161, 1132.
Damon, P. E., and J. L. Kulp (1958) Am. Min. 43, 433.
Ferrara, G., R. Gonfiantini and P. Pistoia (1963) in Tongiorgi, E., ed., Nuclear Geology on Geothermal Areas, Spoleto Consiglio Nazionale della Ricerche Laboratorio di Geologia Nucleare, Pisa, 267.
Fisher, D. E. (1970) Earth Planet. Sci. Letters 9, 331.
Funkhouser, J. G., and J. J. Naughton (1968) Jour. Geophys. Res. 73, 4601.
Gerling, E. K., J. A. Shukoljukov, I. I. Matvejeva, T. V. Koltsova and S. S. Jakovljeva (1962) Geokhimiya 11.
Kaneoka I. (1973) Fortschritte der Mineralogie 50, 85.
Kirsten, T. (1964) Ph. D. Thesis, Univ. Heidelberg.
Kirsten, T., and W. Gentner (1966) Z. Naturforsch. 21a, 119.
Kirsten, T., and O. Müller (1967) in Radioactive Dating and Methods of Low Level Counting, Int. Atomic Energy Agency, Vienna 483.

Lippolt, H. J., and G. J. Wasserburg (1973) Fortschritte der Mineralogie 50, 102.
Mussett, A. E., and G. B. Dalrymple (1968) Earth Planet. Sci. Letters 4, 422.
Ozima, M., and K. Kudo (1972) Nature Physical Science 239, 23.
Schwartzman, D. W. (1971) Ph. D. Thesis, Brown Univ.
Wasserburg, G. J., E. Mazor, and R. E. Zartman (1963) in Geiss, J., and E. D. Goldberg, eds., Earth Science and Meteoritics: Amsterdam, North-Holland Publ. Co., 219.
Zartman, R. E., G. J. Wasserburg and J. H. Reynolds (1961) Jour. Geophys. Res. 66, 277.

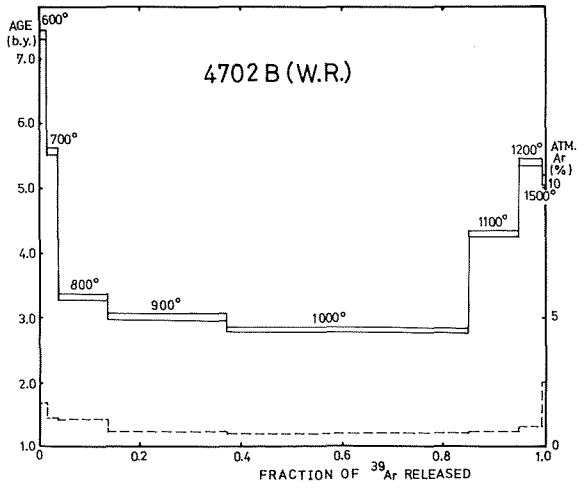

Fig. 1

Release pattern of Ar-40/Ar-39 age for sample 4702B (W.R.) as a function of Ar-39 released. The calculated age is at the center of the box. The height of the box covers ±1σ (standard deviation) in age, based on statistical uncertainties in the Ar-40/Ar-39 ratio and in the J-value. The width of the box is the fractional amount of total Ar-39 released in that fraction. Each number on the box indicates the corresponding degassing temperature. The dotted line indicates the atmospheric Ar contamination level in per cent.

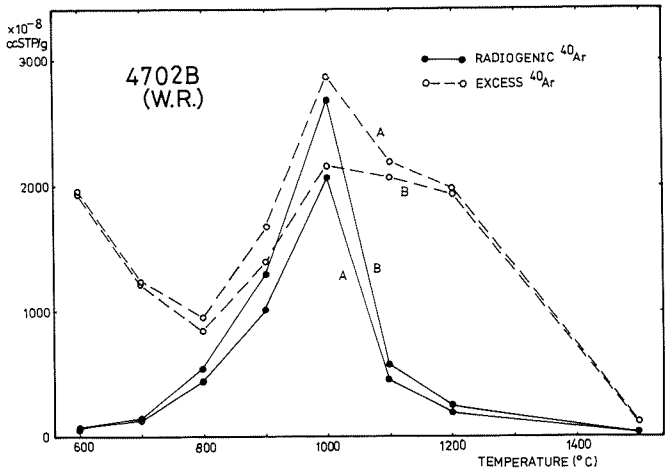

Fig. 2

Release patterns of radiogenic Ar-40 (solid circle) and excess Ar-40 (open circle) from whole rock sample 4702B. The amount of radiogenic Ar-40 is calculated by assuming that the formation age of this rock is; (a) 1.7 b.y. (b) 2.0 b.y., and radiogenic Ar-40 is correlated with Ar-39.

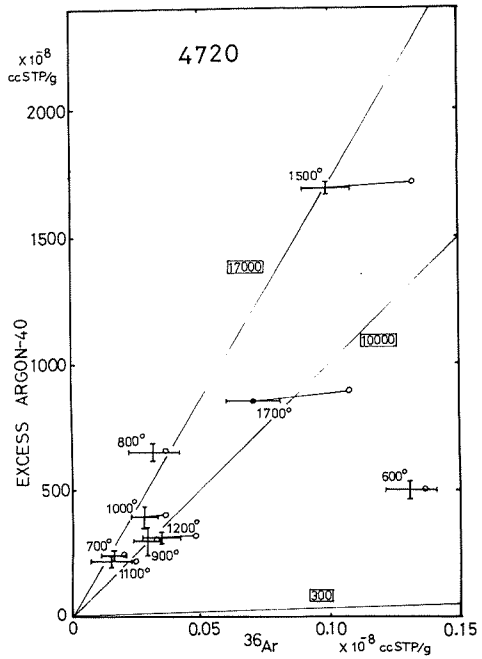

Fig. 3

Excess Ar-40 versus Ar-36 for peridotite 4720 (W.R.). Bars in the amount of excess Ar-40 indicate the range caused by the different assumed reference ages. Bars in the amount of Ar-36 indicate the analytical error (1σ). Open circles indicate the measured values before the blank corrections. The number in the box indicates the excess Ar-40/Ar-36 ratio represented by a straight line.

EVOLUTION OF THE ATMOSPHERE : CONTINUOUS OR CATASTROPHIC ?*)

BY

MINORU OZIMA

GEOPHYSICAL INSTITUTE, UNIVERSITY OF TOKYO

There seems now to be general agreement that the atmosphere has evolved as later degassing from the solid earth. (1, 2, 3) The degassing mechanism, however, is still very controversial. One school considers that the degassing has been a continuous process throughout the history of the earth. (1, 4, 5) For example, Turekian discussed the continuous degassing model on the basis of Ar evolution in the atmosphere. Assuming that the degassing obeys a first order rate process, he obtained the Ar degassing rate of $k = 2.81 \times 10^{-11} yr^{-1}$ from a chondritic earth model (K = 880ppm). It is difficult to judge the model, since there is no experimental determinations which can be directly compared with the degassing rate thus obtained. Taking account of the isotopic ratio Ar40/Ar36 in the present mantle, Ozima and Kudo (5) could show that the first order rate process for Ar degassing yields about 100 ppm of the K-content of the earth. The value is in good agreement with a recent estimate by Larimer (6), offering a criteria to judge the validity of the model.

An alternative view of the origin of the atmosphere is that the degassing was catastrophic (3, 7, 8, 9). Chase and Perry (6) found that oxygen isotopic ratio $^{18}O/^{16}O$ in some sediments decreases with their age. The pattern of the decrease seems to be best explained by a a model which assumes early formation of oceans than a continuous growth model. The similar conclusion was reached by Damon and Kulp(8) who studied Ar40-content in beryls of various ages. The sudden degassing is generally regarded to be due to catastrophic core formation (3, 7, 9). Below we will examine the catastrophic degassing model on the basis of Ar evolution in the atmosphere.

Assuming that the atmosphere has evolved as a later catastrophic degassing, it is shown that the degassing is uniquely defined by specifying two of the following four quantities, that is, (1) the time of the degassing (t), (2) the degassing fraction (f = (Ar)atmosphere/(Ar)earth), (3) K-content of the earth and (4) the isotopic composition of Ar whithin the present solid earth. Also, the model must account for the abundance of Ar (6.55×10^{19} g) and the isotopic composition (Ar40/Ar36 = 295.5) in the present atmosphere. Solving differential equations for the evolution of Ar within the earth, we have sets of solutions which satisfy the Ar abundance and the isotopic ratio in the present atmosphere. This is shown in Figure 1, in which x- and y-axis denote the K-content and the degassing time. Figures assigned to each curve indicate the degassing fraction (f) and the isotopic ratio (Ar40/Ar36) whithin the present solid earth. As seen in the Figure, the catastrophic degassing model can be uniquely defined by specifying any two of the four quantities (1) - (4). For example, if one assumes

*) Nature (1973) in press

that the K-content is 300 ppm and the time of the degassing was 4.0 b.y. B.P., the degassing fraction must be about 95 % and the isotopic ratio Ar40/Ar36 is about 10000 or vice versa.

Recently Ozima and Kudo (5) suggested that the trapped Ar in submarine basalt may represent the isotopic composition of Ar in the mantle. The supposition may also be favoured by a recent hot spot hypothesis (10) which suggested that the dimension of the magma source for seamount extends over a few hundred kilometers. The isotopic ratio Ar40/Ar36 estimated from the submarine basalt is about 1000 (5). It is then obvious from Figure 1 that any catastrophic degassing model can not reconcile with the isotopic ratio, if one accepts the general assumption that the oldest known rocks (about 3.9 b.y.) post-date the core formation, unless one assume unacceptably high K-content, say more than 1500 ppm. One must conclude that the degassing was continuous if the isotopic ratio is about 1000 as estimated from the submarine basalt. However, if the high values (more than 10000) found in the excess Ar in some ultrabasic rocks (11) represent the isotopic ratio in the mantle, as suggested by some authors (9), early catastrophic degassing model can not be ruled out.

We would like to emphasize that study on the trapped Ar in rocks derived from the mantle would yield very crucial informations as to the origin of the atmosphere, since the isotopic composition in the mantle and the degassing fraction may be infered by examining the isotopic ratios and the abundance of the trapped Ar in these rocks.

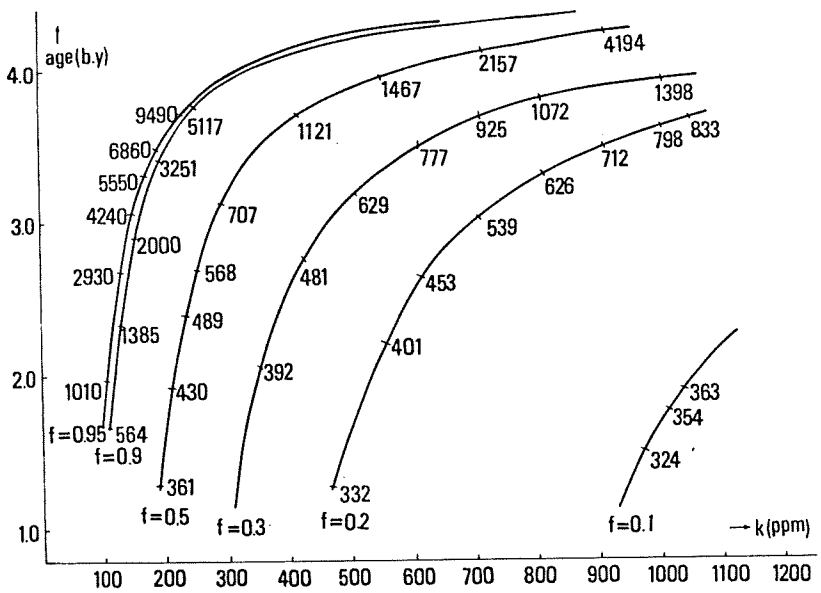

Figure 1. Curves correspond to the catastrophic degassing models which satisfy the Ar abundance and the isotopic ratio in the present atmosphere with respective values of f and the mantle Ar isotopic ratio.

REFERENCES

1) Rubey, W. R., Bull. Geol. Soc. Am., 63, 1111 (1951).
2) Holland, H. O., The origin and evolution of atmospheres and oceans, pp. 86-102, Brancazio and Cameron (ed.), Wiley (1964).
3) Fanale, P. F., Chem. Geol., 8, 79 (1972).
4) Turekian, K. K., Geochim. Cosmochim., Acta, 17, 37 (1959).
5) Ozima, M. and K. Kudo, Nature Phys. Sci., 239, 23 (1972).
6) Larimer, J. W., Geochim. Cosmochim. Acta, 35, 769 (1971).
7) Chase, C. G. and E. C. Perry, Jr., Science, 177, 992 (1972).
8) Damon, P. E. and J. L. Kulp, Amer. Mineralogist, 43, 433 (1958).
9) Schwartzman, D. W., Submitted for publication in Nature.
10) Morgan, W. J., Bull. Am. Assoc. Pet. Geologists, 56, 203 (1972).
11) Kirsten, T. and W. Gentner, Zeit. für Naturforschung, 21a, 119 (1966).

FLUCTUATIONS IN THE EARTH'S SPIN RATE CAUSED BY CHANGES IN THE DIPOLE FIELD

Hidefumi WATANABE[1] and Takeshi YUKUTAKE[2]

1) Geophysical Institute, Univercity of Tokyo, Tokyo
2) Earthquake Research Institute, Univercity of Tokyo, Tokyo

1.Introduction

It is widely believed that electromagnetic core-mantle coupling due to a change in the toroidal field at the core-mantle baundary is one of the most possible causes of the irregular fluctuations in the earth's spin rate, with time scales of decades, centuries or longer (e.g.,Bullard et al,1950; Munk and MacDonald,1960;Rochester,1960,1968,1973;Roden,1963).
There is, however, no direct evidence of such changes in the toroidal field, because the toroidal field is not observable at the surface of the earth. Furthermore, it is not justified to regard the apparent close correlation between the westward drift velocity of the eccentric dipole and the fluctuation in day length, as the evidence of electromagnetic core-mantle coupling (Yukutake,1973b).

It has recently been revealed that the dipole field has been changing its moment with such characteristic periods as about 8000,400 and 65 years. Corresponding to these changes, fluctuations in the earth's spin rate was shown to exist (Yukutake,1972,1973a). Relation between fluctuations in the dipole field and those in the earth's spin rate is examined in this paper for a more detailed model of the earth than that treated in Yukutake's (1972, 1973a).

2. Spherical Shell Model of the Earth

To avoid complexity, the mantle and the core are assumed to be of spherical symmetry (Fig.1). The mantle is devided into three shells; The depths of interfaces are 400 km, 2400 km and 2900 km. The uppermost part is assumed as an insulator. Electrical conductivities of the lower parts are taken to be $\sigma_{m2} = 10^{-10}$emu and $\sigma_{m1} = 10^{-9} - 10^{-7}$emu, as an adjustable parameter.
The core is supposed to consist of four shells (fluid core) and a sphere (solid core). The radii of interfaces are b_0 = 3470 km(core's radius), c_1 = 3300 km, c_2 = 3100 km, c_3 = 2800 km and c_4 = 1200 km(solid core's radius).
The whole core is assumed to have a uniform conductivity $\sigma_c = 3\times10^{-6}$emu and a uniform dencity 10 g·cm^{-3}.

The shear motion that is supposed to exist predominantly in the core is represented by differential rigid rotation of the shells.
Relative velocities of the shells are calculated so that the angular momentum of the fluid particles may be conserved during convectional flow (Fig.2).

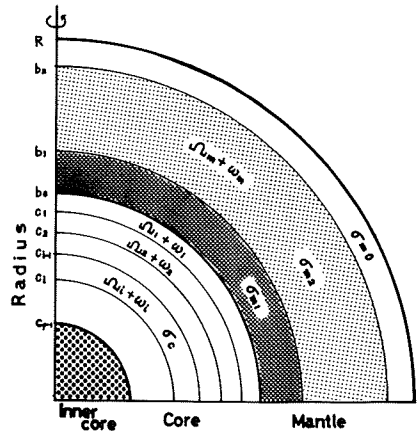

Fig.1 Earth model

3. Electromagnetic Couples acting on the Mantle and the Core Caused by Changes in the Dipole Field

Changes in the dipole field generate toroidal fields both at the core-mantle boundary and at the interfaces within the core. Toroidal fields thus generated diffuse out of the core and exert couples on the mantle to cause fluctuations in the rate of rotation. In this case, the couple acting on the mantle is highly dependent both on the conductivity of the lower mantle and on the distribution of the changes in the dipole field within the core (Yukutake, 1972).
The electromagnetic fields are solved for the earth model described in the previous section, when the dipole field is assumed to originate at various depths in the core and undergo a sinusoidal change. Then the electromagnetic couples acting on the mantle and the core are calculated.

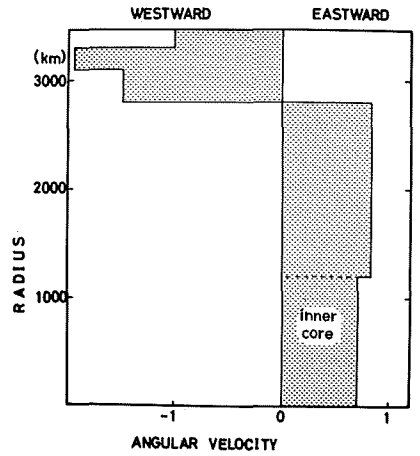

Fig.2 Angular velocity profile of the fluid core in the steady state. Angular velocities are normalized so that mean westward velocity may represent the observed westward drift velocity.

Ignoring cross terms of small quantities, the equations of motion of the mantle and the core become

$$
\left.
\begin{aligned}
I_m \frac{d\tilde{\omega}_m}{dt} &= \frac{2}{5} b_o^3 \, rH_{s10}(b_o) \cdot \varphi\tilde{H}_{t20}(b_o) && \text{for the mantle} \\
I_i \frac{d\tilde{\omega}_i}{dt} &= -\frac{2}{5} C_{i-1}^3 \, (rH_{s10}(C_{i-1}) \cdot \varphi\tilde{H}_{t20}(C_{i-1}) \\
&\qquad + r\tilde{H}_{s10}(C_{i-1}) \cdot \varphi H_{t20}(C_{i-1})) && \text{for the shells} \\
&\quad + \frac{2}{5} C_i^3 \, (rH_{s10}(C_i) \cdot \varphi\tilde{H}_{t20}(C_i) && \text{in the core,} \\
&\qquad + r\tilde{H}_{s10}(C_i) \cdot \varphi H_{t20}(C_i)) && i = 1,2,3,4 \\
I_5 \frac{d\tilde{\omega}_5}{dt} &= -\frac{2}{5} C_4^3 \, rH_{s10}(C_4) \cdot \varphi\tilde{H}_{t20}(C_4) && \text{for the solid core}
\end{aligned}
\right\} \quad (1)
$$

where

I_m, I_i, I_5 ; moment of inertia of the mantle, the shells and the sphere in the core.

rH_{s10}, $r\tilde{H}_{s10}$; radial compornent of the steady and the oscillating dipole field.

φH_{t20}, $\varphi\tilde{H}_{t20}$; azimuthal component of the steady and the oscillating toroidal field induced.

$\varphi H_{t20} = 0$ at the boundaries, $r=b_o$ and C_4 in the fluid core.

Changes in the angular velocity of the mantle are obtained by solving the simultaneous equations (1) .

4. Theoretical Results in Comparison with Observational Data

Effect of change in Ds, the depth at which dipole field changes, on fluctuations in the angular velocity of the mantle is examined over a range of 0 - 670 km, with $\sigma_{m1} = 10^{-8}$emu. The results are shown in Fig.3. The upper diagram shows variation in the amplitude of the angular velocity of the mantle with period, and the lower diagram that of the phase difference between the angular velocity and the dipole change. The amplitude of the angular velocity is reduced to the case when the magnitude of the dipole change is 1 gauss. The observational data taken from Yukutake's(1973a) are also plotted on the same diagrams by solid circles. It is clearly seen that with the increase in Ds, the angular velocity of the mantle increases very rapidly.

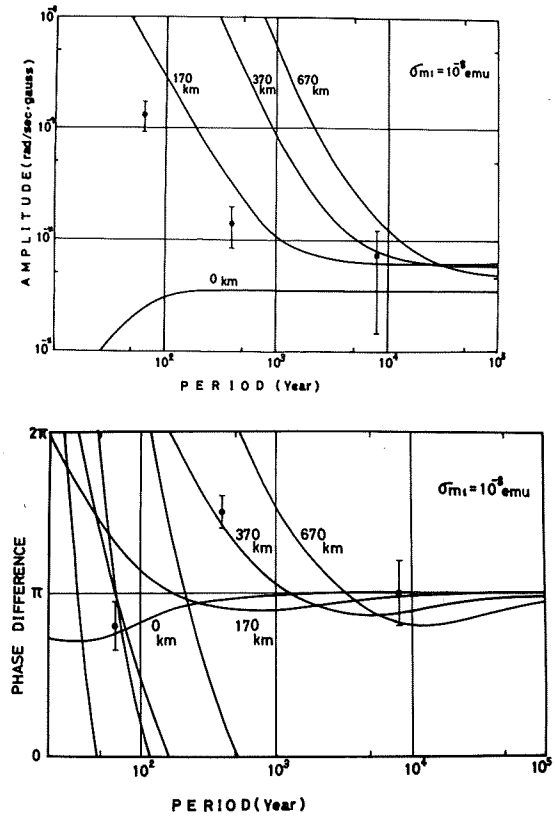

Fig.3. Angular velocity of the mantle caused by a dipole oscillation for Ds of 0 - 670 km, when m1 is assumed to be 10^{-8} emu.

Effect of the conductivity of the lowest mantle is also examined by changing σ_{m1} in a range of 10^{-9}- 10^{-7} emu, with Ds of 170 km and 370 km (Fig.4). As the conductivity σ_{m1} increases, the angular velocity becomes highly dependent on the period of the dipole change.

The depth Ds that accounts for the observed data best is 170 km for the amplitude and 370 km for the phase, as far as σ_{m1} is taken to be 10^{-9}- 10^{-8} emu. Therefore we may conclude that, though there is still slight discrepancy between the depth Ds obtained for the amplitude and that for the phase, the dipole change is most likely to be taking place within a surface part of the core shallower than a few hundreds kilometers, provided that the conductivity of the lowest part of the mantle is 10^{-9}- 10^{-8} emu.

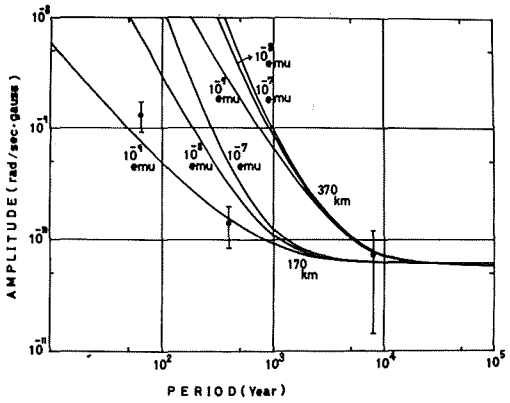

Fig.4. Angular velocity of the mantle caused by a dipole oscillation for Ds of 170 and 670 km, when σm_1 is varied from 10^{-9} to 10^{-7} emu.

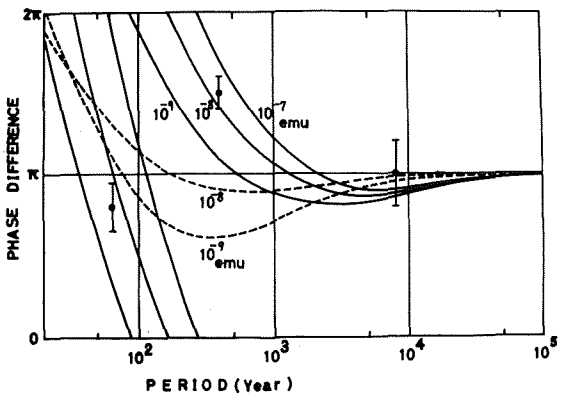

References

Bullard, E.C., C. Freedman, H. Gellman, and J. Nixon (1950) Phil. Trans. Roy. Soc. London, A, 243, 67-92.

Bullard, E.C. (1949b) Proc. Roy. Soc. London, A, 199, 413-443.

Elsasser, W.M. and H. Takeuchi (1955) Trans. Amer. Geophys. Union, 36, 584-590.

Munk, W.H. and G.J.F. MacDonald (1960) Cambridge Univ. Press, London.

Rochester, M.G. (1960) Phil. Trans. Roy. Soc. London, A, 252, 531-555.

Rochester, M.G. (1968) J. Geomag. Geoelectr., 20, 387-402.

Rochester, M.G. (1970) Earthquake Displacement Fields and the Rotation of the Earth, pp. 136- 148, Reidel Pub. Co., Dordrecht.

Rochester, M.G. (1973) EOS, Vol.54, No.8, 769-780.

Vestine, E.H. and A. Kahle (1968) Geophys. J., 15, 29-37.

Yukutake, T. (1972) J. Geomag. Geoelectr., 24, 19-47.

Yukutake, T. (1973a) J. Geomag. Geoelectr., 25, 195-212.

Yukutake, T. (1973b) J. Geomag. Geoelectr., 25, 231-235.

Roden, B.R. (1963) Geophys. J. Roy. Astr. Soc., 7, 361-374.

UNIQUENESS OF THE SPHERICAL HARMONIC ANALYSIS OF THE GEOMAGNETIC FIELD BASED ON THE INCLINATION AND DECLINATION DATA

Masaru KONO

Geophysical Institute, University of Tokyo, Bunkyo-ku, Tokyo 113, Japan.

Fritsche (1899), Kono (1966), Braginskiy (1969), Benkova et al. (1970, 1971, 1973; also Adam et al., 1970a, b; Benkova and Cherevko, 1972), Yukutake (1971) and Creer et al. (1973) attempted to apply spherical harmonic analyses to bodies of data of the geomagnetic field lacking the information on the field strengths; i.e., declination and inclination data between 16th and 19th centuries mostly measured by voyaging ships, archeomagnetic data or paleomagnetic data. Most of these analyses, however, are imcomplete with regard to the uniqueness of the solutions. In the following, we shall first show that the combined data set of inclination and declination on the surface of the earth is really sufficient for the determination of the relative magnitudes of the Gauss coefficients of the geomagnetic field. We shall then demonstrate non-uniqueness of spherical analyses based on some incomplete data set of directions. Lastly, we shall evaluate various author's methods in the light of the uniqueness of the solutions.

Theorem

Consider two curl-free and divergence-free vector fields $\mathbf{F}$ and $\mathbf{F}'$. defined in a region V bounded by a surface S. If $\mathbf{F}$ and $\mathbf{F}'$ are parallel to each other everywhere on S, then $\mathbf{F}' = p\mathbf{F}$ where p is a constant in the entire space V.

Proof

As $\mathbf{F}$ and $\mathbf{F}'$ are curl-free, they can be expressed in terms of scalar potentials

$$\begin{aligned} \mathbf{F} &= -\operatorname{grad} W \\ \mathbf{F}' &= -\operatorname{grad} W' \end{aligned} \tag{1}$$

If we put

$$W' = pW + q \tag{2}$$

where p and q are scalar function of position, the parallelism of $\mathbf{F}$ and $\mathbf{F}'$ on S can be expressed as

$$\mathbf{F}' = p\mathbf{F} = -p \operatorname{grad} W \tag{3}$$

with a subsidary condition for p and q

$$W \operatorname{grad} p + \operatorname{grad} q = 0, \qquad p > 0 \tag{4}$$

Since $\nabla^2 W = \nabla^2 W' = 0$ everywhere by the divergence-free condition, it can be seen by taking the divergence of eq. (3) that

$$\text{grad } p \cdot \text{grad } W = 0 \tag{5}$$

must hold at every point on S. This relation implies that the lines of equal p are everywhere perpendicular to the equipotential lines on S.

Consider an integral $\int F_s' \, ds$ between A and C (Fig. 1). By eqs. (3) and (1)

$$\int_A^C F_s' \, ds = \int_A^C p \, F_s \, ds$$
$$= - \int_A^C p \text{ grad } W \cdot d\mathbf{s}$$

Since the integral does not depend on the choice of the path, we can take a path which goes through AB (where W = const. and $F_s = 0$) and BC (where $p = p_2$).

$$\int_A^C F_s' \, ds = p_2 \int_B^C F_s \, ds$$
$$= p_2 (W_2 - W_1)$$

On the other hand, if we take the path AD and DC

$$\int_A^C F_s' \, ds = p_1 (W_2 - W_1)$$

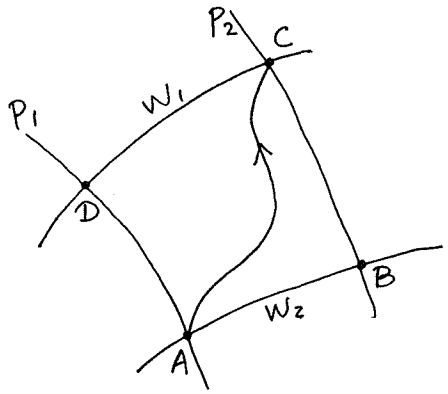

Fig. 1. Integration paths.

This shows that p must be a constant on S and, by virtue of eq. (4), also that q must be another constant on S. But if the potential W' is given on S, the potential field $\mathbf{F}'$ is uniquely determined in the whole space. Therefore, p and q must be constants in the entire space V and $\mathbf{F}' = p\mathbf{F}$.

Thus we have proved that if the data of both the inclination (I) and declination (D) are given over the surface of the earth, then the relative magnitudes of the Gauss coefficients can be uniquely determined.

The procedure employed in the proof of the theorem suggests that an incomplete data set of magnetic directions (such as D only) given on the surface of the earth may not be sufficient for the determination of a unique geomagnetic potential. This is indeed so. Because of this non-uniqueness, the methods used by the above authors except those of Kono (1966) and Braginskiy (1969) are theoretically incorrect, as they used only declination data or only inclination data in their calculation.

Let us express a potential in a familiar form

$$W = a \sum_{n=0}^{\infty} \sum_{m=0}^{n} (a/r)^{n+1} \left(a_{nm} \cos m\phi + b_{nm} \sin m\phi \right) P_n^m(\cos\theta) \tag{6}$$

where r, θ, ϕ are spherical polar coordinates, P_n^m are Legendre's associated polinomials of degree n and order m, and a is the radius of the earth. The northward, eastward, and downward components X, Y, Z of the magnetic field at colatitude θ and longitude ϕ are

$$X = \left(-\frac{\partial W}{r\partial\theta}\right)_a = -\sum\sum\left(a_{nm}\cos m\phi + b_{nm}\sin m\phi\right)\frac{dP_n^m}{d\theta}$$

$$Y = \left(\frac{\partial W}{r\sin\theta\partial\phi}\right)_a = -\sum\sum m\left(a_{nm}\sin m\phi - b_{nm}\cos m\phi\right)P_n^m / \sin\theta \quad (7)$$

$$Z = \left(-\frac{\partial W}{\partial r}\right)_a = -\sum\sum(n+1)\left(a_{nm}\cos m\phi + b_{nm}\sin m\phi\right)P_n^m$$

We can define two independent angles by the three components of force. In the following, we shall show that the distribution on the sphere of one such angle formed by any two of the X, Y, Z components is not enough to determine a unique potential. For the sake of simplicity, we assume that the observed values are the ratios (such as Y/X) and not the angles (such as D). This corresponds to permitting p to take both positive and negative values (see eqs. (3) and (4)). However, the following discussion can easily be extended to the case $p > 0$ on the entire sphere. For, if such a W' is obtained for a particular W, $a\mathbf{F} + b\mathbf{F}'$ can be made to have the same signs as $\mathbf{F}$ on S by appropriate choice of the coefficients a and b, since $\mathbf{F}' = 0$ whenever $\mathbf{F} = 0$ by eq. (3). Then the potential generates a vector field which is truly parallel to - grad W everywhere on S.

Z - X Solutions

The simplest example of non-uniqueness can be shown by considering the two harmonics

$$a\,(a/r)^{n+1}\,a_{nm}\,P_n^m\cos m\phi \;,\quad a\,(a/r)^{n+1}\,b_{nm}\,P_n^m\sin m\phi$$

Obviously the ratio X/Z derived from the above two potentials is the same everywhere.

Y - Z Solutions

For a potential $W_1 = a\,(a/r)^{n+1}\,a_{nm}\,P_n^m\cos m\phi$, the ratio Y/Z is

$$\frac{-m\,a_{nm}\,P_n^m\sin m\phi}{-(n+1)\,a_{nm}\,P_n^m\cos m\phi} = \frac{m}{n+1}\tan m\phi$$

Consider another potential

$$W_2 = \sum_{k=0}^{\infty} a\,(a/r)^{k+1}\,a_k P_k + a\,(a/r)^{2n+2} a_{2n+1,2m}\,P_{2n+1}^{2m}\cos 2m\phi$$

Since P_k forms an orthogonal, complete set, we can define the coefficients a_k so as the following relation is satisfied.

$$\sum_{k=0}^{\infty}(k+1)\,a_k\,P_k = -(2n+2)\,a_{2n+1,2m}\,P_{2n+1}^{2m}$$

The ratio Y/Z for the potential W_2 is then,

$$\frac{-2m\,a_{2n+1,2m}\,P_{2n+1}^{2m}\,\mathrm{sim}\,2m\phi}{-(2n+2)\,a_{2n+1,2m}\,P_{2n+1}^{2m}(\cos 2m\phi + 1)} = \frac{m}{n+1}\tan m\phi$$

which is identical to that derived from the potential W_1.

X - Y Solutions

The general form of a potential on a sphere of radius a is from eq. (6)

$$W_a(\theta, \phi) = a \sum\sum (a_{nm} \cos m\phi + b_{nm} \sin m\phi) P_n^m \qquad (8)$$

The X and Y components (7) can also be derived by partial differentiation of W_a by θ or ϕ.

If we take a k-th power of W_a, it can be expanded by the spherical harmonics , by virtue of the orthogonality and completeness of the set $P_n^m \cos m\phi$ and $P_n^m \sin m\phi$ on a sphere.

$$W_a^k = a \sum_{n=0}^{\infty}\sum_{m=0}^{n} (a_{nm}^{(k)} \cos m\phi + b_{nm}^{(k)} \sin m\phi) P_n^m$$

Since

$$\frac{\partial (W_a^k)}{\partial \theta} = k W_a^{k-1} \frac{\partial W_a}{\partial \theta}, \quad \frac{\partial (W_a^k)}{\partial \phi} = k W_a^{k-1} \frac{\partial W_a}{\partial \phi}$$

the θ and ϕ derivatives of W_a^k form the same ratio as that of the potential W_a (and therefore also that of W). Thus the potential

$$W^{(k)} = a \sum\sum (a/r)^{n+1} (a_{nm}^{(k)} \cos m\phi + b_{nm}^{(k)} \sin m\phi) P_n^m$$

has the same ratio Y/X as that of W over the whole surface of the sphere (if $W_a > 0$ or if k is an odd integer, $W^{(k)}$ has the same declination). By induction, potentials such as

$$c_1 W + c_2 W^{(2)} + c_3 W^{(3)} + \ldots\ldots$$

have the same property with regards to the ratio Y/X.

We can also show that angles such as I cannot decide a unique potential by converting (r, θ, ϕ) coordinate into another curvilinear coordinate system (r, ξ, η) where ξ and η coordinates are measured along field lines and equipotential lines on the surface of the sphere, respectively.

Discussion

In order to obtain the geomagnetic potential for the year 1780, Fritsche (1889) used declination and inclination charts of that epoch and the average magnitude of the magnetic total force for the years 1842 and 1855. He calculated the field components X, Y, Z from the above combination of I, D and the field strength and used them in the ordinary spherical harmonic analysis. For the years 1700, 1650, and 1600, Fritsche used declination data compiled by van Bemmeln and horizontal component, computed from the analysis for later epochs. His methods does not allow the time variation of the field values. Hence, both of his methods are mathematically incorrect because of his assumption of constant intensities in different periods.

Adam et al. (1970a, b), Benkova et al. (1970, 1971, 1973), Benkova and Cherevko (1972), Yukutake (1971), and Creer et al. (1973) used one or more of the following identities,

$$
\begin{aligned}
&X \sin D - Y \cos D = 0 \\
&X \sin I - Z \cos I \cos D = 0 \\
&Y \sin I - Z \cos I \sin D = 0 \\
&(X \cos D + Y \sin D) \sin I - Z \cos I = 0 \\
&X^2 + Y^2 - Z^2 \cot^2 I = 0
\end{aligned}
\tag{9}
$$

Their procedures were to expand X, Y, Z by eq. (7), move the terms containing P_1^0 to the right-hand side, and obtain a set of non-homogeneous equations by assuming a non-zero coefficient of P_1^0 (a_{11} or more usually g_1^0). From the N data of I or D, they determined the relative magnitudes of the Gauss coefficients g_n^m/g_1^0 and h_n^m/g_1^0 by solving the N simultaneous equations by the least square method. Some of the above authors claim the validity of their methods by demonstrating reasonable coincidences between the Gauss coefficients obtained by the I or D analyses and those of the known potential. However, as we have shown above, the analyses based on one of the two independent angles (such as D or I) are not unique. The apparent ability of I or D analyses is probably due to the truncation of the potential (6) at finite terms and depends on the combination of specific harmonics in individual studies.

Braginskiy (1969) assumed that the axial dipole changed in a manner expressed as

$$g_1^0 (t) = - 30400 + 15.7 (t - 1960) \tag{10}$$

where g_1^0 is in gammas and time t in years. He obtained the potential for 1780 from the declination D and inclination I by minimizing the expression

$$\chi^2 = \chi_D^2 + \chi_I^2$$
$$\chi_D^2 = \sum \left[\overline{H_i} (D_i - \overline{D}_i) \right]^2 W_D \ , \quad \chi_I^2 = \sum \left[\overline{F_i} (I_i - \overline{I}_i) \right]^2 W_I$$

where the summation is performed over the grid points, H and F are the horizontal component and the total field vector, W_D and W_I are the statistical weights, and the bars refer to values computed from the potential (6). Apart from the validity of eq. (10) and adequacy of statistical weights, his method is mathematically correct as he used both I and D. However, his analyses for other epochs (1700, 1650, 1600) are not unique, since only D data are used for these epochs.

Kono (1966) attempted to minimize the sum

$$(\cos I_i \cos D_i - X_i/F_i)^2 + (\cos I_i \sin D_i - Y_i/F_i)^2 + (\sin I_i - Z_i/F_i)^2$$

where X, Y, Z are computed from the potential by eq. (7) and $F^2 = X^2+Y^2+Z^2$. This corresponds to the minimization of squared angular error between the calculated and observed directions. It is obviously another mathematically correct expression. As in the case of Braginskiy's 1780 analysis, the equations for minimization condition are non-linear. Kono solved this problem by iteration and obtained a quick convergence.

Conclusion

It is proved that, given the distribution of I and D over the surface of the

earth, the relative magnitudes of the Gauss coefficients can be uniquely determined. It is also demonstrated that potentials obtained from data of D only or I only are not unique.

Many spherical harmonic analyses of directions reported so far are mathematically incorrect because of their non-uniqueness. Only the methods of Kono (1966) and Braginskiy (1969) among them give unique results.

Acknowledgments

Partial financial support from Kudo Foundation is gratefully acknowledged.

References

Adam, N.V., T.N. Baranova, N.P. Benkova and T.N. Cherevko (1970 a) Geomag. Aeronom. 10, 1068.
Adam, N.V., T.N. Baranova, N.P. Benkova and T.N. Cherevko (1970 b) Earth Planet. Sci. Lett. 9, 61.
Benkova, N.P. and T.N. Cherevko (1972) Geomag. Aeron. 12, 727.
Benkova, N.P., N.V. Adam and T.N. Cherevko (1970) Geomag. Aeron. 10, 673.
Benkova, N.P., A.A. Kruglyakov, A.N. Khramov and T.N. Cherevko (1971) Geomag. Aeron. 11, 374.
Benkova, N.P., A.N. Khramov, T.N. Cherevko and N.V. Adam (1973) Earth Planet. Sci. Lett. 18, 141.
Braginskiy, S.N. (1969) Geomag. Aeron. 9, 777.
Creer, K.M., D.T. Georgi and W. Lowrie (1973) Geophys. J. 33, 323.
Fritsche, H. (1889) Die Elemente des Erdmagnetismus für die Epochen 1600, 1650, 1700, 1780, 1842 und 1885, und ihre säcularen Änderungen, St. Petersburg.
Kono, M. (1966) M. Sc. Thesis, University of Tokyo.
Yukutake, T. (1971) J. Geomag. Geoelect. 23, 11.

SPHERICAL HARMONIC ANALYSIS OF THE GEOMAGNETIC FIELD FROM INCLINATION AND DECLINATION DATA

Masaru KONO

Geophysical Institute, University of Tokyo, Bunkyo-ku, Tokyo 113, Japan.

1. Introduction

Spherical harmonic analysis initiated by Gauss in 1938 is a very powerful tool for the study of the geomagnetic field mainly because of its mathematical uniqueness. The ordinary spherical harmonic analysis uses as data the field components X, Y, or Z at grid points or observatories. The applicability of such methods are therefore limited to the ages of Gauss and later, when the absolute values of the geomagnetic field became measurable.

By the progress in archeomagnetic and paleomagnetic studies, it is now possible to obtain considerable information about the inclination and declination at many places and at various epochs in the past. So, if it is possible to determine a unique potential from the field directions, the paleomagnetic field structure may be revealed in a mathematically less ambiguous way. Dipole offset of Wilson (1970) and quiet secular variation in the Pacific of Doell and Cox (1971) are a few of the hypotheses which may be better tested and evaluated by a paleomagnetic potential.

Many authors tried to obtain geomagnetic potentials from either or both of the inclination and declination data. However, all the methods used in these analyses, except those of Kono (1966) and Braginskiy (1969), are mathematically incorrect and give non-unique potentials (Kono, 1973).

In the present paper, mathematical expressions developed by Kono (1966) is presented. The efficiency and convergence of this method is demonstrated by applying this method to the present geomagnetic field data from magnetic observatories. Subsequently, application of this method to paleomagnetic and archeomagnetic data is discussed.

2. Method

The geomagnetic potential at a point is written in the form (external part is neglected)

$$W = a\sum_{n=0}^{\infty}\sum_{m=0}^{n}(a/r)^{n+1}\left(g_n^m \cos m\phi + h_n^m \sin m\phi\right) P_n^m(\cos\theta) \qquad (1)$$

where r, θ, ϕ are spherical polar coordinates, a is the radius of the earth, g_n^m, h_n^m are the Gauss coefficients, and P_n^m are Legendre's associated polinomials in Schmidt's quasi-normalized form. The northward, eastward, downward components of the magnetic field X, Y, Z at colatitude θ and longitude ϕ on the surface of the earth are

$$\begin{aligned} X &= -\sum\sum\left(g_n^m \cos m\phi + h_n^m \sin m\phi\right)(dP_n^m/d\theta) \\ Y &= -\sum\sum m\left(g_n^m \sin m\phi - h_n^m \cos m\phi\right) P_n^m / \sin\theta \qquad (2) \\ Z &= -\sum\sum (n+1)\left(g_n^m \cos m\phi + h_n^m \sin\phi\right) P_n^m \end{aligned}$$

For the sake of simplicity, we shall replace eqs. (2) by a tensor notation. For the i-th data point,

$$X_i = \sum_k a_{ik}\, x_k\,, \quad Y_i = \sum_k b_{ik}\, x_k\,, \quad Z_i = \sum_k c_{ik}\, x_k \tag{3}$$

where

for $k = n^2 + 2m$,	for $k = n^2 + 2m + 1$ $(m = 0, 1, .., n)$
$x_k = g_n^m$	h_n^m
$a_{ik} = -(dP_n^m/d\theta)_{\theta_i} \cos m\phi_i$	$-(dP_n^m/d\theta)_{\theta_i} \sin m\phi_i$ (4)
$b_{ik} = -m\, P_n^m(\cos\theta_i) \sin m\phi_i/\sin\theta_i$	$m\, P_n^m(\cos\theta_i) \cos m\phi_i/\sin\theta_i$
$c_{ik} = -(n+1)\, P_n^m(\cos\theta_i) \cos m\phi_i$	$-(n+1)\, P_n^m(\cos\theta_i) \sin m\phi_i$

As our data consists of magnetic directions I and D, we intend to obtain a potential (1) which will minimize the sum

$$\sum_{i=1}^{N} \left[(\cos I_i \cos D_i - X_i/F_i)^2 + (\cos I_i \sin D_i - Y_i/F_i)^2 + (\sin I_i - Z_i/F_i)^2 \right] \tag{5}$$

where $F_i^2 = X_i^2 + Y_i^2 + Z_i^2$ and N denotes the total number of data points. It is obvious that if we have a set of solutions x_k which minimizes the sum (5), then another set $c\, x_k$, where c is an arbitrary positive constant, will also minimize (5). As we can only determine the relative magnitudes of x_k, it will be convenient to replace them by $x_k' = x_k/x_1$. With such new variables (dropping the primes), components of the magnetic fields are

$$X_i/x_1 = a_{i1} + \sum_k a_{ik}\, x_k\,, \quad \text{etc.} \tag{6}$$

where the summation is taken from $k = 2$, onwards. In the case when the dipole lies near the equatrial plane, we may change the variables to x_k/x_2 or x_k/x_3.

Differentiation of (5) by x_k yields the minimization conditions

$$\sum_{i=1}^{N} \Big[(X_i/F_i - \cos I_i \cos D_i) \frac{\partial}{\partial x_k}(X_i/F_i) + (Y_i/F_i - \cos I_i \sin D_i) \frac{\partial}{\partial x_k}(Y_i/F_i) + (Z_i/F_i - \sin I_i) \frac{\partial}{\partial x_k}(Z_i/F_i) \Big] = 0 \tag{7}$$

which includes non-linear terms $(X_i/F_i)/\ x_k$, etc. However, since the field strength changes slowly over the surface of the earth if the magnetic field is mainly of dipole origin, we can neglect the derivatives of F_i for the first order approximation. Then $(X_i/F_i)/\ x_k$, etc. and we obtain from eq. (7) a set of linear equations of x_k,

$$\begin{pmatrix} A_{22} & A_{23} & \cdots \\ A_{32} & A_{33} & \cdots \\ \cdots & \cdots & \cdots \\ A_{k2} & A_{k3} & \cdots \\ \cdots & \cdots & \cdots \end{pmatrix} \begin{pmatrix} x_2 \\ x_3 \\ \vdots \\ x_k \\ \vdots \end{pmatrix} = \begin{pmatrix} B_2 \\ B_3 \\ \vdots \\ B_k \\ \vdots \end{pmatrix} \tag{8}$$

where

$$A_{jk} = \sum_{i=1}^{N} (a_{ij}\, a_{ik} + b_{ij}\, b_{ik} + c_{ij}\, c_{ik})/F_i^{\,2}$$

$$B_k = \sum_{i=1}^{N} \Big[(a_{ik} \cos I_i \cos D_i + b_{ik} \cos I_i \sin D_i + c_{ik} \sin I_i)/F_i - x_1\, (a_{ik}\, a_{i1} + b_{ik}\, b_{i1} + c_{ik}\, c_{i1})/F_i^{\,2} \Big] \qquad (9)$$

The process of computation is as follows. First, we assume a starting form of the potential (usually, $x_1 = 1$, $x_2 = x_3 = \ldots = 0$ is good enough). The coefficients A_{jk} and B_{jk} are then calculated by (9), using the values F_i derived from (6). By solving the simultaneous linear equations (8), we obtain a set of solutions x_k. These solutions does not actually satisfy the equation (7), as we neglected the derivatives of F_i. A better set of solutions can be obtained by iteration. Using the solutions just obtained, we calculate F_i from (6) and obtain the coefficients A_{jk} and B_k from (9). The equations (8) are again solved and a new set of solutions are obtained. The iteration terminates when a proper convergence is obtained for the solutions x_k.

3. Analysis of the Present Geomagnetic Field

To demonstrate the validity and efficiency of the present method, the geomagnetic potential for the year 1958 was calculated from the data of magnetic observatories in the world (Nagata and Sawada, 1963), both by the ordinary method based on X, Y, Z components and by the direction method based on I and D. Fig. 1 shows the distribution of magnetic observatories used in the analysis of the geomagnetic potential.

The results are given in Fig. 2 and Table 1. A very quick convergence was observed in the direction analysis, showing the ability of this method when dipole components dominate in the magnetic field. The agreement between the two analyses are quite remarkable (Table 1 and Fig. 3). Except h_4^3, which is negligibly small, the relative Gauss coefficients are almost

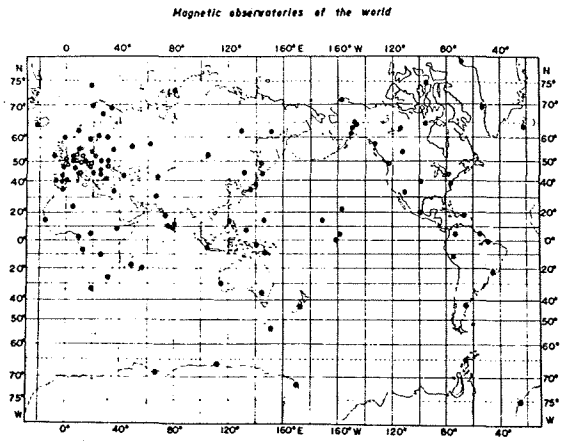

Fig. 1 Magnetic observatories used in the spherical harmonic analysis of the geomagnetic field in 1958.

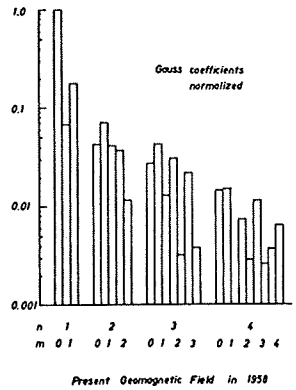

Fig. 2. Relative Gauss coefficients for 1958 determined from I and D.

identical for the two analyses. In Fig. 3, the Gauss coefficients from the two methods are compared. The abscissa is the absolute magnitude of the Gauss coefficient from X, Y, and Z, and the ordinate shows the relative magnitude of the same coefficient from the I and D analysis. White and black circles refers, respectively, to negative and positive coefficients. The circles should lie on the straight line if the two analyses give the identical result.

These results show that the present method is quite adequate, giving correct results and converging quickly. This method may therefore used in the analysis of paleomagnetic data.

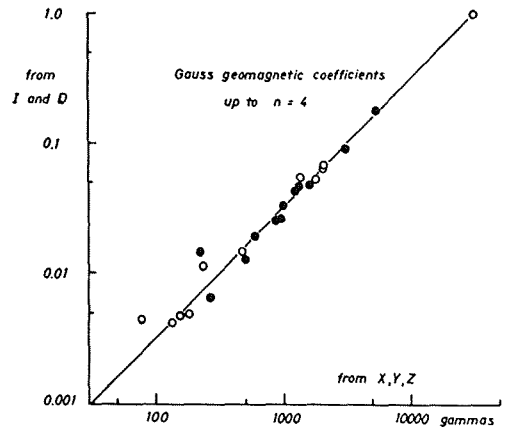

Fig. 3. Comparison of the Gauss coefficients obtained by two methods.

Table 1. Gauss Coefficients for the Year 1958

Coefficient	n	m	From X, Y, Z gammas	From X, Y, Z normalized	From I and D
g	1	0	-30515	-10000	-10000
g	1	1	- 2101	- 688	- 653
h	1	1	5695	1865	1872
g	2	0	- 1454	- 476	- 470
g	2	1	2785	912	864
h	2	1	- 1831	- 600	- 626
g	2	2	1546	507	494
h	2	2	348	114	118
g	3	0	1199	393	375
g	3	1	- 1908	- 625	- 702
h	3	1	- 379	- 124	- 144
g	3	2	1378	452	422
h	3	2	133	44	22
g	3	3	948	311	297
h	3	3	- 72	- 24	- 3
g	4	0	975	320	314
g	4	1	1137	373	355
h	4	1	156	51	55
g	4	2	479	157	153
h	4	2	- 200	- 66	- 85
g	4	3	- 588	- 193	- 166
h	4	3	29	9	- 1
g	4	4	215	71	71
h	4	4	- 351	- 115	- 94

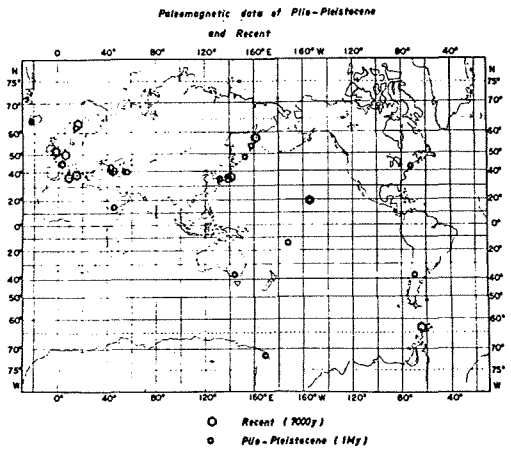

Fig. 4. Distribution of data points for the Recent (7000 years) and Plio-Pleistocene (1 m.y.).

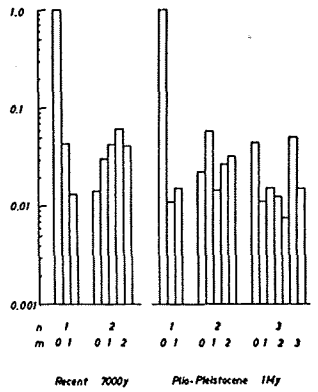

Fig. 5. Relative Gauss coefficients for the Recent and Plio-Pleistocene data.

4. Application to Paleomagnetic Data

For the purpose of preliminary investigation, the present method was applied to (1) 10 recent data (less than 7000years), (2) 27 Plio-Pleistocene data (less than 1 m.y.), (3) 32 upper Tertiary data, and (4) 38 Tertiary data. These data are obtained from Irving (1964). These calculations are of preliminary nature, as the number of data is quite small, and as they are quite irregularly distributed.

Fig. 4 and Fig. 5 show the distribution of the data points and obtained results for the recent and Plio-Pleistocene data. The predominance of the axial dipole g_1^0 can be seen in both cases. Fig. 6 shows the change in the relative magnitudes of the Gauss coefficients when different truncation is used in the potential (1). Although the signs and magnitudes of the coefficients change, they are not very important since g_1^0 is quite large. The root mean square angular difference can be made smaller by including more terms in the potential (1) (Fig. 7).

The relative importance of the dipole and non-dipole components for the present and the paleomagnetic field is compared in Fig. 8 through the quantity

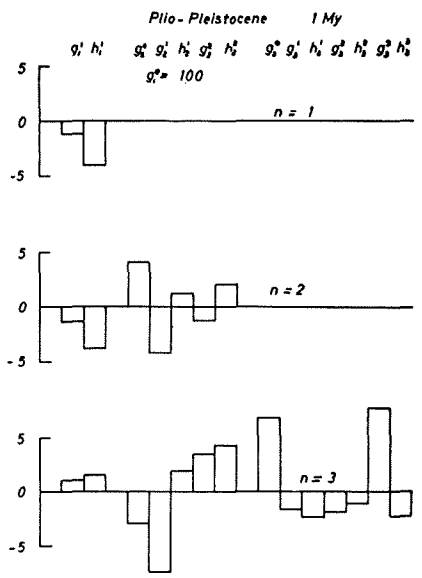

Fig. 7. Chenges in the values of the relative Gauss coefficients when potential has different number of terms.

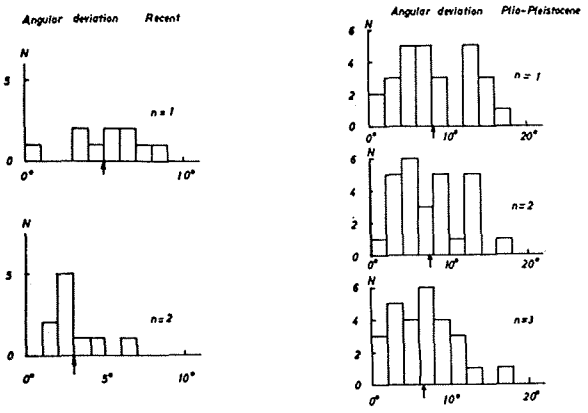

Fig. 7. Histograms of angular differences between observed and calculated angles for potentials with different number of terms. Left: the recent data. Right: the Plio-Pleistocene data. n denotes the maximum order of the harmonics in the potential (1). Arrows indicate the root mean square values.

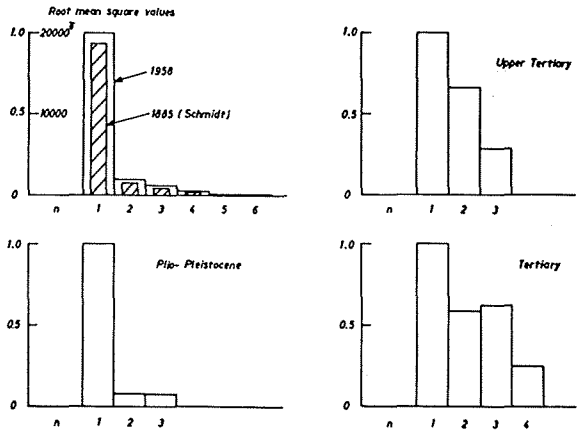

Fig. 8. Relative powers of dipole and non-dipole components in the present and the paleomagnetic fields. Abscissa is the order of the harmonics. See text.

$$\text{Power} = a\left((g_n^{\,0})^2 + (g_n^{\,1})^2 + (h_n^{\,1})^2 + \ldots + (g_n^{\,n})^2 + (h_n^{\,n})^2\right)^{\frac{1}{2}}/(2n+1)^{\frac{1}{2}}$$

Schmidt's value for 1885 (Chapman and Bartels, 1940) are also shown in this figure. The large powers of non-dipole terms for Tertiary may indicate that the movements of landmasses over the sphere cannot be neglected for the older periods.

References

Braginskiy, S.N. (1969) Geomag. Aeron. 9, 777.
Capman, S. and J. Bartels (1940) Geomagnetism, Vol. 2, p. 639, Oxford.
Doell, R.R. and A. Cox (1971) Science 171, 248.
Irving, E. (1964) Paleomagnetism and Its Application to Geological and Geophysical Problems, John Wiley, New York.
Kono, M. (1966) M. Sc. Thesis, University of Tokyo.
Kono, M. (1973) Rock Mag. Paleogeophys. 1, 118.
Nagata, T. and M. Sawada (1963) J. Geomag. Geoelect. 15, Suppl. 1.
Wilson, R.L. (1970) Geophys. J.Roy. Astr. Soc. 19, 417.

GALACTIC ROTAION AND GEOMAGNETIC REVERSALS

Nobuaki NIITSUMA

Department of Earth Sciences, College of Arts & Sciences
Tohoku University, 980 SENDAI

A chronologic correspondence between the passage of the Sun through the spiral arms of our Galaxy and geomagnetic reversals is suggested.

In our Galaxy the distribution of the spiral arms has been recognized by the positions of young stars and radio waves radiated from interstellar gas (Schmidt-Kaler, 1964; Kerr, 1970b; Weaver, 1970). According to " Density wave theory " (Lin et al., 1964; Lin et al., 1969) the spiral pattern is formed by a density wave in the galactic plane and the pattern is quasi-stationary. The rotation and distribution of mass in our Galaxy are explained approximately by the Schmidt Model (Schmidt, 1965), in which the Sun is moving with a velocity of 250 km/s along a circular orbit with radius of 10 kpc about the center of the Galaxy. Using the Schmidt Model, the angular velocity of the spiral pattern is calculated to be 13.5 km/s/kpc, therefore the materials pass the pattern with the velocity of 115 km/s. The Sun takes 620 million years to complete circular tour of the spiral pattern in our galactic plane (Fig. 1). If the position of the spiral arms in our Galaxy can be decided, we will be able to calculate the time when the Sun passed through the spiral arms. For deciding the positions of the spiral arms of our Galaxy on the orbit of the Sun, the

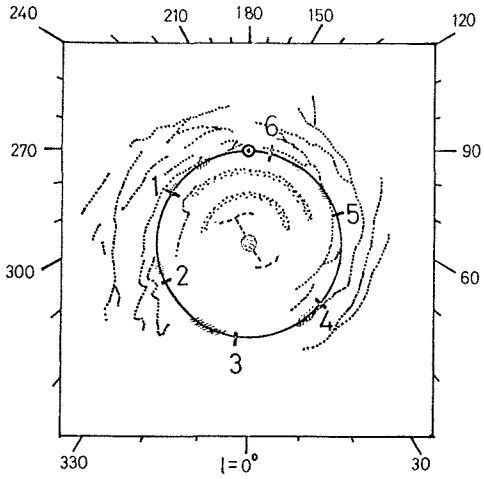

Fig. 1 Sketch of the main features of the neutral hydrogen spiral structure (Kerr, 1970b) and the orbit of the Sun.

The orbit of the Sun is shown by circle; the positions of the Sun during these 620 million years interval started from the small circle indicating the present position; the shaded area on the orbit is showing the area of high density of H_I.

intensities of 21-cm radio waves radiated by neutral hydrogen (H_I) with zero radial velocity in the directions of galactic latitude (b)=0°, and galactic longitude (l) between 270 to 90° are plotted in Fig. 2, using the data of Westhout (1966) and Kerr (1969, 1970a). In general there is a tendency for the intensity to increase towards l=0°, because in this direction radial velocity of all H_I in the Galaxy is zero. General increase of the intensity is also recognized around l=265 and 85°, where the directions are oblique and/or parallel to the spiral arms. Under the consideration of these general tendencies, eight locations of high density of H_I in galactic longitude are found in Fig. 2, which are shown with arrow heads. If the density of H_I was controlled by a density wave and the high density area composed the spiral arm, the above-mentioned locations are the intersecting areas of the spiral arms and the orbit of the Sun. The times when the Sun passed through the spiral arms can be calculated as 50, 80, 180, 270, 370, 440, 510, and 560 million years before present.

The magnetic field of the Earth has repeatedly changed between two stable directions, normal and reversed. It is known that the magnetic field is not stable in the intermediate direction, and the transition from one stable direction to another occurs within only a few thousand years (Niitsuma, 1971), although the cause and mechanism of magnetic field reversal have not been explained completely. Recently behaviour of the geomagnetic field has been traced back to 600 million years before present by the interpretation of

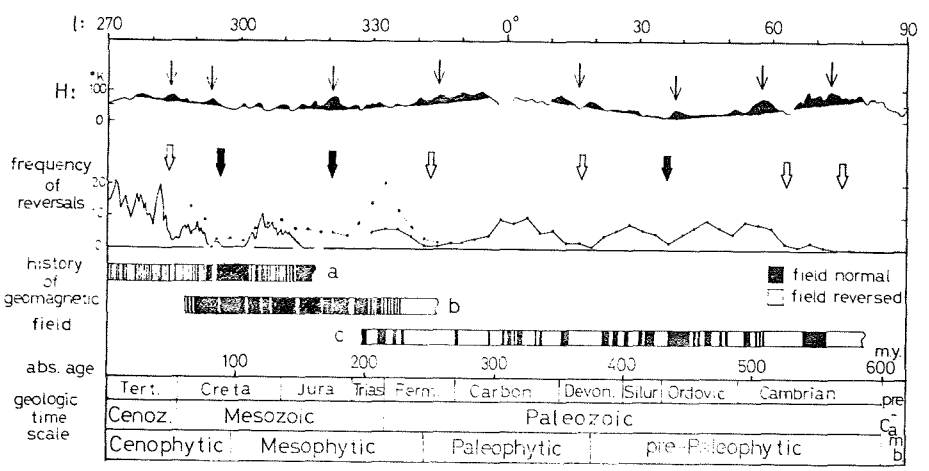

Fig. 2 Correlation of the locus of the Sun in the spiral pattern of our Galaxy with history of the Earth. In the history of geomagnetic field, column a is quated from Larson & Pitman (1972), b from McElhinny & Burek (1971), and c from Khramov et al. (1965).

magnetic anomalies over oceanic areas, and measurements of the remanent magnetization of rocks dated by isotopes and fossils (Larson & Pitman, 1972; McElhinny & Burek, 1971; Khramov et al., 1965). Three columns of the history of geomagnetic reversals together with frequency curves of reversals are shown in Fig. 2. The frequency curves are drawn from the number of reversals during a moving 5 million year window for column a, and a 30 million year window for b and c. In this figure, the frequency curves show eight remarkable intervals in which the geomagnetic field scarely reversed. They are shown with black (prevailing field normal) and white (reversed) arrows. Their ages are 50, 100, 180, 250, 370, 440, 530, and 570 million years before present, which correspond very well with those of passage of the Sun through the spiral arms.

The chronologic correspondence between passage of the Sun through the spiral arms and geomagnetic reversals suggests a causal relation among them. It has been derived theoretically that the density of gas and magnetic field should be increased by 4-6 times at the front of the spiral arm in our Galaxy and decreased gently behind it, because the interstellar gas makes a shock wave when it enters into the spiral arm with supersonic velocity (Roberts, 1969; Tosa, 1973). Because the direction of the galactic magnetic field is nearly parallel to spiral arms (Spitzer, 1968) and the rotation axes of solar system are nearly parallel to the direction of spiral arms, the influence of galactic magnetic field appeared most effectively on the magnetic field of the Earth. Looking at the correspondence between the ages of the passage of the Sun through the spiral arms and of the times of low frequency of geomagnetic reversals, and the fact that the geomagnetic field had the same polarity during the passage of the solar system through axial-symmetric pairs of the spiral arms except a pair of l=320° and 57°, it is suggested that reversals of the geomagnetic field are controlled by the intensity of the galactic magnetic field during the low frequency interval of reversals was influenced by the direction of the magnetic field in the spiral arms.

I thank Prof. K. Takakubo and Mr. Y. Sabano of Institute of Astronomy, and Prof. H. Nakagawa of Institute of Geology and Paleontology of Tohoku University, and Prof. B. M. Funnell of School of Environmental Sciences in University of East Anglia for discussion and reading of the manuscript.

Refereces

Kerr, F.J. (1969) Australian J. Phys. Astrophys. Suppl., 9.
Kerr, F.J. (1970a) ibid. 18.
Kerr, F.J. (1970b) in The Spiral Structure of our Galaxy, 95, (D. Reidel., Dordrecht-Holland)
Khramov, A.N., Rodinonov, V.P., and Komissarova, R.A.,

(1965) in The Present and Past of the Geomagnetic Field, 206, (Nauka Press, Moscow)
Larson, R.L. and Pitman, W.C. III (1972) Geol. Soc. Amer., Bull., 83, 3627.
Lin, C.C. and Shu, F.H. (1964) Astrophys. J. 140, 646.
Lin, C.C., Yuan, C. and Shu, F.H. (1969) ibid. 155, 721.
McElhinny, M.W. and Bureck, P.J. (1971) Nature, 237, 98.
Niitsuma, N. (1971) Tohoku Univ., Sci. Rep. 2nd Ser. (Geol.) 43, 1.
Roberts, W.W. (1969) Astrophys. J. 158, 123.
Schmidt, M. (1965) Stars and Stellar Systems, 5, 513.
Schmidt-Kaler, T. (1964) Trans. IAU. 12B, 416.
Spitzer, L.Jr. (1968) Diffuse Matter in Space, (John Wiley Sons, New York)
Tosa, M. (1973) Publ. Astron. Soc. Japan, 25, 191.
Weaver, H. (1970) in The Spiral Structure of our Galaxy, 122, (D. Reidel., Dordrecht-Holland)
Westhout, G. (1966) Maryland-Green Bank Galactic 21-cm line Survey.

AUTHOR INDEX